UNIVERSIDADE FEDERAL DO ESPÍRITO SANTO

CENTRO DE CIÊNCIAS HUMANAS E NATURAIS

PROGRAMA DE PÓS-GRADUAÇÃO EM BIOLOGIA VEGETAL

ROSIANE CIPRIANO

SILÍCIO COMO AGENTE MITIGADOR DE ESTRESSE EM *Aechmea blanchetiana* (BROMELIACEAE) *IN VITRO*: UMA ABORDAGEM ANATÔMICA E FISIOLÓGICA

VITÓRIA - ES
2022

ROSIANE CIPRIANO

SILÍCIO COMO AGENTE MITIGADOR DE ESTRESSE EM *Aechmea blanchetiana* (BROMELIACEAE) *IN VITRO*: UMA ABORDAGEM ANATÔMICA E FISIOLÓGICA

Tese de Doutorado apresentada ao Programa de Pós-Graduação em Biologia Vegetal do Centro de Ciências Humanas e Naturais da Universidade Federal do Espírito Santo como parte dos requisitos exigidos para a obtenção do título de Doutora em Biologia Vegetal.

Área de concentração: Fisiologia Vegetal.

Orientador(a): Prof. Dr. Antelmo Ralph Falqueto

Coorientador: Dr. João Paulo Rodrigues Martins

Coorientadora: Prof.ª. Dr.ª Andreia Barcelos Passos Lima Gontijo

VITÓRIA - ES
2022

Ficha catalográfica disponibilizada pelo Sistema Integrado de Bibliotecas - SIBI/UFES e elaborada pelo autor

---

Cipriano, Rosiane, 1990-
C577s Silício como agente mitigador de estresse em Aechmea blanchetiana (Bromeliaceae) in vitro: uma abordagem anatômica e fisiológica / Rosiane Cipriano. - 2022.
141 f. : il.

Orientador: Antelmo Ralph Falqueto.
Coorientadores: João Paulo Rodrigues Martins, Andreia Barcelos Passos Lima Gontijo.
Tese (Doutorado em Biologia Vegetal) - Universidade Federal do Espírito Santo, Centro de Ciências Humanas e Naturais.

1. Anatomia vegetal. 2. Cádmio. 3. Fluorescência da Clorofila a. 4. Salinidade. 5. Cultura de Tecidos Vegetais. I. Falqueto, Antelmo Ralph. II. Martins, João Paulo Rodrigues. III. Gontijo, Andreia Barcelos Passos Lima. IV. Universidade Federal do Espírito Santo. Centro de Ciências Humanas e Naturais. V. Título.

CDU: 57

Rosiane Cipriano

SILÍCIO COMO AGENTE MITIGADOR DE ESTRESSE EM *Aechmeablanchetiana* (BROMELIACEAE) *IN VITRO*: UMA ABORDAGEM ANATÔMICA E FISIOLÓGICA

Tese apresentada ao Programa de Pós-Graduação em Biologia Vegetal do Centro de Ciências Humanas e Naturais, da Universidade Federal do Espírito Santo, como requisito parcial para obtenção do Grau de Doutor em Biologia Vegetal.

Aprovada em 26 de agosto de 2022.

Comissão Examinadora:

Prof. Dr. Antelmo Ralph Falqueto (UFES)
Orientador e Presidente da Comissão

Profª. Drª. Diolina Moura Silva (UFES)
Examinadora Interna

Profª. Drª. Camilla Rozindo Dias Milanez (UFES)
Examinadora Interna

Profª. Drª. Eugenia Jacira Bolacel Braga (UFPEL)
Examinadora Externa

Prof. Dr. Wagner Campos Otoni (UFV)
Examinador Externo

UNIVERSIDADE FEDERAL DO ESPÍRITO SANTO

PROTOCOLO DE ASSINATURA

O documento acima foi assinado digitalmente com senha eletrônica através do Protocolo Web, conforme Portaria UFES nº 1.269 de 30/08/2018, por
ANTELMO RALPH FALQUETO - SIAPE 1648734
Departamento de Ciências Agrárias e Biológicas - DCAB/CEUNES
Em 18/10/2022 às 16:11

Para verificar as assinaturas e visualizar o documento original acesse o link:
https://api.lepisma.ufes.br/arquivos-assinados/586020?tipoArquivo=O

UNIVERSIDADE FEDERAL DO ESPÍRITO SANTO

PROTOCOLO DE ASSINATURA

O documento acima foi assinado digitalmente com senha eletrônica através do Protocolo Web, conforme Portaria UFES nº 1.269 de 30/08/2018, por
CAMILLA ROZINDO DIAS MILANEZ - SIAPE 2578589
Departamento de Ciências Biológicas - DCB/CCHN
Em 18/10/2022 às 17:51

Para verificar as assinaturas e visualizar o documento original acesse o link:
https://api.lepisma.ufes.br/arquivos-assinados/586147?tipoArquivo=O

UNIVERSIDADE FEDERAL DO ESPÍRITO SANTO

PROTOCOLO DE ASSINATURA

O documento acima foi assinado digitalmente com senha eletrônica através do Protocolo Web, conforme Portaria UFES nº 1.269 de 30/08/2018, por
DIOLINA MOURA SILVA - SIAPE 294671
Departamento de Ciências Biológicas - DCB/CCHN
Em 20/10/2022 às 09:42

Para verificar as assinaturas e visualizar o documento original acesse o link:
https://api.lepisma.ufes.br/arquivos-assinados/587537?tipoArquivo=O

gov.br Documento assinado digitalmente
WAGNER CAMPOS OTONI
Data: 20/10/2022 22:03:36-0300
Verifique em https://verificador.iti.br

gov.br Documento assinado digitalmente
EUGENIA JACIRA BOLACEL BIRAGA
Data: 27/10/2022 13:45:10-0300
Verifique em https://verificador.iti.br

DEDICATÓRIA

Aos meus pais Jorge Cipriano e Marlene da Costa Silva Cipriano e aos meus irmãos Francisco de Assis Cipriano e Marlucia da Penha Cipriano. Ao meu noivo Lucas Conseição Nascimento de Lima. Aos meus avós (in memoriam).

Dedico.

AGRADECIMENTOS

À Universidade Federal do Espírito Santo (UFES);
Ao Departamento de Ciências Agrárias e Biológicas, do Centro Universitário Norte do Espírito Santo;

Ao Programa de Pós-Graduação em Biologia Vegetal (PPGBV);

À Coordenação de Aperfeiçoamento de Pessoal de Nível Superior (CAPES) que subsidiou a bolsa de pesquisa e projeto de pesquisa;

À Deus pela minha vida, por me dar força e fé.

Ao meu orientador, Prof. Dr. Antelmo Ralph Falqueto, por toda orientação, pela confiança no meu trabalho, dedicação, direcionamentos, ensinamentos, apoio e amizade.

Ao Dr. João Paulo Rodrigues Martins por toda orientação durante toda minha trajetória do doutorado, pela atenção dada ao meu trabalho, pelos ensinamentos, conselhos, por ser sincero e verdadeiro, por toda amizade, pela paciência e apoio.

À prof Dra. Andreia Barcelos Passos Lima Gontijo pelas correções na escrita dos meus trabalhos, pelos ensinamentos, conselhos e pela amizade.

Aos ilustres membros da banca, que aceitaram corrigir este trabalho e por todas as contribuições para o aperfeiçoamento deste.

Aos amigos do laboratório de Cultura de Tecidos Vegetais Lorenzo, Samuel, Evens, Franciele, Leandro, Diana, Júlia, Luna, Samira e Thayna. Obrigada pela amizade, pelo apoio e por toda ajuda nos trabalhos.

Ao Laboratório de Ecofisiologia Vegetal-Ceunes/Ufes e ao Núcleo de Estudos da Fotossíntese-CCHN-Ufes.

À prof. Dra. Diolina Moura Silva e Dra. Mariela Mattos da Silva pelas contribuições nas análises da atividade das enzimas antioxidantes. Ao doutorando Marcel Merlo Mendes pela ajuda nas análises estatísticas do primeiro capítulo. Ao Dr. Luiz Carlos de Almeida Rodrigues pelas formatações em minhas figuras e gráficos.

Aos meus pais, irmãos e sobrinhos (Cecília e Paulo) por todo o amor, apoio, por serem minha força, pelas orações para que eu nunca desanimasse e persistisse com os meus objetivos e pela compreensão. Obrigada por tudo. Aos meus avós (Santina, Pedro e Amélia (*in memoriam*)) que foram minha força propulsora.

Ao meu amado noivo Lucas por todo amor, pelo companheirismo, pelas risadas, força, por acreditar em mim e no meu sonho e pela compreensão nos momentos que eu não estive tão presente.

À minha sogra, Maria Leide, por todo amor, carinho, apoio diário, amizade e compreensão nos meus momentos de ausência.

Aos meus parentes (primos, tios) e ao meu cunhado Guido por todo apoio, força e orações.

À minha turma do doutorado 2018, pela amizade e por compartilharem todos os momentos.

Às minhas amigas e amigos de Vitória (amigas da graduação), de Venda Nova do Imigrante e de São Mateus, pela amizade, por todo apoio, companheirismo, conselhos, presença em minha vida e ajuda.

À todos vocês que contribuíram para a realização deste sonho, meus sinceros agradecimentos!

RESUMO

As plantas estão expostas a frequentes fontes de estresses abióticos como pela alta salinidade e por elementos-traço, dentre eles o cádmio (Cd). A utilização do silício (Si) é uma alternativa que pode amenizar os efeitos deletérios desses estresses. O primeiro manuscrito (capítulo 1) teve como objetivo analisar a influência de diferentes fontes e concentrações de Si em respostas anatômicas e na atividade fotoquímica efetiva do fotossistema II (FSII) em plantas de *Aechmea blanchetiana* em condições *in vitro*. O segundo manuscrito (capítulo 2) avaliou o efeito do estresse salino *in vitro* e o potencial amenizador do Si em plantas de *A. blanchetiana*. O terceiro manuscrito (capítulo 3) investigou as modulações anatômicas e fisiológicas de *A. blanchetiana* expostas ao Cd *in vitro* e a co-exposição ao Cd e Si. No primeiro experimento brotos laterais de plantas previamente estabelecidas *in vitro* foram transferidos para meio de cultura. Meios sem Si foram usados como controle. Os tratamentos consistiram em silicato de cálcio ($CaSiO_3$), silicato de potássio (K_2O_3Si) e silicato de magnésio (MgO_3Si) em três concentrações (8, 16, 32 µM). Após 45 dias de cultivo foram realizadas análises anatômicas e fisiológicas. O estudo comprovou que o Si aumentou o diâmetro dos vasos do xilema, área do floema e crescimento das plantas. Dentre as fontes de Si testadas, o $CaSiO_3$ foi o que apresentou maior contribuição para o aumento do funcionamento efetivo do FSII e do crescimento das plantas. No segundo experimento, plantas já estabelecidas *in vitro* foram transferidas para meio de cultura com 0 ou 14 µM de Si ($CaSiO_3$). Após 30 dias de crescimento foram acrescentados nos frascos meio líquido estacionário contendo diferentes concentrações de NaCl (0, 100, 200 ou 300 µM). Após 45 dias foram realizadas análises anatômicas e fisiológicas. Plantas cultivadas com excesso de NaCl apresentaram redução do rendimento quântico fotoquímico efetivo do FSII e aumento da dissipação não-fotoquímica de fluorescência. Plantas em presença de Si tiveram aumento do conteúdo de pigmentos fotossintéticos, da atividade de enzimas do sistema antioxidante e do coeficiente de dissipação fotoquímica de fluorescência (q_P). Respostas anatômicas, fisiológicas e bioquímicas induzidas pelo Si tiveram efeito amenizador do estresse salino em *A. blanchetiana* cultivadas *in vitro*. No terceiro experimento, plantas previamente estabelecidas *in vitro* foram transferidas para meio de cultura com 0 ou 14 µM de Si. Após 30 dias de crescimento, foram adicionados aos recipientes meio MS líquido estacionário contendo concentrações crescentes de Cd

(0, 50, 100 ou 200 µM). Após 45 dias, foram realizadas análises anatômicas e fisiológicas. Plantas cultivadas com Si mostraram uma exoderme mais fina, diminuição na concentração de Chl *a/b* e aumento de Chl *total*/Car. O Cd induziu danos ao complexo de evolução do oxigênio (W_K) e alterou o rendimento quântico da dissipação de energia não regulada (ΦNO). Na presença de Si houve aumento da atividade fotoquímica do FSII e transporte de elétrons, mesmo quando as plantas foram expostas ao Cd. Respostas anatômicas e fisiológicas induzidas pelo Si foram eficazes em aliviar o estresse das plantas de *A. blanchetiana* crescidas *in vitro* com Cd.

Palavras-chave: Anatomia vegetal • cádmio • Fluorescência da clorofila *a* • Fluorescência modulada • salinidade •

ABSTRACT

Plants are exposed to frequent sources of abiotic stresses such as high salinity and trace elements, including cadmium (Cd). The use of silicon (Si) is an alternative that can alleviate the deleterious effects of these stresses. The first manuscript (chapter 1) aimed to analyze the influence of different sources and concentrations of Si on anatomical responses and on the effective photochemical activity of photosystem II (PSII) in *Aechmea blanchetiana* plants under *in vitro* conditions. The second manuscript (chapter 2) evaluated the effect of saline stress *in vitro* and the mitigating potential of Si in *A. blanchetiana* plants. The third manuscript (chapter 3) investigated the anatomical and physiological modulations of *A. blanchetiana* exposed to Cd *in vitro* and co-exposure to Cd and Si. In the first experiment lateral shoots of plants previously established *in vitro* were transferred to culture medium. Media without Si were used as a control. The treatments consisted of calcium silicate ($CaSiO_3$), potassium silicate (K_2O_3Si) and magnesium silicate (MgO_3Si) in three concentrations (8, 16, 32 µM). After 45 days of cultivation, anatomical and physiological analyzes were performed. The study proved that Si increased xylem vessel diameter, phloem area and plant growth. Among the Si sources tested, $CaSiO_3$ was the one that presented the greatest contribution to increase the effective functioning of PSII and plant growth. In the second experiment, plants already established *in vitro* were transferred to a culture medium with 0 or 14 µM of Si ($CaSiO_3$). After 30 days of growth, stationary liquid medium containing different concentrations of NaCl (0, 100, 200 or 300 µM) was added to the flasks. After 45 days, anatomical and physiological analyzes were performed. Plants grown with excess NaCl showed a reduction in the effective photochemical quantum yield of PSII and an increase in the non-photochemical dissipation of fluorescence. Plants in the presence of Si had an increase in the content of photosynthetic pigments, in the activity of enzymes of the antioxidant system and in the coefficient of photochemical fluorescence dissipation (qP). Anatomical, physiological and biochemical responses induced by Si had a mitigating effect of saline stress in *A. blanchetiana* cultivated *in vitro*. In the third experiment, plants previously established in vitro were transferred to a culture medium with 0 or 14 µM of Si. After 30 days of growth, stationary liquid MS medium containing increasing concentrations of Cd (0, 50, 100 or 200 µM) was added to the containers. After 45 days, anatomical and physiological analyzes were performed. Plants grown with Si showed a thinner exoderm, decreased concentration of Chl *a/b* and higher *total* Chl/Car ratio. Cd induced damage to the oxygen-evolution complex (W_K) and altered the quantum yield of non-regulated energy dissipation (ΦNO). In the presence of Si there was an increase in the photochemical activity of PSII and electron transport, even when the plants were exposed to Cd. Anatomical and physiological responses induced by Si were effective in easing the stress of *A. blanchetiana* plants grown *in vitro* with Cd.

Keywords: Plant anatomy • cadmium • Chlorophyll *a* fluorescence • Modulated fluorescence • salinity •

LISTA DE FIGURAS

CAPÍTULO 1: Melhoria na eficiência fotoquímica efetiva e no crescimento de *Aechmea blanchetiana* (BROMELIACEAE) in vitro são dependentes da fonte de silício*.....57*

Figura 1: Análise do controle (0 µM de Si) comparado aos demais tratamentos com Si ($CaSiO_3$, MgO_3Si, K_2O_3Si). Médias (± erro padrão) seguidas por um asterisco (*) são significativamente diferentes de acordo com o teste de Tukey ($p<0.05$). ns – diferença não significativa. Os dados foram normalizados com o controle (0 µM Si) igual a 1……62

Figura 2: Cortes transversais de raízes de plantas de *Aechmea blanchetiana* cultivadas *in vitro* em função de diferentes fontes de Si ($CaSiO_3$, MgO_3Si, K_2O_3Si) e concentrações (8, 16 e 32 µM). A) Controle (0 µM Si). en-endoderme, ex-exoderme, ep- epiderme, mx- vasos de metaxilema, fl-floema. Barras = 100 µm. 60

Figura 3: Espessura da parede celular da exoderme (µm) e diâmetro das raízes (µm) de *Aechmea blanchetiana* em função de fontes de Si ($CaSiO_3$, MgO_3Si, K_2O_3Si) e de concentrações (8, 16, 32 µM). Médias (± erro padrão) seguidos pela mesma letra não diferem de acordo com o teste de Tukey ($p<0.05$).....64

Figura 4: Secções paradérmicas e secções transversais de folhas de plantas de *Aechmea blanchetiana* cultivadas *in vitro* em função de diferentes fontes de Si ($CaSiO_3$, MgO_3Si, K_2O_3Si) e concentrações (0, 8, 16 e 32 µM). ad, epiderme adaxial; ab, epiderme abaxial; cl, clorênquima; hi, hidrênquima; ev, elementos de vasos (vasos do xilema); fl, floema; fb-fibras do esclerênquima; fv- feixes vasculares; es, estômatos. Barras = 100 µm. Secções paradérmicas (A1) Controle (0 µM Si); (B1, C1, D1; E1, F1, G1, H1; I1, J1) e secções transversais (A2, A3) Controle (B2; B3; C2, C3; D2, D3; E2, E3; F2, F3; G2; G3; H2, H3; I2, I3; J2, J3).....66

Figura 5: Densidade dos estômatos (0.01 mm^{-2}) (A), tamanho dos estômatos (μm^2) (B), área do esclerênquima (C), diâmetro de vasos do xilema (D), área do floema (E), espessura da epiderme adaxial e abaxial e do hidrênquima (F) de folhas de *Aechmea blanchetiana* em função das fontes de Si ($CaSiO_3$, MgO_3Si, K_2O_3Si) e das concentrações (8, 16, 32µM). (A – E) Médias (± erro padrão) seguidas da mesma letra (minúscula em função das fontes em cada concentração e maiúscula em função das

concentrações em cada fonte), não diferem pelo teste de Tukey ($p<0.05$). (F) Valores (± erro padrão) seguidos da mesma letra em função das fontes não diferem de acordo com o teste de Tukey ($p<0.05$). Médias (± erro padrão) em função das concentrações seguidas por um asterisco (*) são significativamente diferentes de acordo com o teste de Tukey ($p<0.05$). ns – diferença não significativa. Os dados foram normalizados com o tratamento 8 µM Si igual a 1……67

Figura 6: Conteúdo de pigmentos fotossintéticos clorofila *a* (Chl *a*), clorofila b (Chl *b*), carotenoides (Car), razão clorofila *a/b* (Chl *a/b*), clorofila *total*/car e clorofila *total* em plantas de *Aechmea blanchetiana* em função de fontes de Si ($CaSiO_3$, MgO_3Si, K_2O_3Si) e de concentrações (8, 16, 32 µM) em *Aechmea blanchetiana*. Valores (± erro padrão) seguidos pela mesma letra em cada pigmento fotossintético não diferem de acordo com o teste de Tukey ($p<0.05$)……...68

Figura 7: Parâmetros da fluorescência modulada de plantas de *Aechmea blanchetiana* em função das fontes de Si ($CaSiO_3$, MgO_3Si, K_2O_3Si) e das concentrações (8, 16, 32 µM). (A - C) Valores (± erro padrão) seguidos da mesma letra em cada parâmetro não diferem de acordo com o teste de Tukey ($p<0.05$). (A) Médias (± erro padrão) em função das concentrações seguidas por um asterisco (*) são significativamente diferentes de acordo com o teste de Tukey ($p<0.05$). ns – diferença não significativa. Os dados foram normalizados com o tratamento 8 µM Si igual a 1. (D – E) Valores (± erro padrão) seguidos da mesma letra para cada parâmetro (minúsculas em função das fontes em cada concentração e maiúsculas em função das concentrações em cada fonte), não diferem de acordo com o teste de Tukey ($p<0.05$)……68

Figura 8: Massa fresca total (parte aérea + raiz) (g $plant^{-1}$) de plantas de *Aechmea blanchetiana* em função das fontes de Si ($CaSiO_3$, MgO_3Si, K_2O_3Si) e das concentrações (8, 16, 32 µM). Valores (± erro padrão) seguidos pela mesma letra não diferem de acordo com o teste de Tukey ($p<0.05$)……..70

Figura 9: Coeficiente de Correlação de Pearson de plantas de *Aechmea blanchetiana* em função das fontes de Si ($CaSiO_3$, MgO_3Si, K_2O_3Si) e de concentrações (8, 16, 32 µM). Símbolos em vermelho indicam correlação negativa; símbolos em azul indicam correlação positiva……71

CAPÍTULO 2: Anatomical and physiological responses of *Aechmea blanchetiana* (Bromeliaceae) induced by silicon and salt stress during *in vitro* culture……81

Fig. 1. Cross-sections (A–H) and anatomical traits (I–J) of roots of *Aechmea blanchetiana* plants in the function of different concentrations of sodium chloride (NaCl) in the absence and presence of silicon (Si) during *in vitro* culture. Root transverse diameter (I) and cell wall thickness of root exodermis (J) of *Aechmea blanchetiana* in the function of the NaCl concentration (µM) and in the absence and presence of silicon (Si) during *in vitro* culture. (I) Means (± SE), *n* = 6, followed by the same letter do not differ according to the Tukey test at 5% significance. (J) Means (± SE), *n* = 6, followed by the same letter (lowercase for 0 µM Si and uppercase for 14 µM Si), at each NaCl concentration, do not differ according to the Tukey test at 5% significance. For each Si concentration analyzed (0 and 14 µM Si), the means followed by an asterisk are significantly different according to the Tukey test at 5% significance. ct – cortex, ed – endodermis, ep – epidermis, ex – exodermis, rh – root hair, xl – xylem, and phl – phloem. Bars =100 µm……102

Fig. 2. Paradermal sections (A – P) and stomatal traits of leaves of *Aechmea blanchetiana* plants in the function of different concentrations of sodium chloride (NaCl) in the absence and presence of silicon (Si) during *in vitro* culture. Means (± SE), *n* = 6, followed by the same letter, do not differ according to the Tukey test at 5% significance. st – stomata. Bars = 100 µm……..103

Fig. 3. Cross-sections of leaves of *Aechmea blanchetiana* plants in the function of different concentrations of sodium chloride (NaCl) in the absence and presence of silicon (Si) during *in vitro* culture. ad – adaxial epidermis, ab – abaxial epidermis, chl – chlorenchyma, hy – hydrenchyma, ph – phloem, sc – sclerenchyma, xl – xylem. Bars = 100 µm……104

Fig. 4. The thickness of the adaxial and abaxial faces of the epidermis (µm) (A – B) and the chlorenchyma (C) of leaves of *Aechmea blanchetiana* in the function of the concentrations of NaCl (0, 100, 200, 300 µM). Means (± SE), *n* = 6, followed by the same letter, do not differ according to the Tukey test at 5% significance……105

Fig. 5. Contents of macronutrients and micronutrients in *Aechmea blanchetiana* plants in the function of NaCl concentrations (0, 100, 200, 300 µM) combined with 0 or 14 µM Si. For each nutrient, the means (± SE), *n* = 3, followed by the same letter (lowercase

for 0 µM Si and uppercase for 14 µM Si), at each NaCl concentration, do not differ according to the Tukey test at 5% significance. For each Si concentration analyzed (0 and 14 µM Si), the means followed by an asterisk are significantly different according to the Tukey test at 5% significance. S = sulfur, Mg = magnesium, B = boron, Na = sodium……...106
Fig. 6. Contents of nutrients in *Aechmea blanchetiana* plants in the function of the concentrations of NaCl (0, 100, 200, 300 µM) or concentration of Si (0 or 14 µM Si). For each content of nutrients, the means (± SE), *n* = 3, followed by the same letter do not differ according to the Tukey test at 5% significance. Fe = iron, Zn = zinc, Mn = manganese, Ca = calcium, N = nitrogen, K = potassium, Na = sodium.....107
Fig. 7. The activity of superoxide dismutase (SOD), catalase (CAT), and ascorbate peroxidase (APX), respectively, in the leaves (A-C-E) and roots (B-D-F) of *Aechmea blanchetiana* plants cultivated *in vitro* in the function of the concentrations of NaCl (0, 100, 200, 300 µM) and concentration of Si (0 or 14 µM Si). Means (± SE), *n* = 5, followed by the same letter (lowercase for 0 µM Si and uppercase for 14 µM Si), at each NaCl concentration, do not differ according to the Tukey test at 5% significance. For each Si concentration analyzed (0 and 14 µM Si), the means followed by an asterisk are significantly different according to the Tukey test at 5% significance (A-D). Means (± SE), *n* = 5 followed by the same letter at each NaCl concentration, do not differ between Si content according to the Tukey test at 5% significance……108
Fig. 8. Contents of the photosynthetic pigments in *Aechmea blanchetiana* plants in the function of the presence or absence of Si (0 or 14 µM Si). Means (± SE), *n* = 8, followed by the same letter in each photosynthetic pigment, do not differ according to the Tukey test at 5% significance……109
Fig. 9. The effective photochemical quantum yield of PSII (ΦPSII) (A) and electron transport rate (ETR) (B) in the function of the concentrations of NaCl (0, 100, 200, 300 µM). Non-photochemical dissipation of fluorescence (non-photochemical quenching) (NPQ) (C) and maximum quantum yield of PSII (F_V/F_M) (D) in *Aechmea blanchetiana* plants in the function of the presence or absence of Si (0 or 14 µM Si). Means (± SE), *n* = 12, followed by the same letter for each parameter, do not differ according to the Tukey test at 5% significance……110
Fig. 10. Modulated fluorescence parameters of *Aechmea blanchetiana* plants in the function of the concentrations of NaCl (0, 100, 200, 300 µM) combined with 0 µM Si (A) or 14 µM Si (B). For each parameter, means (*n* = 12) followed by an asterisk (*)

denote significant differences between the concentrations of NaCl at each level of Si, while two asterisks (⁑) denote significant differences between the presence and absence of Si according to the Tukey test at 5% probability. ns = no significant……108
Fig. 11. Shoot (A) and root (B) fresh weights of *Aechmea blanchetiana* plants in the function of the concentrations of NaCl combined with 0 or 14 µM Si. Means (± SE), *n* = 5, followed by the same letters (lowercase for 0 µM Si and uppercase for 14 µM Si) at each NaCl concentration, do not differ according to the Tukey test at 5% significance. For each Si concentration analyzed (0 and 14 µM Si), the means followed by an asterisk are significantly different according to the Tukey test at 5% significance……...112

CAPÍTULO 3: Anatomical, physiological, and biochemical modulations of silicon in *Aechmea blanchetiana* (Bromeliaceae) cultivated in vitro in response to cadmium……..113

Fig. 1 Schematic representation of the experimental design from the first day of cultivation in agar-solidified culture media supplemented with 0 or 14 µM Si. After 30 days of growth, stationary liquid media with 0, 50, 100, or 200 µM Cd covered just the basal part of the leaves……131

Fig. 2 Root cross-sections of *Aechmea blanchetiana* plants in the function of concentrations (0, 50, 100 and, 200 µM) of Cd and Si (0 and 14 µM) during *in vitro* culture. en-endodermis, ex-exodermis, tr- trichome (root hair), mx- metaxylem vessels and, phl-phloem. Bars = 100 µm……133
Fig. 3 Anatomical traits of the root of *Aechmea blanchetiana* with 0 or 14 µM of Si. Means (±SE), *n* = 5, followed by an asterisk (*) in each anatomical feature are significantly different according to the Tukey test with a 5% probability……...134

Fig. 4 Paradermal sections (a–d and m–p) and cross-sections (e–l and q–x) of leaves of *Aechmea blanchetiana* plants as a function of concentrations (0, 50, 100 and, 200 µM) of Cd and Si (0 and 14 µM) during *in vitro* culture. ad-adaxial epidermis, ab-abaxial epidermis, chl-chlorenchyma, hy-hydrenchyma, ph-phloem, sc-sclerenchyma, st-stomata, vb-vascular bundles, and ve-vessel elements (xylem vessels). Bars = 100 µm……..135

Fig. 5 (A) Stomatal density and (B) size of the stomata of leaves of *Aechmea blanchetiana* as a function of Si (0 or 14 µM) and Cd concentrations (0, 50, 100, 200 µM). (a) Means (±SE), *n* = 5, followed by the different letters in each Si concentration (lower case for 0 µM Si and upper case for 14 µM Si, comparing the Cd concentrations) and asterisk (*) in each Cd concentration (comparing the Si concentrations) are significantly different according to the Tukey test at 5% probability. (b) For each Si concentration analyzed (0 and 14 µM Si), the means (±SE) followed by an asterisk are significantly different according to the Tukey test at 5% significance……135

Fig. 6 Anatomical characteristics of *Aechmea blanchetiana* leaves as a function Si (0 and 14 µM) and Cd concentrations (0, 50, 100, 200 µM). For each anatomical trait, means (±SE), *n* = 5, followed by an asterisk (*) (comparing the Si treatments) and different letters (comparing the Cd treatments) are significantly different according to the Tukey test at 5% significance……136

Fig. 7 Photosynthetic pigment content: chlorophyll *a/b* ratio (Chl *a/*b), total chlorophyll ratio for carotenoids (*total* Chl / Car) in *Aechmea blanchetiana* plants with 0 or 14 µM Si. Means (±SE), *n* = 8, followed by an asterisk (*) in each photosynthetic pigment ratio are significantly different according to the Tukey test with a 5% probability……136

Fig. 8 Kinetic differences of *Aechmea blanchetiana* plants grown in medium with different concentrations of Cd [µM] and Si [µM]. (A) kinetic differences between steps O and K [$V_{OK} = (F_t - F_0)/(F_K - F_0)$], showing the L-band; W_L - represents changes in the fluidity of the thylakoid membrane and damage to its function and structural integrity. (B) kinetic differences between steps O and J [$V_{OJ} = (F_t - F_0)/(F_J - F_0)$], showing the K-band; W_K - represents the damage to the oxygen evolving complex (OEC); For each parameter, means (±SE), *n* = 15, followed by the same letter do not differ significantly according to the Tukey test, with a 5% probability……137

Fig. 9 Parameters of the JIP test in *Aechmea blanchetiana* plants as a function of Cd concentrations (0, 50, 100, 200 µM). Means (±SE), *n* = 15, followed by an asterisk (*) are significantly different according to the Tukey test with a 5% probability. All parameters of the JIP test were normalized in relation to the control data (0 µM Cd = 1). ^{ns} = not significant……..138

Fig. 10 Parameters of modulated chlorophyll *a* fluorescence related to energy dissipation in *Aechmea blanchetiana* plants as a function of Cd concentrations (0, 50,

100, 200 µM). Means (±SE), *n* = 12, followed by the same letter do not differ according to the Tukey test at 5% significance……..…138

Fig. 11 Total fresh mass (shoot + roots) (g plant^{-1}) in *Aechmea blanchetiana* plants as a function of Cd concentrations (0, 50, 100, 200 µM) combined with 0 or 14 µM Si. Means (±SE), *n* = 5, followed by the different letters in each Si concentration (lower case for 0 µM Si and upper case for 14 µM Si, comparing the Cd concentrations) and asterisk (*) in each Cd concentration (comparing the Si concentrations) are significantly different according to the Tukey test at 5% probability……..140

LISTA DE TABELAS

CAPÍTULO 3: Anatomical, physiological, and biochemical modulations of silicon in *Aechmea blanchetiana* (Bromeliaceae) cultivated in vitro in response to cadmium……..114

Table 1 Abbreviations of the parameters, formulas and description of the data derived from the transient fluorescence of chlorophyll *a*.....132
Table 2 Abbreviations, formulas and description of the parameters of modulated chlorophyll fluorescence.....132
Table 3 JIP test parameters in *Aechmea blanchetiana* plants as a function of the absence or presence of Si (0 or 14 µM Si).....137
Table 4 Modulated fluorescence parameters related to energy dissipation in *Aechmea blanchetiana* plants as a function of the absence or presence of Si (0 or 14 µM Si).....139
Table 5 Effective photochemical quantum yield of PSII (ΦPSII), photochemical quenching (qP), and electron transport rate (ETR) as a function of Cd concentrations (0, 50, 100, 200 µM) in *Aechmea blanchetiana* plants.....139

SUMÁRIO

1. INTRODUÇÃO GERAL 25

2. OBJETIVO GERAL 288

3. OBJETIVOS ESPECÍFICOS 288

4. REVISÃO BIBLIOGRÁFICA 299

4.1 Cultura de Tecidos Vegetais 299

4.2 Estresse salino 30

4.3 Estresse por elemento-traço 31

4.4 Silício 33

4.5 Anatomia Vegetal 35

4.6 Fluorescência da Clorofila a.....36

4.7 Atividade de Enzimas do sistema antioxidante.....37

4.8 Bromeliaceae.....38

CAPÍTULO 1 – Silício induz incremento na eficiência fotoquímica efetiva e no crescimento de *Aechmea blanchetiana* (BROMELIACEAE) cultivadas *in vitro*.....57

RESUMO. 57

INTRODUÇÃO 58

MATERIAL E MÉTODOS 59

Material Vegetal e condições de cultivo in vitro 60

Análise da anatomia foliar e radicular 60

Conteúdo de pigmentos fotossintéticos 60

Análise da fluorescência modulada 61

Análise de características de crescimento 61

Análise estatística 61

RESULTADOS 62

Análise do controle (0 µM) *comparado aos demais tratamentos* (fontes de Si).....62

Análise anatômica em função das fontes e concentrações de Si......63

Conteúdo de pigmentos fotossintéticos em função das fontes e concentrações de Si.....68

Análise da Fluorescência modulada da clorofila a em função das fontes e concentrações de Si.. 69

*Análise de crescimento em função das fontes e concentrações de Si..*70

Análise de correlação.....70

DISCUSSÃO 71
CONCLUSÃO 75
REFERÊNCIAS 76
CAPÍTULO 2 – Anatomical and physiological responses of *Aechmea blanchetiana* (Bromeliaceae) induced by silicon and salt stress during *in vitro* culture..... 81
ABSTRACT 81
INTRODUCTION 82
MATERIALS E METHODS 84
In vitro culture conditions 84
Analysis of the leaf and root anatomy 85
Analysis of the mineral nutrient levels 85
Analysis of enzymatic activity 86
Contents of protosynthetic pigments 86
Measurement of modulated chlorophyll a fluorescence 87
Analysis of the growth traits 87
Statistical analysis 87
RESULTS 87
Anatomical analysis 87
Contents of nutrients 88
Antioxidant enzyme activity 89
Contents of photosynthetic pigments 89
Analysis of modulated chlrophyll a fluorescence 89
Analysis of growth 90
DISCUSSION 90
CONCLUSION 94
REFERENCES 95
CAPÍTULO 3 - Anatomical, physiological, and biochemical modulations of silicon in *Aechmea blanchetiana* (Bromeliaceae) cultivated *in vitro* in response to cadmium……113
ABSTRACT 114
INTRODUCTION 115
MATERIAL AND METHODS 116
Plant material and in vitro culture conditions 116

Analysis of leaf and root anatomy 117
Analysis of photosynthetic pigment contents 117
Analysis of chorophyll a fluorescence 117
Modulated fluorescence analysis 118
Analysis of growth traits *118*
Statistical analysis *118*
RESULTS 118
Root anatomy 118
Leaf anatomy 119
Photosynthetic pigments content 119
Analysis of chlorophyll a fluorescence 119
Analysis of modulated chlorophyll a fluorescence 119
Analysis of growth traits 120
DISCUSSION 120
CONCLUSION 124
REFERENCES 124
CONCLUSÕES GERAIS 140

1. INTRODUÇÃO GERAL

As plantas são continuamente expostas a várias condições ambientais que podem causar efeitos prejudiciais durante todos os estádios de desenvolvimento (ZHU et al., 2019; KIM et al., 2021). Estresses abióticos e bióticos são fatores que influenciam os organismos em um ambiente específico e que afetam negativamente o crescimento e o desenvolvimento de plantas (ZHANG et al., 2019). Dentre esses estresses está a alta salinidade, seca, inundação, resfriamento, calor e toxicidade por elementos-traço (REZENDE et al., 2018; ZHANG et al., 2019; ZHU et al., 2019). As plantas desenvolveram estratégias para lidar com tais estresses, e a elucidação dos mecanismos subjacentes é, portanto, cada vez mais útil (AHMED et al., 2021; KIM et al., 2021).

A alta salinidade é um tipo de estresse que as plantas estão constantemente sujeitas. A salinidade é responsável por múltiplos efeitos que reduzem o crescimento, desenvolvimento e a sobrevivência das plantas por meio de diversos mecanismos, incluindo alterações nas relações hídricas nas plantas (MORTON et al., 2019), deficiências ou toxicidades de íons (HNILIČKOVÁ et al., 2019) e estresse oxidativo (CARILLO, 2018; ZHU et al., 2019; CHUNG et al., 2020).

A contaminação por elementos-traço, outro tipo de estresse, representa um problema ambiental global. É decorrente principalmente de atividades antropogênicas, atividades industriais e agrícolas, como dispersão de resíduos de mineração, adubos, fertilizantes fosfatados e pesticidas à base de metais (MALČOVSKÁ et al., 2014; PAUNOV et al., 2018; KAYA et al., 2020). O cádmio (Cd) é um dos mais perigosos elementos-traço devido a sua alta mobilidade no sistema solo-planta (FENG et al., 2018). As plantas que crescem em ambiente com alto teor de Cd podem apresentar distúrbios bioquímicos e alterações morfofisiológicas. Dentre os vários sintomas de toxicidade, inclui-se a inibição da germinação, clorose, necrose, inibição do crescimento, alterações na homeostase iônica, distúrbios graves nas relações hídricas e no transporte de nutrientes (MALČOVSKÁ et al., 2014; OLIVEIRA et al., 2017), além de poder induzir a redução no conteúdo de pigmentos, na condutância estomática e no acesso ao CO_2 (PAUNOV et al., 2018).

Um mecanismo que têm sido empregado para reduzir os efeitos nas plantas do estresse salino e por elementos-traço é a suplementação com o Si (SAHEBI et al., 2016). Muitos estudos relataram os efeitos atenuantes do Si de estresses salino e por

elementos-traço (WU et al., 2015; COSKUN et al., 2016; MANIVANNAN et al., 2017; RIOS et al. 2017; ZHU et al. 2019; CIPRIANO et al. 2021b). O Si é o segundo elemento mais abundante da crosta terrestre, que pode ser absorvido por plantas superiores por meio do solo, principalmente, na forma de ácido silícico (H_4SiO_4) (ZHANG et al., 2019). É um elemento essencial que promove o crescimento e o desenvolvimento de várias espécies vegetais (SAHEBI et al., 2016; HU et al., 2018). O Si também possui potencial em aumentar a tolerância das plantas a ampla gama de estresses bióticos e abióticos, além dos expostos acima, como por patógenos vegetais, pragas, seca, calor, frio e estresse nutricional (LIU et al., 2014; SIVANESAN e JEONG, 2014; CUONG et al., 2017; HU et al., 2018; MARTINS et al., 2018; SOUNDARARAJAN et al., 2018; BHAT et al., 2019). O Si pode aumentar o conteúdo de pigmentos fotossintéticos e promover mudanças benéficas nas plantas, como na anatomia e no aumento da atividade fotossintética, redução da perda de água e aumento no crescimento (ASMAR et al., 2015; KHALIQ et al., 2016; DIAS et al., 2017, MANIVANNAN et al., 2017; D'ADDAZIO et al. 2020). O Si também pode atuar no balanço de nutrientes e na resistência mecânica, aumentando a estabilidade estrutural das células, especialmente sob condições estressantes (LIANG et al., 2015; TRIPATHI et al., 2016; MANIVANNAN et al., 2017; SOUNDARARAJAN et al., 2018; ZHANG et al., 2019).

A técnica de cultivo *in vitro* é vantajosa porque permite isolar os efeitos do elemento de interesse de estudo no metabolismo das plantas a partir dos efeitos de outros estresses (GIAMPAOLI et al., 2012). Estudos fisiológicos de estresses, como o salino e por elementos-traço, além de estudos das funções fisiológicas do Si, em condições *in vitro* são considerados uma alternativa viável por representar o ambiente externo com suas condições adversas (CLAYES et al., 2014; SIVANESAN e PARK, 2014). Avaliações por meio da técnica de fluorescência da clorofila *a* podem permitir verificar o estado fisiológico das plantas *in vitro* com base na detecção de alterações em alguns componentes do fotossistema II (FSII), componentes da cadeia de transporte de elétrons e nas reações fotoquímicas dependente da luz (LOTFI et al., 2018). Essa análise é amplamente utilizada para verificar a performance fotoquímica de plantas sob condições estressantes (KALAJI et al., 2016; 2017a; 2017b; 2018; STIRBET et al., 2018), tal como, expostas a diferentes elementos-traço (ZUREK et al., 2014; FRANIĆ et al., 2017; PAUNOV et al., 2018; MARTINS et al., 2020a). Vários estudos investigaram mudanças na fisiologia e na anatomia de plantas expostas ao

Cd *in vitro* (SON et al., 2014; ANJU et al., 2015; MANQUIÁN-CERDA et al., 2016; RODRIGUES et al., 2017). Assim como estudos de estresse salino *in vitro* também já foram realizados (HARTER et al., 2014; PANDEY e CHIKARA, 2015; CANTABELLA et al., 2017; ZUSHI e MATSUZOE, 2017; REZENDE et al., 2018; JAVED e GÜREL, 2019;), os quais enalteceram as vantagens dessas técnicas para pesquisas voltadas para fisiologia vegetal. Alterações anatômicas de plantas podem ser utilizadas como indicativo da qualidade ambiental (STOLÁRIKOVÁ-VACULÍKOVÁ et al., 2015; RODRIGUES et al., 2017). Essas alterações específicas são a chave para o processo de adaptação das plantas à determinadas condições ambientais (GOMES et al., 2012).

O estresse salino e por elementos-traço também se manifestam como estresse oxidativo e leva a produção de espécies reativas de oxigênio (ERO), com todos esses fatores contribuindo para os efeitos deletérios desses estresses nas plantas (ACOSTA- MOTOS et al., 2015; ZHU et al., 2019). As ERO podem alterar o metabolismo celular normal por meio de danos oxidativos em organelas e às membranas por peroxidação lipídica. Os sistemas antioxidantes das plantas podem ser estimulados para combater lesões oxidativas induzidas pelo estresse salino. Essas respostas incluem a remoção de ERO por enzimas como ascorbato peroxidase (APX), superóxido dismutase (SOD) e catalases (CAT) (ZHU et al., 2019).

No presente estudo, a espécie *Aechmea blanchetiana* (Baker) L.B. Smith (Bromeliaceae) foi escolhida como modelo vegetal, por ocorrer amplamente em áreas de restinga, um ambiente caracterizado por ser salino e com a presença de Si, onde se adaptou (COSTA et al., 2020). Além disso, as bromélias podem ser fundamentais em estudos com elementos-traço devido à formação de um sistema de tanque com suas folhas na base da roseta da planta, que pode armazenar grande quantidade de detritos do ambiente e água, resultando em exposição prolongada aos metais (SCHRECK et al., 2016; MARTINS et al., 2020a). Nesse contexto, é importante entender quais são os mecanismos morfo-fisiológicos que permitiram mitigar os danos induzidos pelo estresse salino e pelo Cd. Ainda não está claro como a co-exposição do Si e NaCl, bem como Si e Cd, podem influenciar na anatomia, performance do aparato fotossintético e na atividade de enzimas antioxidantes das plantas de restinga. Parte-se das hipóteses que: (1) Em condições de estresse *in vitro*, o NaCl e o Cd, são prejudiciais para o crescimento de plantas de *A. blanchetiana*, já que afetam a anatomia, a absorção de nutrientes e a fisiologia das plantas. (2) A suplementação

com o Si ameniza os danos e aumenta a resistência ao NaCl e ao Cd devido ao menor nível dos efeitos deletérios no conteúdo de pigmentos fotossintéticos, na atividade do sistema antioxidante e no desempenho do aparato fotossintético.

2. OBJETIVO GERAL

Avaliar os efeitos de fontes de Si, do NaCl e do Cd em plantas de *Aechmea blanchetiana* cultivadas *in vitro* e investigar o potencial amenizador de estresse do Si com a co-exposição ao NaCl e Si e Cd e Si.

3. OBJETIVOS ESPECÍFICOS

1. Avaliar o efeito de fontes de Si, do estresse salino e pelo Cd na anatomia radicular e foliar e no crescimento em plantas de *A. blanchetiana in vitro*;
2. Analisar as respostas fotoquímicas de plantas de *A. blanchetiana* cultivadas *in vitro* em diferentes fontes de Si, concentrações de NaCl e de Cd por meio de análises da fluorescência da clorofila *a* e do conteúdo de pigmentos fotossintéticos;
3. Investigar as modulações bioquímicas resultantes do estresse salino em *A. blanchetiana* cultivada *in vitro*, por meio da análise da atividade de enzimas do sistema antioxidante;
4. Avaliar o potencial do Si como amenizador do estresse por NaCl e por Cd em plantas de *A. blanchetiana* cultivadas *in vitro* na anatomia radicular e foliar, no conteúdo de pigmentos, na fisiologia, na bioquímica e no crescimento.

4. REVISÃO BIBLIOGRÁFICA

4.1 Cultura de Tecidos Vegetais

A cultura de tecidos vegetais compreende um conjunto de técnicas nas quais um explante (célula, tecido ou órgão) é isolado e cultivado em condições assépticas, em um meio nutritivo artificial e em condições controladas (THORPE, 2007). O seu princípio básico é baseado na exploração da pluripotência das células vegetais, que é a capacidade que possuem as células somáticas de, em condições adequadas, voltarem a dividir-se, sofrendo desdiferenciação, seguida de rediferenciação em outros tipos celulares, podendo regenerar, então, até mesmo uma planta completa (TERMIGNONE, 2012; SOUZA et al., 2018).

As técnicas de cultivo *in vitro* são amplamente utilizadas para a rápida multiplicação de muitas espécies de plantas, tais como espécies hortícolas, principalmente espécies ornamentais como orquídeas e bromélias (ERIG e SCHUCH, 2005; SILVA et al., 2017a; LEMBRECHTS et al., 2017; ROSA et al., 2018; MARTINS et al., 2019; 2020a; 2020b; CIPRIANO et al., 2021a). A multiplicação *in vitro* de bromélias pode ser realizada por meio de organogênese direta ou indireta (MARTINS et al., 2014; SIMÃO et al., 2016). No processo de organogênese direta, o crescimento e a formação de brotos resulta da ligação e interação entre reguladores de crescimento de plantas com proteínas receptoras, promovendo rápidas respostas bioquímicas e fisiológicas (HARUTA e SUSSMAN, 2017). Os reguladores de crescimento vegetais são compostos sintéticos adicionados ao meio de cultivo (JIMÉNEZ, 2005). Na multiplicação *in vitro*, para induzir brotos, é comum o uso de citocininas para estimular um desequilíbrio hormonal endógeno na parte aérea, ativando os meristemas laterais (MACKOVÁ et al., 2013). Para quebrar a dominância apical em bromélias *in vitro*, a fonte de citocinina utilizada mais comumente é o 6-benzilaminopurina (BAP) (SOUZA et al., 2016; SIMÃO et al., 2016; MARTINS et al., 2020a). No entanto, existem também estudos com a utilização de 6-furfurilaminopurina (cinetina - KIN) (MARTINS et al., 2014; FERMINO JÚNIOR et al., 2014), e de forma menos comum, o thidiazuron (TDZ), que geralmente não é recomendado (GUERRA e VESCO, 2010; BADR-ELDEN, 2013). A auxina sintética mais comumente utilizada para indução de raízes adventícias na propagação *in vitro* de bromélias é o ácido-1-naftalenoacético (ANA) (MARTINS et al., 2020c).

Estudos relacionados ao crescimento e fisiologia de bromélias *in vitro* também têm sido documentados (MARTINS et al., 2014, 2016b, 2018; SIMÃO et al., 2016; CORREDOR-PRADO et al., 2019; CIPRIANO et al., 2021a). A técnica de cultivo *in vitro* também é vantajosa porque permite isolar os efeitos do elemento de interesse de estudo no metabolismo das plantas a partir dos efeitos de outros estresses (GIAMPAOLI et al., 2012). Neste contexto, estudos fisiológicos de estresses, como estresse salino e por elementos-traço em condições *in vitro* são considerados uma alternativa viável por representar o ambiente externo com suas condições adversas (CLAYES et al., 2014). Além disso, este tipo de técnica oferece controle do nível e início do estresse, e baixa variabilidade (LAWLOR, 2013). Estudos *in vitro* também oferecem melhores perspectivas durante estádios iniciais do processo de aclimatização (REZENDE et al., 2018).

4.2 Estresse Salino

O estresse salino é considerado um dos principais estresses abióticos que podem limitar o crescimento das plantas e causar o declínio na produtividade das culturas (MORTON et al., 2019; CASTRO et al., 2020). Um conhecimento biológico dos efeitos do estresse salino é necessário para compreender as respostas da planta e encontrar maneiras de mitigar os danos. Atualmente, mais de 20% das terras irrigadas agrícolas do mundo são afetadas por concentrações excessivas de sal, e este problema continua a piorar em todo o mundo por causa da aplicação inadequada de fertilizantes, poluição industrial e práticas deficientes de irrigação (ZHU et al., 2019).

O estresse salino pode afetar diretamente o desempenho da planta de várias maneiras (MORTON et al., 2019; HNILIČKOVÁ et al., 2019; ZHU et al., 2019; CASTRO et al., 2020). A alta salinidade causa redução no nível osmótico e no potencial hídrico do meio de cultivo, impedindo a absorção de água. Isso, bem como os altos níveis de íons sódio, também podem afetar a absorção de nutrientes e os mecanismos de captação. Os íons sódio também são capazes de entrar na raiz através de canais iônicos e transportadores, eventualmente se espalhando por toda a planta via sistema vascular (ZHAO et al., 2019). Durante a exposição prolongada, os íons sódio podem se acumular a níveis que podem resultar em efeitos citotóxicos ou causar desequilíbrios osmóticos na planta. O acúmulo e, portanto, os danos, tendem

a ser maiores nos tecidos aéreos porque os íons sódio são entregues lá como solutos no fluxo de transpiração. Como a água é perdida através da transpiração, os íons sódio são depositados cumulativamente (MORTON et al., 2019).

Esses efeitos combinados levam ao comprometimento de processos biológicos vitais. As plantas podem responder de várias maneiras a esses danos ao estresse (ZHU et al., 2019). Os mecanismos fisiológicos das plantas para minimizar os danos do estresse salino ocorrem em raízes e brotos, no órgão, tecido, célula e escalas subcelulares. Respostas fisiológicas comuns incluem processos como detecção e sinalização de estresse, regulação da homeostase de íons, do metabolismo, diminuição da abertura estomática, da transpiração e da fotossíntese, inibição da divisão e expansão celular, assim como mudanças na morfologia da planta, fenologia e alocação de recursos (NEGRÃO et al., 2017; MORTON et al., 2019).

Os efeitos iônicos se desenvolvem gradualmente conforme o acúmulo de sódio (Na) progride e geralmente envolve um declínio gradual nas taxas de fotossíntese, metabolismo e crescimento, danos no aparato fotossintético e senescência precoce. Por exemplo, uma redução nas taxas de transpiração pode ser esperada como um efeito direto do reduzido potencial hídrico do meio de cultivo, mas também pode ser uma resposta da planta que limita o acúmulo de Na (ACOSTA- MOTOS et al., 2015; ZHU et al., 2019).

Estudos de estresse salino *in vitro* já foram realizados para mogango (*Cucurbita pepo*) (HARTER et al., 2014), estévia (*Stevia rebaudiana* Bertoni) (PANDEY e CHIKARA, 2015; CANTABELLA et al., 2017; JAVED e GÜREL, 2019), tomate (*Solanum lycopersicum*) (ZUSHI e MATSUZOE, 2017), fisális (Cape gooseberry)(*Physalis peruviana* L.) (REZENDE et al., 2018), erva-cidreira (*Lippia alba* L.) (Verbenaceae) (CASTRO et al., 2020) os quais enalteceram as vantagens dessas técnicas para pesquisas voltadas para fisiologia vegetal.

4.3 Estresse por elementos-traço

A contaminação por elementos-traço é um problema ambiental global devido aos seus potenciais riscos prejudiciais ao ecossistema e à saúde humana (CHANG et al., 2019; CLEMENS, 2019; KAMRAN et al., 2020; RIAZ et al., 2021). É decorrente principalmente de atividades antropogênicas, atividades industriais e agrícolas, como emissões de fundidores e incineradores, dispersão de resíduos de mineração, uso de

lodo de esgoto contaminado, adubos, fertilizantes fosfatados e pesticidas à base de metais (PAUNOV et al., 2018; KAYA et al., 2020). Os elementos-traço são altamente estáveis, não biodegradáveis e, portanto, facilmente transportáveis e acumulados através da cadeia alimentar, que pode ameaçar significativamente os seres vivos (YOUNIS et al., 2016; FENG et al., 2018).

O cádmio (Cd) é um metal relativamente móvel em comparação com outros metais pesados e as raízes das plantas podem facilmente absorver e translocar para as partes aéreas, devido à sua alta mobilidade no floema (CHANG et al., 2019; ADHIKARI et al., 2018). O Cd é translocado do solo para a raiz por diferentes transportadores que são usados para a absorção de nutrientes essenciais para as plantas. O Cd é um elemento não essencial e tóxico que perturba os processos bioquímicos, fisiológicos, morfológicos e moleculares essenciais para o crescimento e a produtividade das plantas (RIZWAN et al., 2016; 2018; REHMAN et al., 2019). O Cd pode causar danos ao metabolismo das plantas mesmo em níveis muito baixos (5-10 μg g^{-1}), exceto em plantas acumuladoras de Cd que podem sobreviver sob uma concentração considerável de Cd (100 μg g^{-1}). Nestas plantas, podem se acumular em seus tecidos sem apresentar sintomas de toxicidade (CLEMENS et al., 2013). A toxicidade do Cd afeta a fotossíntese, reduz a biomassa vegetal e dificulta a absorção de nutrientes essenciais do solo, o que resulta na redução do crescimento de várias espécies de plantas (CAO et al., 2018; ALYEMENI et al., 2018; QIN et al., 2018; ISMAEL et al., 2019; SHAHID et al., 2019; SEPEHRI e GHAREHBAGHLI, 2019; REN et al., 2020).

Os nutrientes minerais são uma parte essencial para o crescimento e produtividade das plantas. A deficiência de micro e macronutrientes causa um efeito negativo no crescimento e desenvolvimento das plantas (DING et al., 2017). Os nutrientes minerais foram relatados para aliviar a toxicidade de elementos-traço e aumentar a atividade dos sistemas de defesa das plantas. Esse mecanismo protege as plantas dos danos oxidativos de elementos-traço, incluindo a toxicidade do Cd (LIU et al., 2020b).

O estresse oxidativo gerado pela toxicidade do Cd pode causar a interrupção de uma série de processos fisiológicos e biológicos (WU et al., 2015; CLAIRVIL et al., 2022). A geração de espécies reativas de oxigênio (ERO) induzida por Cd interrompe direta ou indiretamente as funções moleculares nas plantas. Pode causar disfunção de DNA, genes, proteínas, ruptura de membrana e, em casos de severidade, causar

morte celular (RIAZ et al., 2018; YAN et al., 2018). A raiz é a parte principal de absorção da planta e o Cd danifica a estrutura radicular (YAN et al., 2018; RIAZ et al., 2021).

A capacidade de absorção, transporte, desintoxicação e acumulação de Cd varia entre diferentes espécies e genótipos de plantas (CLAIRVIL et al., 2022). Várias estratégias têm sido sugeridas para amenizar a toxicidade do Cd em plantas (ADREES et al., 2015; RIZWAN et al., 2016b, 2016c; YOUNIS et al., 2016). Pesquisas têm sido realizadas com o objetivo de minimizar os sintomas de toxicidade de Cd através de aplicações de silício (Si) (CIPRIANO et al., 2021b). O sequestro vacuolar, a formação de fitoquelatinas e a adsorção da parede celular têm sido relatados como mecanismos eficazes para a desintoxicação do Cd.

4.4 Silício

O silício (Si) é o segundo elemento, depois do oxigênio (O), mais abundante no solo, que pode ser absorvido pelas plantas principalmente na forma de ácido silícico (H_4SiO_4) (ZHANG et al., 2019; TREJO-TÉLLEZ et al., 2020). As concentrações de Si nas plantas geralmente variam entre 0,1% e 10% da massa seca total (EPSTEIN, 1994). Essa concentração depende principalmente dos genótipos das plantas e, em segundo lugar, de propriedades como fontes de Si (COSKUN et al., 2019; TREJO-TÉLLEZ et al., 2020). Vale ressaltar que sete das dez culturas mais produzidas no mundo (classificadas por quantidade) são acumuladoras de Si (GUNTZER, KELLER e MEUNIER, 2012) e a maioria responde positivamente às aplicações de Si (GÓMEZ-MERINO e TREJO-TÉLLEZ, 2018). Essas culturas incluem arroz (*Oryza sativa* L.), trigo (*Triticum aestivum* L.), cevada (*Hordeum vulgare* L.), cana-de-açúcar (*Saccharum* spp. L.), soja [*Glycine max* (L.) Merr.] e beterraba (*Beta vulgaris* L. subsp. *vulgaris*) (GUNTZER, KELLER e MEUNIER, 2012 ; ELSOKKARY, 2018 ; ARTYSZAK, GOZDOWSKI e KUCIŃSKA, 2019). O Si foi introduzido com sucesso no meio de cultura de plantas ornamentais como as orquídeas e bromélias como um elemento benéfico para a cultura de tecidos, melhorando as características morfológicas, anatômicas e fisiológicas de mudas *in vitro* (MANTOVANI et al., 2020).

O Si melhora características das plantas, especialmente sob estresses bióticos e abióticos, como salinidade, seca, toxicidade de metais pesados, frio, calor, hipóxia,

patógenos vegetais, deficiência de nutrientes e radiação ultravioleta (SIVANESAN e JEONG, 2014; LIU et al., 2014; MARTINS et al., 2018; HU et al., 2018; SOUNDARARAJAN et al., 2018; D'ADDAZIO et al. 2020; CIPRIANO et al., 2021b; NEDUKHA et al., 2022). Em plantas sob estresse a elementos-traço, o Si está envolvido em mecanismos de mitigação da toxicidade desses metais. O aumento da absorção de nutrientes, a estimulação de sistemas antioxidantes enzimáticos e não enzimáticos, o aumento da precipitação de íons tóxicos e o sequestro de íons em vacúolos e paredes celulares, podem funcionar como importantes mecanismos internos (SIL et al., 2019; ZHANG et al., 2019; ZHU et al., 2019; CIPRIANO et al., 2021).

Em pesquisas sobre estresse salino, os estudos envolveram o efeito regulatório do Si no metabolismo, na fotossíntese, no estresse oxidativo, no conteúdo de íons, em hormônios, poliaminas e transportadores de Si (ZHU et al., 2019). Os materiais de pesquisa envolveram monocotiledôneas, como cevada (*Hordeum vulgare* L.), trigo (*Triticum aestivum* L.) (CHEN et al., 2014), arroz (*Oryza sativa* L.) (SONG et al. 2015), milho (*Zea mays*) e sorgo (*Sorghum bicolor* L.) (YIN et al., 2016); eudicotiledôneas, incluindo pepino (*Cucumis sativus*), tomate (*Solanum lycopersicum* L.), tabaco (*Nicotiana tabacum*), abóbora (*Cucurbita maxima*) e amendoim (*Arachis hypogaea* L.); e plantas lenhosas (por exemplo, manga (*Mangifera indica* L.) e banana (*Musa* spp.).

O Si pode ser adicionado ao meio de cultura *in vitro* por meio de diferentes fontes e concentrações, que podem ter diferentes influências nas plantas *in vitro*. Dentre essas fontes está o silicato de potássio (K_2O_3Si), silicato de cálcio ($CaSiO_3$) e o silicato de magnésio (MgO_3Si). Estudos demonstraram que o K_2O_3Si melhorou a indução da parte aérea em comparação com o silicato de sódio ($NaSiO_3$) (SOARES et al., 2011). O K_2O_3Si também estimulou o comprimento da raiz, o crescimento vegetativo e a osmorregulação e melhorou processos fisiológicos, como aumento de pigmentos de clorofila, movimento dos estômatos e equilíbrio iônico (HAFEZ et al., 2021). O K_2SiO_3 mostrou potencial para atenuar estresse por deficiência de fósforo, melhorando a fotossíntese, o potencial antioxidante e a absorção dos nutrientes (ZHANG et al., 2019). O K_2SiO_3 é utilizado como bioestimulante vegetal e fonte de potássio (K) e Si altamente solúvel. O K é um dos elementos essenciais da planta e desempenha papel fundamental na formação de açúcares e amido, síntese de proteínas, divisão celular, crescimento, tamanho e qualidade de sementes (HAFEZ et al., 2021). A aplicação $CaSiO_3$ aumentou o potencial de indução de calos do arroz

(ISLAMET al., 2005), desencadeou o enraizamento e aumentou a espessura das folhas de banana (ASMAR et al., 2015). A suplementação com $CaSiO_3$ aumentou o conteúdo de pigmentos fotossintéticos, o desempenho do aparato fotossintético e o peso fresco em plantas *in vitro* (RODRIGUES et al., 2017; MARTINS et al., 2019; CIPRIANO et al., 2021). O MgO_3Si promoveu efeito na parte aérea das plantas e formação de raízes, além de desempenhar papel importante no processo de fotossíntese (SIPAHUTAR et al., 2021). Tomados em conjunto, o Si pode ser utilizado como fonte adicional para a melhoria da propagação *in vitro* de plantas (MANIVANNAN et al., 2017). Esses estudos enaltecem a necessidade de pesquisas voltadas para as especificidades de cada fonte e concentração dos silicatos em plantas de *Aechmea blanchetiana.*

4.5 Anatomia Vegetal

A análise da anatomia vegetal de plantas propagadas *in vitro*, por meio de cortes transversais e paradérmicos de folhas e raízes, é de grande importância para estudos comparativos do desenvolvimento de seus tecidos e de estruturas adaptativas (REZENDE et al., 2018). Dentro dessa análise está a caracterização da espessura da epiderme adaxial e abaxial, área do esclerênquima e do floema, tamanho e densidade de estômatos, entre outros (MARTINS et al. 2019; 2020b). Da mesma forma, análises anatômicas também são úteis para verificar como os componentes do meio de cultura podem influenciar as plantas cultivadas *in vitro* (ROSA et al., 2018).

Esses estudos também podem servir de base para pesquisas relacionadas ao desenvolvimento durante o processo de aclimatização, a qual se caracteriza por uma elevada mortalidade, muitas vezes, inviabilizando a micropropagação de algumas espécies (ABBADE et al., 2009).

Os estudos referentes à anatomia foliar e radicular podem ser uma ferramenta importante para avaliar as adequações morfológicas das plantas frente a agentes de estresse (PAEZ-GARCIA et al., 2015; MARTINS et al., 2019). Alterações anatômicas de plantas podem ser utilizadas como indicativo da qualidade ambiental (RODRIGUES et al., 2017). Essas alterações específicas são a chave para o processo de adaptação das plantas à determinadas condições ambientais (GOMES et al., 2012).

4.6 Fluorescência da Clorofila a

Avaliações por meio da técnica de fluorescência da clorofila *a* podem permitir verificar o estado fisiológico das plantas com base na detecção de alterações em alguns componentes do fotossistema II (FSII), componentes da cadeia de transporte de elétrons e nas reações fotoquímicas dependente da luz (LOTFI et al., 2018). Por meio das medições é possível detectar alterações no estado bioenergético geral do aparelho fotossintético das plantas (BORAWSKA-JARMUŁOWICZ et al., 2014), apresentando inúmeras vantagens. É um método preciso, não destrutivo e que possibilita analisar grande número de amostras em curto espaço de tempo (GOLTSEV et al., 2016). Por meio do teste OJIP, é possível obter informações visuais qualitativas e quantitativas sobre todo o aparato fotossintético ou sobre pontos específicos do FSII, intersistema e fotossistema I (FSI). Além disso, as curvas do teste OJIP podem ser quantificadas pelo teste JIP. Este fornece informações quantitativas sobre a produtividade e eficiência do aparato fotossintético (KALAJI et al., 2016; ROSA et al., 2018).

As análises de fluorescência da clorofila *a* mais comuns e amplamente usadas são realizadas em amostras de folhas adaptadas ao escuro e subsequentemente diferentes parâmetros que caracterizam o status de estado estacionário do aparelho fotossintético são calculados (KALAJI et al., 2016). O teste JIP é baseado em medições da cinética da fluorescência da clorofila *a*, fornecendo informações detalhadas sobre a estrutura e função do aparelho fotossintético, principalmente FSII. Os modelos subjacentes ao teste JIP descrevem as reações fotossintéticas primárias, levando em consideração a estrutura do aparelho fotossintético em total consistência com a teoria dos fluxos de energia que ocorrem na membrana dos tilacóides entre os complexos de pigmentos fotossintético no FSII. Esse teste é amplamente utilizado para analisar o desempenho da planta sob condições estressantes (KALAJI et al., 2016; 2017a; 2017b; 2018; STIRBET et al., 2018). Essa análise também foi aplicada para avaliar o desempenho do aparato fotossintético de plantas expostas a diferentes metais (ZUREK et al., 2014; FRANIĆ et al., 2017; PAUNOV et al., 2018; MARTINS et al., 2020; CIPRIANO et al., 2021).

Entre as medições de fluorescência, a cinética da fluorescência da clorofila baseada no pulso de amplitude modulada (PAM), pode sondar o desempenho do aparato fotossintético e avaliar características fisiológicas das plantas (YAO et al., 2018; BHAGOOLI et al., 2021). Essa análise permite a aquisição de importantes informações à cerca dos processos de dissipação fotoquímica e não fotoquímica da energia de excitação que ocorrem nas membranas dos tilacóides em presença de luz. Além de descrever também o rendimento quântico fotoquímico efetivo do FSII (CIPRIANO et al., 2021; CLAIRVIL et al., 2022).

4.7 Atividade de enzimas do sistema antioxidante

O estresse salino e por elementos-traço podem induzir ao estresse oxidativo e levar a produção de espécies reativas de oxigênio (ERO), malondialdeído (MDA) e ao extravasamento de eletrólitos (NAHAR et al., 2016; KAYA et al., 2020). As ERO tais como oxigênio singleto ($^1O_2$), ânion superóxido ($O_2^{\bullet-}$), radical hidroxila ($OH^{\bullet-}$) e peróxido de hidrogênio (H_2O_2), podem alterar o metabolismo celular normal através de danos oxidativos em organelas e às membranas por peroxidação lipídica, reduzindo o crescimento das plantas (GIAMPAOLI et al., 2012; AHMAD et al., 2019). Todos esses fatores podem contribuir para os efeitos deletérios da salinidade e elementos-traço nas plantas, podendo alterar as atividades de várias enzimas-chave e até causar morte celular (YOUNIS et al., 2016; NAHAR et al., 2016; ZHU et al., 2019; CLAIRVIL et al., 2022).

As plantas possuem mecanismos do sistema antioxidante, enzimáticos e não enzimáticos, que são estimulados para combater lesões oxidativas induzidas por condições de estresse. As respostas de enzimas antioxidantes incluem a remoção de ERO por enzimas como ascorbato peroxidase (APX), superóxido dismutase (SOD) e catalase (CAT) (ZHU et al., 2019). As enzimas CAT e APX são classificadas como os principais antioxidantes enzimáticos, pois participam na decomposição do H_2O_2 em água. O Si induz várias respostas fisiológicas, tal como o aumento da atividade de enzimas do sistema antioxidante como de APX, SOD, CAT e não-enzimático como da glutationa (GSH) (SHI et al., 2014; TRIPATHI et al., 2015; KIM et al., 2016; 2017; RIZWAN et al., 2019; CHUNG et al., 2020). Além disso, está bem estabelecido que o Si regula significativamente a atividade das enzimas antioxidantes (CAT, APX e SOD)

para mitigar estresses abióticos, por meio da redução da geração de ROS (ABDEL LATEF e TRAN, 2016; AHMAD et al., 2019; CHUNG et al., 2020).

4.8 Bromeliaceae

As bromélias ornamentais, nativas de zonas tropicais e subtropicais da América do Sul e Central, estão entre as plantas ornamentais comercialmente mais importantes do mundo, ocupando uma posição valiosa na horticultura e a indústria de flores (ZHANG et al., 2012).

A espécie *Aechmea blanchetiana* (Baker) L. B. Sm. (Subfamília Bromelioideae) é uma bromélia tanque-dependente e nativa do estado do Espírito Santo e Bahia. Ocorre amplamente em áreas de restinga por ser heliófita, um ambiente caracterizado por ser salino e com a presença de Si, onde se adaptou (COSTA et al., 2020). Possui hábito terrestre e epifítico com folhagem amarelada devido à irradiação solar e possui valor comercial em todo o território brasileiro, sendo muito utilizada em projetos paisagísticos (GOMES e SILVA, 2013; SANTA-ROSA et al., 2013).

As bromélias podem ser fundamentais em estudos com elementos-traço devido à formação de um sistema de tanque com suas folhas na base da roseta da planta. O tanque pode armazenar uma grande quantidade de detritos do ambiente e água, resultando em uma exposição prolongada aos metais (SCHRECK et al., 2016; MARTINS et al., 2020a). Estes podem ser prontamente assimilados por meio dos tricomas escamiformes. Essas ultra-estruturas foliares são responsáveis pela absorção quando a superfície da folha de bromélias está úmida (GOMES et al., 2015) e as raízes também podem absorver nutrientes a partir do solo. Várias espécies de bromélias possuem potencial como bioindicadoras de metais pesados e este potencial já foi constatado em condições *in vitro* (GIAMPAOLI et al., 2012; 2016; PIAZZETTA et al., 2018; MARTINS et al., 2016; 2020a). Já foi verificado que *A. blanchetiana* tolera altas concentrações de um metal pesado (Cu) e tem potencial para uso como bioindicador (MARTINS et al., 2020a). Essa exposição a metais pesados pode levar a modificações anatômicas e fisiológicas nessas plantas, indicando a qualidade do ambiente (MARTINS et al., 2016). Essas características descritas justificam a escolha da espécie *Aechmea blanchetiana* (Baker) L.B. Smith (Bromeliaceae) como modelo vegetal do presente estudo.

REFERÊNCIAS

ABDEL LATEF, A. A.; TRAN, L.S.P. Impacts of priming with silicon on the growth and tolerance of maize plants to alkaline stress. **Frontiers in Plant Science**, v. 7, p. 243, 2016.

ACOSTA-MOTOS, J.R.; DÍAZ-VIVANCOS, P.; ÁLVAREZ, S.; FERNÁNDEZ-GARCÍA, N.; SÁNCHEZ- BLANCO, M.J.; HERNÁNDEZ, J.A. NaCl-induced physiological and biochemical adaptative mechanisms in the ornamental *Myrtus communis* L. plants. **Journal of Plant Physiology**, v. 183, p. 41-51, 2015.

ADHIKARI, S; GHOSH, S.; AZAHAR, I.; ADHIKARI, A.; SHAW, A.K.; KONAR, S.; ROY, S.; HOSSAIN, Z. Sulfate improves cadmium tolerance by limiting cadmium accumulation, modulation of sulfur metabolism and antioxidant defense system in maize. **Environmental and Experimental Botany**, v. 153, p. 143–162, 2018.

AHMAD, P.; AHANGER, M. A.; ALAM, P.; ALYEMENI, M. N.; WIJAYA, L.; ALI, S.; et al. Silicon (Si) supplementation alleviates NaCl toxicity in mung bean [*Vigna radiata* (L.) Wilczek] through the modifications of physio-biochemical attributes and key antioxidant enzymes. **Journal of Plant Growth Regulation**, v. 38, n. 1, p. 70–82, 2019.

AHMED, H.A.I.; SHABALA, L.; SHABALA, S. Tissue-specificity of ROS-induced K^+ and Ca^{2+} fluxes in succulent stems of the perennial halophyte *Sarcocornia quinqueflora* in the context of salinity stress tolerance. **Plant Physiology and Biochemistry**, v. 166, p. 1022–1031, 2021.

ALYEMENI, M.N.; AHANGER, M.A.; WIJAYA, L.; ALAM, P.; BHARDWAJ, R.; AHMAD, P. Selenium mitigates cadmium-induced oxidative stress in tomato (*Solanum lycopersicum* L.) plants by modulating chlorophyll fluorescence, osmolyte accumulation, and antioxidant system. **Protoplasma**, v. 255, p. 459-469, 2018.

ANJU, M.; SANSKRITI, G.; SURESH, B.S.; NIDHI, S. *In vitro* accumulation of cadmium chloride in papaya seedling and its impact on plant protein. **International Journal of Ayurveda and Pharma Research**, v. 2, p. 54–62, 2015.

ASMAR, A.S.; SOARES, J.D.R.; SILVA, R.A.L.; PASQUAL, M.; PIO, L.A.S.; CASTRO, E.M. Anatomical and structural changes in response to application of silicon (Si) *in vitro* during the acclimatization of banana cv. 'Grand Naine'. **Australian Journal of Crop Science**, v. 9, p. 1236–1241, 2015.

ARTYSZAK, A.; GOZDOWSKI, D.; KUCIŃSKA, K. Impact of foliar fertilization on the content of silicon and macronutrients in sugar beet. **Plants**, v. 8, n. 5, p. 136, 2019.

BHAGOOLI, R.; MATTAN-MOORGAWA, S.; KAULLYSING, D.; LOUIS, Y.D.; GOPEECHUND, A.; RAMAH, S.; SOONDUR, M.; PILLY, S.S.; BEESOO, R.; WIJAYANTI, D.P.; BACHOK, Z.B.; MONRÁS, V.C.; CASARETO, B.E.; SUZUKI, Y.; BAKER, A.C. Chlorophyll fluorescence – A tool to assess photosynthetic performance and stress photophysiology in symbiotic marine invertebrates and seaplants. **Marine Pollution Bulletin**, v. 165, p. 112059. 2021.

BHAT, J.A.; SHIVARAJ, S.M.; SINGH, P.; NAVADAGI, D.B.; TRIPATHI, D.K.; DASH, P.K.; SOLANKE, A.U.; SONAH, H.; DESHMUKH, R. Role of Silicon in Mitigation of Heavy Metal Stresses in Crop Plants. **Plants** (Basel), v.8, n. 3, p. 71, 2019.

BORAWSKA-JARMUŁOWICZ, B.; MASTALERCZUK, G.; KALAJI, M.H.; CARPENTIER, R.; PIETKIEWICZ, S.; ALLAKHVERDIEV, S.I. Photosynthetic efficiency and survival of *Dactylis glomerata* and *Lolium perenne* following low temperature stress. **Russian Journal of Plant Physiology**, v. 61, p. 281-288, 2014.

CANTABELLA, D.; PIQUERAS, A.; ACOSTA-MOTOS, J.R.; BERNAL-VICENTE, A.; HERNÁNDEZ, J.A.; DÍAZ-VIVANCOS, P. Salt-tolerance mechanisms induced in *Stevia rebaudiana* Bertoni: Effects on mineral nutrition, antioxidative metabolism and steviol glycoside content. **Plant Physiology and Biochemistry**, v. 115, p. 484–496, 2017.

CAO, Z.Z.; QIN, M.L.; LIN, X.Y.; ZHU, Z.W.; CHEN, M.X. Sulfur supply reduces cadmium uptake and translocation in rice grains (*Oryza sativa* L.) by enhancing iron plaque formation, cadmium chelation and vacuolar sequestration. **Environmental Pollution**, v. 238, p. 76-84, 2018.

CARILLO, P. GABA Shunt in Durum Wheat. **Frontiers in Plant Science**, v. 9, p. 100, 2018.

CHANG, C.; YIN, R.; ZHANG, H.; YAO, L. Bioaccumulation and health risk assessment of heavy metals in the soilerice system in a typical seleniferous area in Central China. **Environmental Toxicogy and Chemistry**, v. 38, p. 1577-1584, 2019.

CHEN, D.; YIN, L.; DENG, X.; WANG, S. Silicon increases salt tolerance by influencing the two-phase growth response to salinity in wheat (*Triticum aestivum* L.). **Acta Physiologiae Plantarum**, v. 36, p. 2531–2535, 2014.

CHUNG, Y.S.; KIM K.S.; HAMAYUN, M.; KIM, Y. Silicon Confers Soybean Resistance to Salinity Stress Through Regulation of Reactive Oxygen and Reactive Nitrogen Species. **Frontiers in Plant Science**, v. 10, p. 1725, 2020.

CIPRIANO, R.; MARTINS, J.P.R.; RODRIGUES, L.C.A.; FALQUETO, A.R.; GONTIJO, A.B.P.L. Impact of saline solution on growth and photosystem II during *in vitro* cultivation of *Bromelia antiacantha* (Bromeliaceae). **Rodriguésia**, v. 72, 2021a.

CIPRIANO, R.; MARTINS, J.P.R.; CONDE, L.T.; MOREIRA, S.W.; CLAIRVIL, E.; BRAGA, P.C.S.; GONTIJO, A.B.P.L.; FALQUETO, A.R. Anatomical, physiological, and biochemical modulations of silicon in *Aechmea blanchetiana* (Bromeliaceae) cultivated *in vitro* in response to cadmium. **Plant Cell, Tissue and Organ Culture**, v. 147, p. 271-285, 2021b.

CLAYES, H. et al. What is stress?: dose-response effects in commonly used *in vitro* stress assays. **Plant Physiology**, v.165, n.1, p.519-517, 2014.

CLEMENS, S.; AARTS, M.G.; THOMINE, S.; VERBRUGGEN, N. Plant science: the key to preventing slow cadmium poisoning. **Trends in Plant Science**. v. 18, p. 92-99, 2013.

CLEMENS, S. Safer food through plant science: reducing toxic element accumulation in crops. **Journal of Experimental Botany**, v. 70, p. 5537- 5557, 2019.

CLAIRVIL, E.; MARTINS, J.P.R.; BRAGA, P.D.C.D.S.; CIPRIANO, R.; CONDE, L.T.; MOREIRA, S.W.; ROSSINI, F.P.; FALQUETO, A.R.; GONTIJO, A.B.P.L. Modulation of physiological responses and tolerance of *Alternanthera tenella Colla* (Amaranthaceae) to cadmium during in vitro cultivation. **Israel Journal of Plant Sciences**, v. 69, n. 3-4, p. 181-192, 2022.

COSKUN, D.; BRITTO, D.T.; HUYNH, W.Q.; KRONZUCKER, H.J. The role of silicon in higher plants under salinity and drought stress. **Frontiers in Plant Science**, v. 7, p. 1072, 2016.

COSKUN, D.; DESHMUKH, R; SONAH, H.; MENZIES, J.G.; REYNOLDS, O.; MA, J. F.; KRONZUCKER, H.J.; BÉLANGER, R.R. The controversies of silicon's role in plant biology. **New Phytologist**, v. 221, p. 67-85, 2019.

COSTA, W.S.; YAMAMURA, R.H.R.; MORCELLI, C.P.R.; SÍGOLO, J.B. Adição de resíduo de marmoraria em pastas cimentícias, avaliação de suas propriedades mecânicas e caracterização química. INOVAE - **Journal of Engineering, Architecture and Technology Innovation**, São Paulo, v.8, p.1-18, 2020.

CORREDOR-PRADO, J.P.; DE CONTI, D.; ROECKER JÚNIOR, D.; CANGAHUALA-INOCENTE, G.C.; GUERRA, M.P.; VESCO, L.L.D.; PESCADOR, R. Proteomic identification of differentially altered proteins during regeneration from nodular cluster cultures in *Vriesea reitzii* (Bromeliaceae). **Journal of Plant Growth Regulation**, v. 38, p. 586-599, 2019.

CUONG, T.X.; ULLAH, H.; DATTA, A.; HANH, T.C. Effects of Silicon-Based Fertilizer on Growth, Yield and Nutrient Uptake of Rice in Tropical Zone of Vietnam. **Rice Science**, v. 24, n. 5, p. 283–290, 2017.

D'ADDAZIO, V.; SILVA, J.V.G.; JARDIM, A.S.; LONGUE, L.L.; SANTOS, R.A.A.; FERNANDES, A.A.; ... FALQUETO, A.R. Silicon improves the photosynthetic performance of black pepper plants inoculated with *Fusarium solani* f. sp. *piperis*. **Photosynthetica**, v. 58, n. 3, p. 692-701, 2020.

CASTRO, K.M.; BATISTA, D.S., SILVA, T.D. et al. Salinity modulates growth, morphology, and essential oil profile in *Lippia alba* L. (Verbenaceae) grown *in vitro*. **Plant Cell, Tissue and Organ Culture**, v. 140, p. 593–603, 2020.

DIAS, G.M.G.; SOARES, J.D.R.; RIBEIRO, S.F.; MARTINS, A.D.; PASQUAL, M., ALVES E. Morphological and physiological characteristics *in vitro* anthurium plantlets exposed to silicon. **Crop Breeding and Applied Biotechnology**, v. 17, p. 18–24, 2017.

DING, Y.; WANG, Y.; ZHENG, X.; CHENG, W.; SHI, R.; FENG, R. Effects of foliar dressing of selenite and silicate alone or combined with different soil ameliorants on the accumulation of as and Cd and antioxidant system in *Brassica campestris*. **Ecotoxicology and Environmental Safety**, v. 142, p. 207-215, 2017.

ELSOKKARY, I.H. Silicon as a beneficial element and as an essential plant nutrient: an outlook. **Alexandria Science Exchange Journal**, v. 39, n. 3, p. 534-550, 2018.

EPSTEIN, E. The anomaly of silicon in plant biology. **Proceedings of the National Academy of Sciences of the United States of America**, v. 91, n. 1, p. 11-17, 1994.

ERIG, A. C.; SCHUCH, M. W. Micropropagação fotoautotrófica e uso da luz natural. **Ciência Rural**, Santa Maria, v. 35, n. 4, p. 961-965, 2005.

FENG, J.; LIN, Y.; YANG, Y.; SHEN, Q.; HUANG, J.; WANG, S.; ZHU, X.; LI, Z. Tolerance and bioaccumulation of Cd and Cu in *Sesuvium portulacastrum*. **Ecotoxicology and Environmental Safety**, v. 147, p. 306–312, 2018.

FRANIĆ, M.; GALIĆ, V.; MAZUR, M.; ŠIMIĆ, D. Effects of excess cadmium in soil on JIP-test parameters, hydrogen peroxide content and antioxidant activity in two maize inbreds and their hybrid. **Photosynthetica**, v. 55, n. 1–10, 2017.

GIAMPAOLI, P.; TRESMONDI, F.; LIMA, G.P.P.; KANASHIRO, S.; ALVES, E.S.; DOMINGOS, E.; TAVARES, A.R. Analysis of tolerance to copper and zinc in *Aechmea blanchetiana* grown *in vitro*. **Biologia Plantarum**, v. 56, p. 83–88, 2012.

GIAMPAOLI, P.; WANNAZ, E.D.; TAVARES, A.R.; DOMINGOS, M. Suitability of *Tillandsia usneoides* and *Aechmea fasciata* for biomonitoring toxic elements under tropical seasonal climate. **Chemosphere**, v. 149, p. 14-23, 2016.

GOMES, J.M.L.; SILVA, N.N.F. Bromeliaceae das restingas do Estado do Espirito Santo, Brasil. **Natureza online,** v. 11, n. 2, p. 79-89, 2013.

GOLTSEV, V.N.; KALAJI, H.M.; PAUNOV, M.; BĄBA, W.; HORACZEK, T.; MOJSKI, J.; KOCIEL, H.; ALLAKHVERDIEV, S.I. Variable chlorophyll fluorescence and its use for assessing physiological condition of plant photosynthetic apparatus. **Russian Journal of Plant Physiology**, v. 63, p. 869-893, 2016.

GÓMEZ-MERINO, F.C.; TREJO-TÉLLEZ, L.I. The role of beneficial elements in triggering adaptive responses to environmental stressors and improving plant performance. In: Vats S, ed. *Biotic and Abiotic Stress Tolerance in Plants*. Singapore: **Springer Nature**, p. 137-172, 2018.

GUNTZER, F.; KELLER, C.; MEUNIER, J.D. Benefits of silicon for crops: a review. **Agronomy for Sustainable Development,** v. 32, n. 1, p. 201-213, 2012.

HAFEZ, E.M.; OSMAN, H.S.; EL-RAZEK, U.A.A.; ELBAGORY, M.; OMARA, A.E.-D.; EID, M.A.; GOWAYED, S.M. Foliar-Applied Potassium Silicate Coupled with Plant

Growth-Promoting Rhizobacteria Improves Growth, Physiology, Nutrient Uptake and Productivity of Faba Bean (*Vicia faba* L.) Irrigated with Saline Water in Salt-Affected Soil. **Plants**, v. 10, n. 5, p. 894, 2021.

HARTER, L.S.H.; HARTER, F.S.; DEUNER, C.; MENEGHELLO, G.E.; VILLELA, F.A. Effect of salinity on physiological performance of mogango seeds and seedlings. **Horticultura Brasileira**, v. 32, p. 80-85, 2014.

HARUTA, M.; SUSSMAN, M.R. Chapter ten-ligand receptor-mediated regulation of growth in plants. **Current Topics in Developmental Biology**, v. 123, p. 331–363, 2017.

HNILIČKOVÁ, H.; HNILIČKA, F.; ORSÁK, M.; HEJNÁK, V. Effect of salt stress on growth, electrolyte leakage, Na^+ and K^+ content in selected plant species. **Plant, Soil and Environmental**, v. 65, p. 90–96, 2019.

HU, A.Y.; CHE, J.; SHAO, J.F.; YOKOSHO, K.; ZHAO, X.Q.; SHEN, R.F.; MA, J.F. Silicon accumulated in the shoots results in down-regulation of phosphorus transporter gene expression and decrease of phosphorus uptake in rice. **Plant and Soil**, v. 423, n. 1-2, p. 317–325, 2018.

ISMAEL, M.A.; ELYAMINE, A.M.; MOUSSA, M.G.; CAI, M.; ZHAO, X.; HU, C. Cadmium in plants: uptake, toxicity, and its interactions with selenium fertilizers. **Metall**, v. 11, p. 255-277, 2019.

JAVED, R.; GUREL, E. Salt stress by NaCl alters the physiology and biochemistry of tissue culture-grown *Stevia rebaudiana* Bertoni. **Turkish Journal of Agriculture and Forestry**, v. 43, p. 11-20, 2019.

KALAJI, H.M.; JAJOO, A.; OUKARROUM, A.; BRESTIC, M.; ZIVCAK, M.; SAMBORSKA, I.A.; CETNER, M.D.; ŁUKASIK, I.; GOLTSEV, V.; LADLE, R.J. Chlorophyll *a* fluorescence as a tool to monitor physiological status of plants under abiotic stress conditions. **Acta Physiologiae Plantarum**, v. 4, n. 1-11, p. 38-102, 2016.

KALAJI, M.H.; GOLTSEV, V.N.; ZUK-GOŁASZEWSKA, K.; ZIVCAK, M.; BRESTIC, M. **Chlorophyll Fluorescence: Understanding Crop Performance— Basics and Applications**. CRC Press, T&F Group, Abingdon, UK; p. 240, 2017a.

KALAJI, M.H.; SCHANSKER, G.; BRESTIC, M.; BUSSOTTI, F.; CALATAYUD, A.; FERRONI, L.; GOLTSEV, V.; GUIDI, L.; JAJOO, A.; LI, P. et al. Frequently asked questions about chlorophyll fluorescence, the sequel. **Photosynthesis Research,** v. 132, p. 13–66, 2017b.

KALAJI, H.M.; RASTOGI, A.; ŽIVČAK, M. et al. Prompt chlorophyll fluorescence as a tool for crop phenotyping: an example of barley landraces exposed to various abiotic stress factors. **Photosynthetica**, n. 56, p. 953–961, 2018.

KAMRAN, M.; PARVEEN, A.; AHMAR, S.; MALIK, Z.; HUSSAIN, S.; CHATTHA, M.S.; SALEEM, M.H.; ADIL, M.; HEIDARI, P.; CHEN, J.-T. An overview of hazardous impacts of soil salinity in crops, tolerance mechanisms, and amelioration through selenium supplementation. **International Journal of Molecular Sciences**, v. 21, p. 148, 2020.

KAYA, C.; ASHRAF, M.; ALYEMEN, M.N.; AHMAD, P. Responses of nitric oxide and hydrogen sulfide in regulating oxidative defence system in wheat plants grown under cadmium stress. **Physiologia Plantarum**, v. 168, p. 345–360, 2020.

KIM, Y.H.; KHAN, A.L.; AND LEE, I.J. Silicon: a duo synergy for regulating crop growth and hormonal signaling under abiotic stress conditions. **Critical Reviews in Biotechnology**, v. 36, p. 1099–1109, 2016.

KIM, Y.H.; KHAN, A.L.; WAQAS, M.; AND LEE, I.J. Silicon regulates antioxidant activities of crop plants under abiotic-induced oxidative stress: A review. **Frontiers in Plant Science**, v. 8, p. 510, 2017.

LAWLOR, D.W. Genetic engineering to improve plant performance under drought: physiological evaluation of achievements, limitations, and possibilities. **Journal of Experimental Botany**, v. 64, p. 83-108, 2013.

KIM, B.; LEE, H.; SONG, Y.H.; KIM, H. Effect of salt stress on the growth, mineral contents, and metabolite profiles of spinach. **Journal of the Science of Food and Agriculture**, n. 101, p. 3787-3794, 2021.

LEMBRECHTS, R.; CEUSTERS, N.; DE PROFT, M.; CEUSTERS, J. Sugar and starch dynamics in the medium-root-leaf system indicate possibilities to optimize plant tissue culture. **Scientia Horticulturae**, v. 224, p. 226-231, 2017.

LIANG, X.; WANG, H.; HU, Y.; MAO, L.; SUN, L.; DONG, T.; NAN, W.; BI, Y. Silicon does not mitigate cell death in cultured tobacco BY-2 cells subjected to salinity without ethylene emission. **Plant Cell Reports**, v. 34, p. 331–343, 2015.

LIU, P.; YIN, L.; DENG, X.; WANG, S.; TANAKA, K.; ZHANG, S. Aquaporin-mediated increase in root hydraulic conductance is involved in silicon-induced improved root water uptake under osmotic stress in *Sorghum bicolor* L. **Journal of Experimental Botany**, v. 65, p. 4747–4756, 2014.

LIU, B.; SOUNDARARAJAN, P.; MANIVANNA, A. Mechanisms of Silicon-Mediated Amelioration of Salt Stress in Plants. **Plants**, v. 8, n. 9, p. 307, 2019.

LOTFI, R.; KALAJI, H.M.; VALIZADEH, G.R.; KHALILVAND BEHROZYAR, E.; HEMATI, A.; GHARAVI-KOCHEBAGH, P.; GHASSEMI, A. Effects of humic acid on photosynthetic efficiency of rapeseed plants growing under different watering conditions**. Photosynthetica**, v. 56, p. 962-970, 2018.

MACKOVÁ, H.; HRONKOVÁ, M.; DOBRÁ, J.; TUREČKOVÁ. V.; NOVÁK, O.; LUBOVSKÁ, Z.; MOTYKA, V.; HAISEL, D.; HÁJEK, T.; PRÁŠIL, I.T.; GAUDINOVÁ, A.; ŠTORCHOVÁ, H.; GE, E.; WERNER, T.; SCHMÜLLING, T.; VANKOVÁ, R. Enhanced drought and heat stress tolerance of tobacco plants with ectopically enhanced cytokinin oxidase/dehydrogenase gene expression. **Journal of Experimental Botany**, v. 64, p. 2805–2815, 2013.

MALČOVSKÁ SM, DUČAIOVÁ Z, MASLAŇÁKOVÁ I, BAČKOR M. Effect of silicon on growth, photosynthesis, oxidative status and phenolic compounds of maize (*Zea mays* L.) grown in cadmium excess. **Water, Air, & Soil Pollution**, v. 225, p. 2056, 2014.

MANIVANNAN, A.; AHN, Y.K. Silicon regulates potential genes involved in major physiological processes in plants to combat stress. **Frontiers in Plant Science**, n. 8, p. 1346, 2017.

MANQUIÁN-CERDA, K.; ESCUDEY, M.; ZÚÑIGA, G.; ARANCIBIA-MIRANDA, N.; MOLINA, M.; CRUCES, E. Effect of cadmium on phenolic compounds, antioxidant enzyme activity and oxidative stress in blueberry (*Vaccinium corymbosum* L.) plantlets grown in vitro. **Ecotoxicology and Environmental Safety**, v. 133, p. 316–326, 2016.

MANTOVANI, C.; PIVETTA, K.F.L.; DE MELLO PRADO, R.; DE SOUZA, J.P.; NASCIMENTO, C.S.; NASCIMENTO, C.S.; GRATÃO, P.L. Silicon toxicity induced by different concentrations and sources added to in vitro culture of epiphytic orchids. **Scientia Horticulturae**, v. 265, p. 109272, 2020.

MARTINS, J.P.R.; SCHIMILDT, E.R.; ALEXANDRE, R.S.; CASTRO, E.M.; NANI, T.F.; PIRES, M.F.; PASQUAL, M. Direct organogenesis and leaf-anatomy modifications *in vitro* of *Neoregelia concentrica* (Vellozo) L.B. Smith (Bromeliaceae). **Pakistan Journal of Botany**, v. 46, p. 2179-2187, 2014.

MARTINS, J.P.R.; MARTINS, A.D.; PIRES, M.F.; JUNIOR, R.A.B.; REIS, R.O.; DIAS, G.D.M.G.; PASQUAL, M. Anatomical and physiological responses of *Billbergia zebrina* (Bromeliaceae) to copper excess in a controlled microenvironment. **Plant Cell, Tissue and Organ Culture**, v. 126, n. 1, p. 43–57, 2016.

MARTINS, A.D.; MARTINS, J.P.R.; BATISTA, L.A.; DIAS, G.M.G.; ALMEIDA, M.O.; PASQUAL, M.; SANTOS, H.O. Morpho-physiological changes in *Billbergia zebrina* due to the use of silicates *in vitro*. **Anais da Academia Brasileira de Ciências**, v. 90, p. 3449–3462, 2018.

MARTINS, J.P.R.; RODRIGUES, L,C,A.; SILVA, T.S.; SANTOS, E.R.; FALQUETO, A.R.; GONTIJO, A.B.P.L. Sources and concentrations of silicon modulate the physiological and anatomical responses of *Aechmea blanchetiana* (Bromeliaceae) during *in vitro* culture. **Plant Cell, Tissue and Organ Culture**, v. 137, p. 397-410, 2019.

MARTINS, J.P.R.; RODRIGUES, L.C.A.; SILVA, T.S.; ROSSINI, F.P.; GONTIJO, A.B.P.L.; FALQUETO, A.R. Morphophysiological responses of *Aechmea blanchetiana* (Bromeliaceae) to excess copper during *in vitro* culture. **Plant Biosystems - An International Journal Dealing with all Aspects of Plant Biology**, v. 155, n. 3, p. 447-456, 2020a.

MARTINS, J.P.R.; SOUZA, A.F.C.; RODRIGUES, L.C.A.; BRAGA, P.C.S.; GONTIJO, A.B.P.L.; FALQUETO, A.R. Zinc and selenium as modulating factors of the anatomy and physiology of *Billbergia zebrina* (Bromeliaceae) during *in vitro* culture. **Photosynthetica**, v. 58, n. 5, p. 1068-1077, 2020b.

MARTINS, J.P.R.; RODRIGUES, L.C.A.; SANTOS, T.S.; GONTIJO, A.B.P.L.; FALQUETO, A.R. Modulation of the anatomical and physiological responses of *in vitro* grown *Alcantarea imperialis* induced by NAA and residual effects of BAP. **Ornamental Horticulture**, v. 26, p. 283-297, 2020c.

MORTON, M.J.L.; AWLIA, M.; AL-TAMIMI, N.; SAADE, S.; PAILLES, Y.; NEGRÃO, S.; TESTER, M. Salt stress under the scalpel–dissecting the genetics of salt tolerance. **The Plant Journal**, v. 97, p. 148–163, 2019.

NAHAR, K.; RAHMAN, M.; HASANUZZAMAN, M.; ALAM MM, R.A.; SUZUKI, T.; FUJITA, M. Physiological and biochemical mechanisms of spermine-induced cadmium stress tolerance in mung bean (*Vigna radiata* L.) seedlings. **Environmental Science and Pollution Research**, v. 23, n. 21, p. 21206–21218, 2016.

NEDUKHA, O.M. The role of silicon in plant under normal conditions and stress. **Notulae Scientia Biologicae**, v. 14, n. 1, p. 10973, 2022.

NEGRÃO, S.; SCHMÖCKEL, S.M.; TESTER, M. Evaluating physiological responses of plants to salinity stress. **Annals of Botany**, v. 119, p. 1–11, 2017.

OLIVEIRA, J.P.V.; PEREIRA, M.P.; DUARTE, V.P.; CORRÊA, F.F.; CASTRO, E.M.; PEREIRA, F.J. Cadmium tolerance of *Typha domingensis* Pers. (Typhaceae) as related to growth and leaf morphophysiology. **Brazilian Journal of Biology**, v. 78, n. 3, p. 509–516, 2017.

PAEZ-GARCIA, A.; MOTES, C.M; SCHEIBLE, W.; CHEN, R.; BLANCAFLOR, E.B.; MONTEROS, M.J. Root traits and phenotyping strategies for plant improvement. **Plants**, v. 4, p. 334–355, 2015.

PANDEY, M.; CHIKARA, S.K. Effect of salinity and drought stress on growth parameters, glycoside content and expression level of vital genes in steviol glycosides biosynthesis pathway of *Stevia rebaudiana* (Bertoni). **International Journal of Genetics and Genomics,** v. 7, p. 153-160, 2015.

PAUNOV, M.; KOLEVA, L.; VASSILEV, A.; VANGRONSVELD, J.; GOLTSEV, V. Effects of different metals on photosynthesis: cadmium and zinc affect chlorophyll fluorescence in durum wheat. **International Journal of Molecular Sciences,** v. 19, p. 787, 2018.

PIAZZETTA, K.D.; RAMSDORF, W.A.; MARANHO, L.T. Use of airplant *Tillandsia recurvata* L., Bromeliaceae, as biomonitor of urban air pollution. **Aerobiologia**, v. 35, n. 1, p. 125-137, 2018.

QIN, X.; NIE, Z.; LIU, H.; ZHAO, P.; QIN, S.; SHI, Z. Influence of selenium on root morphology and photosynthetic characteristics of winter wheat under cádmium stress. **Environmental and Experimental Botany**, v. 150, p. 232-239, 2018.

LIU, J.; HOU, H.; ZHAO, L.; SUN, Z.; LI, H. Protective Effect of foliar application of sulfur on photosynthesis and antioxidative defense system of rice under the stress of Cd. **Science of The Total Environment**, v. 710, p. 136230, 2020.

REHMAN, S.; ABBAS, G.; SHAHID, M.; SAQIB, M.; FAROOQ, A.B.U.; HUSSAIN, M.; MURTAZA, B.; AMJAD, M.; NAEEM, M.A.; FAROOQ, A. Effect of salinity on cádmium tolerance, ionic homeostasis and oxidative stress responses in conocarpus exposed to cadmium stress: implications for phytoremediation. **Ecotoxicology and Environmental Safety**, v.171, p. 146-153, 2019.

REN, M.; QIN, Z.; LI, X.; WANG, L.; WANG, Y.; ZHANG, J.; HUANG, Y.; YANG, S. Selenite antagonizes the phytotoxicity of Cd in the cattail Typha angustifolia. **Ecotoxicology and Environmental Safety**, v. 189, p. 109959, 2020.

REZENDE, R.A.L.S.; RODRIGUES, F.A.; SOARES, J.D.R.; SILVEIRA, H.R.O.; PASQUAL, M.; DIAS, G.M.G. Salt stress and exogenous silicon influence physiological and anatomical features of *in vitro*-grown cape gooseberry. **Ciência Rural,** v. 48, p. 1, 2018.

RIAZ, M.; YAN, L.; WU, X.; HUSSAIN, S.; AZIZ, O.; WANG, Y.; IMRAN, M.; JIANG, C. Boron alleviates the aluminum toxicity in trifoliate orange by regulating antioxidante defense system and reducing root cell injury. **Journal of Environmental Management,** v. 208, p. 149-158, 2018.

RIAZ, M.; KAMRAN, M.; RIZWAN, M.; ALI, S.; PARVEEN, A.; MALIK, Z.; WANG, X. Cadmium uptake and translocation: selenium and silicon roles in Cd detoxification for the production of low Cd crops: a critical review. **Chemosphere***,* v. 273, p. 129690, 2021.

RIOS, J.J.; MARTÍNEZ-BALLESTA, M.C.; RUIZ, J.M.; BLASCO, B.; CARVAJAL, M. Silicon- mediated improvement in plant salinity tolerance: The role of aquaporins. **Frontiers in Plant Science**, n. 8, p. 948, 2017.

RIZWAN, M.; ALI, S.; ADREES, M.; RIZVI, H.; ZIA-UR-REHMAN, M.; HANNAN, F.; QAYYUM, M.F.; HAFEEZ, F.; OK, Y.S. Cadmium stress in rice: toxic effects, tolerance mechanisms, and management: a critical review. **Environmental Science and Pollution Research**, v. 23, p. 17859-17879, 2016.

RIZWAN, M.; ALI, S.; UR REHMAN, M.Z.; RINKLEBE, J.; TSANG, D.C.; BASHIR, A.; MAQBOOL, A.; TACK, F.; OK, Y.S. Cadmium phytoremediation potential of *Brassica crop* species: a review. **Science of The Total Environmental**, v. 631, p. 1175-1191, 2018.

RIZWAN, M.; ALI, S.; REHMAN, M. Z.; MALIK, S.; ADREES, M.; QAYYUM, M. F.; et al. Effect of foliar applications of silicon and titanium dioxide nanoparticles on growth, oxidative stress, and cadmium accumulation by rice (*Oryza sativa*). **Acta Physiologiae Plantarum**, v. 41, n. 3, p. 35, 2019.

RODRIGUES, L.C.A.; MARTINS, J.P.R.; ALMEIDA JÚNIOR, O.; GUILHERME, L.R.G.; PASQUAL, M.; CASTRO, E.M. Tolerance and potential for bioaccumulation of *Alternanthera tenella Colla* to cadmium under *in vitro* conditions. **Plant Cell, Tissue and Organ Culture**, v. 130, n. 3, p. 507–519, 2017.

ROSA, W.S.; MARTINS, J.P.R.; RODRIGUES, E.S.; RODRIGUES, L.C.A.; GONTIJO, A.B.P.L.; FALQUETO, A,R. Photosynthetic apparatus performance in function of the cytokinins used during the *in vitro* multiplication of *Aechmea blanchetiana* (Bromeliaceae). **Plant Cell, Tissue and Organ Culture,** v. 133, p. 339-350, 2018.

SANTA-ROSA, S.; SOUZA, F.V.D.; VIDAL, Á.M.; LEDO, C.A.S.; SANTANA, J.R.F. Micropropagação das bromélias ornamentais vulneráveis *Aechmea blanchetiana* e *Aechmea distichantha*. **Horticultura Brasileira**, v. 31, n.1, p. 112-118, 2013.

SAHEBI, M.; HANAFI, M.M.; PARISA, A. Application of silicon in plant tissue culture. **In Vitro Cellular & Developmental Biology – Plant**, n. 52, p. 226–232, 2016.

SCHRECK, E.; SARRET, G.; OLIVA, P.; CALAS, A.; SOBANSKA, S.; GUÉDRON, S.; BARRAZA, F.; POINT, D.; HUAYTA, C.; COUTURE, R.M.; PRUNIER, J.; HENRY, M.; TISSERAND, D.; GOIX, S.; CHINCHEROS, J.; UZU, G. Is *Tillandsia capillaris* an efficient bioindicator of atmospheric metal and metalloid deposition? Insights from five months of monitoring in an urban mining area. **Ecological Indicators**, v. 67, p. 227–237, 2016.

SEPEHRI, A.; GHAREHBAGHLI, N. Selenium alleviate cadmium toxicity by improving nutrient uptake, antioxidative and photosynthetic responses of garlic. **Russian Journal of Plant Physiology**, v. 66, p. 152-159, 2019.

SHAHID, M.A.; BALAL, R.M.; KHAN, N.; ZOTARELLI, L.; LIU, G.D.; SARKHOSH, A.; FERNANDEZ-ZAPATA, J.C.; NICOLAS, J.J.M.; GARCIA-SANCHEZ, F. Selenium impedes cadmium and arsenic toxicity in potato by modulating carbohydrate and nitrogen metabolism. **Ecotoxicology and Environmental Safety,** v. 180, p. 588-599, 2019.

SHI, Y.; ZHANG, Y.; YAO, H.; WU, J.; SUN, H.; GONG, H. Silicon improves seed germination and alleviates oxidative stress of bud seedlings in tomato under water deficit stress. **Plant Physiology and Biochemistry**, v. 78, p. 27–36, 2014.

SIL, P.; DAS, P.; BISWAS, S.; MAZUMDAR, A.; BISWAS, A.K. Modulation of photosynthetic parameters, sugar metabolism, polyamine and ion contents by silicon amendments in wheat *(Triticum aestivum L.)* seedlings exposed to arsenic. **Environmental Science and Pollution Research**, v. 26, n. 13, p. 13630-13648, 2019.

SILVA, C.S.; ARAÚJO, L.G.; SOUSA, K.C.I.; SILVA, D.M.; SIBOV, S.T.; FARIA, P.R. *In vitro* germination and development of the Cerrado epiphytic orchid. **Ornamental Horticulture,** v. 23, p. 96-100, 2017.

SIMÃO, M.J.; FONSECA, E.; GARCIA, R., MANSUR, E.; PACHECO, G. Effects of auxins and different culture systems on the adventitious root development of *Passiflora pohlii* Mast. and their ability to produce antioxidant compounds. **Plant Cell, Tissue and Organ Culture**, v. 124, p. 419-430, 2016.

SIVANESAN, I.; JEONG, B.R. Silicon promotes adventitious shoot regeneration and enhances salinity tolerance of *Ajuga multiflora* Bunge by altering activity of antioxidant enzyme. **The Scientific World Journal**, v. 2014, p. 1-10, 2014.

SIVANESAN, I.; PARK, S.W. The role of silicon in plant tissue culture. **Frontiers in Plant Science**, v. 5, p. 571, 2014.

SOARES, J.D.R.; PASQUAL, M.; RODRIGUES, F.A., VILLA, F., ARAUJO, A.G.D., Silicon sources in the micropropagation of the Cattleya group orchid. **Acta Scientiarum Agronomy,** v. 33, p. 503–507, 2011.

SON, J.A.; NARAYANANKUTTY, D.P.; ROH, K.S. Influence of exogenous application of glutathione on rubisco and rubisco activase in heavy metal-stressed tobacco plant grown in vitro. **Saudi Journal of Biological Sciences**, v. 21, p. 89–97, 2014.

SONG, A.; NING, D.; FAN, F.; LI, Z.; PROVANCE-BOWLEY, M.; LIANG, Y. The potential for carbon bio-sequestration in China's paddy rice (*Oryza sativa* L.) as impacted by slag-based silicate fertilizer. **Scientific Reports**, v. 5, p. 17354, 2015.

SOUZA, T.V.; THIESEN, J.F.; GUERRA, M.P.; SANTOS, M. Morpho-and histodifferentiation of shoot regeneration of *Billbergia zebrina* (Helbert) Lindley nodular cultures. **Plant Cell, Tissue and Organ Culture**, v. 127, p. 393–403, 2016.

SOUZA, J.C.; RESCAROLLI, C.L.S.; NUNEZ, C.V. Produção de metabólitos secundários por meio da cultura de tecidos vegetais. **Revista Fitos**, Rio de Janeiro, v. 12, n. 3, p. 269-280, 2018.

SOUNDARARAJAN, P.; MANIVANNAN, A.; KO, C.H.; JEONG, B.R. Silicon Enhanced Redox Homeostasis and Protein Expression to Mitigate the Salinity Stress in *Rosa hybrida* 'Rock Fire'. **Plant Growth Regulators**, v. 37, p. 16–34, 2018.

STIRBET, A.; LAZÁR, D.; KROMDIJK, J. Chlorophyll *a* fluorescence induction: Can just a one-second measurement be used to quantify abiotic stress responses? **Photosynthetica**, v. 56, n. 1, p. 86-104, 2018.

STOLÁRIKOVÁ-VACULÍKOVÁ, M.; ROMEO, S.; MINNOCCI, A.; LUXOVÁ, M.; VACULÍK, M.; LUX, A.; SEBASTIANI, L. Anatomical, biochemical and morphological

responses of poplar *Populus deltoides* clone Lux to Zn excess. **Env Exp Bot**, v. 109, p. 235–243, 2015.

TERMIGNONE, R.R. **Cultura de Tecidos Vegetais**. Editora da UFRGS, Porto Alegre, 182p. ISBN: 85- 7025-810-0, 2012.

TREJO-TÉLLEZ, L.I.; GARCÍA-JIMÉNEZ, A.; ESCOBAR-SEPÚLVEDA, H.F.; RAMÍREZ-OLVERA, S.M.; BELLO-BELLO, J.J.; GÓMEZ-MERINO, F.C. Silicon induces hormetic dose-response effects on growth and concentrations of chlorophylls, amino acids and sugars in pepper plants during the early developmental stage. **PeerJ** 8:e9224, 2020.

TRIPATHI, D.K.; SINGH, V.P.; PRASAD, S.M.; CHAUHAN, D.K.; AND DUBEY, N.K. Silicon nanoparticles (SiNp) alleviate chromium (VI) phytotoxicity in *Pisum sativum* (L.) seedlings. **Plant Physiology and Biochemistry**, v. 96, p. 189–198, 2015.

YAO, J.; SUN, D.; CEN, H.; XU, H.; WENG, H.; YUAN, F.; HE, Y. Phenotyping of Arabidopsis drought stress response using Kinetic Chlorophyll Fluorescence and Multicolor Fluorescence Imaging. **Frontiers in Plant Science,** v. 9, p. 603, 2018.

YAN, L.; RIAZ, M.; WU, X.; DU, C.; LIU, Y.; JIANG, C. Ameliorative effects of boron on aluminum induced variations of cell wall cellulose and pectin components in trifoliate orange (*Poncirus trifoliate* (L.) Raf.) rootstock. **Environmental Pollution**, v. 240, p. 764-774, 2018.

YIN, L.; WANG, S.; TANAKA, K.; FUJIHARA, S.; ITAI, A.; DEN, X.; ZHANG, S. Silicon-mediated changes in polyamines participate in silicon-induced salt tolerance in *Sorghum bicolor* L. **Plant, Cell & Environment**, v. 39, p. 245–258, 2016.

YOUNIS, U.; MALIK, S.A.; RIZWAN, M.; QAYYUM, M.F.; OK, Y.S.; SHAH, M.H.R.; REHMAN, R.A.; AHMAD, N. Biochar enhances the cadmium tolerance in spinach (*Spinacia oleracea*) through modification of Cd uptake and physiological and biochemical attributes. **Environmental Science and Pollution Research,** v. 23, n. 21, p. 21385–21394, 2016.

WU, J.; GUO, J.; HU, Y.; GONG, H. Distinct physiological responses of tomato and cucumber plants in silicon-mediated alleviation of cadmium stress. **Frontiers in Plant Science,** n. 6, p. 453, 2015.

ZHANG, Y.; LIANG, Y.; ZHAO, X.; JIN, X.; HOU, L.; SHI, Y.; AHAMMED, G.J. Silicon Compensates Phosphorus Deficit-Induced Growth Inhibition by Improving Photosynthetic Capacity, Antioxidant Potential, and Nutrient Homeostasis in Tomato. **Agronomy**, v. 9, n. 11, p. 733, 2019.

ZHAO, X.; BAI, X.; JIANG, C.; LI, Z. Phosphoproteomic Analysis of Two Contrasting Maize Inbred Lines Provides Insights into the Mechanism of Salt-Stress Tolerance. **International Journal of Molecular Sciences**, v. 20, p. 1886, 2019.

ZHU, Y.X.; GONG, H.J.; YIN, J.L. Role of Silicon in Mediating Salt Tolerance in Plants: A Review. **Plants**, v. 8, p. 147, 2019.

ZUREK, G.; RYBKA, K.; POGRZEBA, M.; KRZY ZAK, J.; PROKOPIUK, K. Chlorophyll *a* Fluorescence in Evaluation of the Effect of Heavy Metal Soil Contamination on Perennial Grasses. **PLoS ONE**, v. 9, n. 3, e91475, 2014.

ZUSHI, K.; MATSUZOE, N. Using of chlorophyll a fluorescence OJIP transients for sensing salt stress in the leaves and fruits of tomato. **Scientia Horticulturae**, v. 219, p. 216–221, 2017.

CAPÍTULO 1

Silício induz incremento na eficiência fotoquímica efetiva e no crescimento de *Aechmea blanchetiana* (BROMELIACEAE) cultivadas *in vitro*

Resumo

Fontes de silício (Si) têm especificidades que podem beneficiar o crescimento de plantas cultivadas *in vitro* e amenizar estresses. Ainda não são totalmente compreendidos como fontes e concentrações afetam o transporte de elétrons e o desempenho efetivo do aparato fotossintético de plantas *in vitro*. O objetivo desse estudo foi analisar a influência de diferentes fontes e concentrações de Si nas respostas anatômicas e na atividade fotoquímica efetiva do fotossistema II (FSII) de *Aechmea blanchetiana in vitro*. Brotos laterais de plantas previamente estabelecidas *in vitro* foram extraídos e transferidos para meio de cultura. Meios sem Si foram usados como controle. Os tratamentos consistiram em silicato de cálcio ($CaSiO_3$), silicato de potássio (K_2O_3Si) e silicato de magnésio (MgO_3Si) em três concentrações (8, 16, 32 μM). Após 45 dias de cultivo, foram realizadas análises anatômicas e fisiológicas. A presença de Si independente da fonte e concentração aumentou o diâmetro dos vasos do xilema, área do floema e crescimento das plantas. Plantas com $CaSiO_3$ reduziram a espessura da epiderme, aumentaram a taxa de transporte de elétrons (ETR) e atividade fotoquímica efetiva do FSII (ΦPSII). Aumento no conteúdo de clorofila *a* e clorofila *total* foi verificado em plantas com MgO_3Si. A utilização do K_2O_3Si aumentou parâmetros de dissipação não-fotoquímica e reduziu ΦPSII. O estudo comprovou que o $CaSiO_3$ é a fonte de Si dentre as testadas que tem maior contribuição no aumento da atividade fotoquímica efetiva do FSII e do crescimento de plantas de *A. blanchetiana* cultivadas *in vitro*.

Palavras-chave: Silicato de potássio, Silicato de cálcio, Silicato de magnésio, Fluorescência Modulada, Fluorescência da clorofila *a*.

Abreviações: ΦPSII = Y(II) = Φ(II)- Rendimento quântico fotoquímico efetivo de FSII; ETR - Taxa de fluxo linear de elétrons; NPQ - Dissipação não-fotoquímica de fluorescência (*quenching* não-fotoquímico); qP - *Quenching* fotoquímico; qL – *Quenching* fotoquímico de fluorescência assumindo antenas interconectadas do FSII; qN - *Quenching* não-fotoquímico; ΦNPQ - Rendimento quântico de luz induzida (ΔpH e dependente de zeaxantina) a partir de dissipação não-fotoquímica de fluorescência; ΦNO - Rendimento quântico de dissipação de energia não regulada. F_V/F_M – Eficiência fotoquímica máxima do FSII.

Introdução

O silício (Si) é o segundo elemento mais abundante da crosta terrestre, que pode ser absorvido por plantas superiores por meio do solo, principalmente, na forma de ácido silícico (H_4SiO_4) (Zhang *et al.* 2019). É um elemento benéfico que promove o crescimento e o desenvolvimento de várias espécies vegetais (Sahebi *et al.* 2016; Hu *et al.* 2018). O Si pode atuar contribuindo no funcionamento do aparato fotossintético, no balanço nutricional, na estimulação de sistemas antioxidantes enzimáticos e não enzimáticos, na resistência mecânica, o que conferem estabilidade estrutural as células, especialmente sob condições de estresse (Khaliq *et al.* 2016; Tripathi *et al.* 2016; Manivannan *et al.* 2017). O Si aumenta a tolerância das plantas a uma ampla gama de estresses bióticos e abióticos, como patógenos vegetais, pragas, seca, salinidade, calor, frio, toxicidade de metais pesados e estresse nutricional (Duan *et al.* 2013; Sivanesan e Jeong 2014; Soundararajan *et al.* 2015; Martins *et al.* 2018; Hu *et al.* 2018; Cipriano *et al.* 2021).

O Si foi introduzido com sucesso no meio de cultura de bromélias como um elemento benéfico para o cultivo *in vitro*, melhorando as características morfológicas, anatômicas, fisiológicas e o crescimento das plantas *in vitro* (Martins *et al.* 2018; Martins *et al.* 2019; Cipriano *et al.* 2021). O uso de Si no cultivo *in vitro* pode elevar o teor de hemicelulose e lignina, estimulando a rigidez da parede celular e a sobrevivência das plantas na aclimatização (Camargo *et al.* 2007). O Si também pode aumentar o conteúdo de pigmentos fotossintéticos (Dias *et al.* 2017; Manivannan *et al.* 2017).

O Si pode ser adicionado ao meio de cultura a partir de diferentes fontes, que podem promover respostas diferenciadas nas plantas. Dentre essas fontes está o silicato de potássio (K_2O_3Si), silicato de cálcio ($CaSiO_3$) e o silicato de magnésio (MgO_3Si). Sob condições *in vitro* a inclusão de Si contribui com o potencial morfogenético dos tecidos vegetais (Sivanesan e Park 2014; Asmar *et al.* 2015; Sahebi *et al.* 2016; Rodrigues *et al.* 2017). Estudos demonstraram que o K_2O_3Si pode induzir o crescimento da parte aérea em comparação com o silicato de sódio ($NaSiO_3$) (Soares *et al.* 2011). O K_2O_3Si também pode estimular o comprimento da raiz, o crescimento vegetativo e a osmorregulação, podendo ainda contribuir com processos fisiológicos, como aumento de pigmentos de clorofila, movimento dos estômatos e equilíbrio iônico (Hafez *et al.* 2021). A aplicação de $CaSiO_3$ aumentou o potencial de indução de calos do arroz (Islam *et al.* 2005), desencadeou o enraizamento e promoveu maior espessura das folhas de banana (Asmar *et al.* 2015). A suplementação com $CaSiO_3$ elevou o conteúdo de pigmentos

fotossintéticos, o desempenho do aparato fotossintético e a massa fresca em plantas *in vitro* (Rodrigues *et al.* 2017; Martins *et al.* 2019; Cipriano *et al.* 2021). O MgO_3Si teve efeito na parte aérea das plantas e formação de raízes, além de desempenhar um papel importante no processo de fotossíntese (Sipahutar *et al.* 2021). Esses estudos enaltecem a necessidade de pesquisas voltadas para as especificidades de cada fonte de Si em plantas de *Aechmea blanchetiana.*

Técnicas de cultivo *in vitro* são amplamente utilizadas para a rápida multiplicação de muitas espécies de plantas, além de oferecer benefícios em estudos relacionados com a fisiologia vegetal (Giampaoli *et al.* 2012; Kalaji *et al.* 2018). Dentre os estudos fisiológicos, a técnica da fluorescência da clorofila baseada no pulso de amplitude modulada (PAM), é uma ferramenta que permite avaliar o desempenho efetivo do aparato fotossintético (Yao *et al.* 2018; Bhagooli *et al.* 2021). Da mesma forma, análises anatômicas também são úteis para verificar como as condições da cultura podem influenciar as plantas cultivadas *in vitro* (Rosa *et al.* 2018).

As fontes de Si têm especificidades que podem beneficiar o crescimento da planta. Este benefício é acompanhado por riscos de toxicidade que podem induzir danos para a fisiologia das plantas e ainda não são totalmente compreendidos (Mantovani *et al.* 2020). Em plantas de *Aechmea blanchetiana* (Baker) L.B. Smith (Bromeliaceae) já foi comprovado uma melhor eficiência fotoquímica potencial do FSII na presença de $CaSiO_3$ quando comparado ao silicato de sódio (Na_2SiO_3), que apresentou sintomas de estresse salino (Martins *et al.* 2019). Entretanto, considerando outras fontes de Si como K_2O_3Si e MgO_3Si, faz-se necessário compreender como estas fontes podem afetar a eficiência fotoquímica efetiva do FSII comparada ao $CaSiO_3$. Portanto, o objetivo desse estudo foi analisar a influência de diferentes fontes e concentrações de Si em respostas anatômicas e na atividade fotoquímica efetiva do FSII em plantas de *A. blanchetiana* em condições *in vitro*.

Material e Métodos

Material Vegetal e condições de cultivo *in vitro*

Plantas de *A. blanchetiana* foram previamente multiplicadas *in vitro* conforme descrito por Rosa *et al.* (2018). Brotos laterais de aproximadamente 2,5cm de comprimento de parte aérea foram transferidos para frascos de vidro contendo meio de cultura MS (Murashige e Skoog 1962) conforme descrito por Martins *et al.* (2018). Ao meio foram adicionados 30 g L^{-1} de sacarose e 4μM de Ácido 1-naftalenoacético e solidificado com 7 g L de ágar. As plantas cultivadas sem Si (0 μM Si) foram utilizadas como controle. Os tratamentos consistiram em

três fontes distintas de Si, o silicato de cálcio ($CaSiO_3$), silicato de potássio (K_2O_3Si) e silicato de magnésio (MgO_3Si) em três concentrações (8, 16 e 32 μM). O experimento consistiu em um total de dez tratamentos (3 fontes x 3 concentrações + controle). Essa etapa foi conduzida com dez frascos por tratamento, contendo cinco explantes por frasco. Os meios de cultura tiveram o pH ajustado para 5,8 antes da autoclavagem a 120ºC, por 20 minutos. O material vegetal foi mantido em uma sala de crescimento, por 45 dias, a 26 ± 2 °C e fotoperíodo de 16 h sob lâmpadas de LED (Luminaria LED Slim 36 W Bi-Volt 2800 lm).

Análise da anatomia foliar e radicular

Após os 45 dias de cultivo com as diferentes fontes e concentrações de Si foram realizadas as análises anatômicas utilizando seis plantas por tratamento. Estas foram coletadas ao acaso, fixadas por 72 horas em solução de FAA 50% (formaldeído, ácido acético e álcool 50% na proporção 0.5:0.5:9.0) e conservadas em etanol 70% (Johansen, 1940). As secções transversais das folhas e raízes, e as secções paradérmicas obtidas, foram clarificadas e coradas conforme descrito por Cipriano *et al.* (2021). As secções foram observadas em microscópio óptico (Bioval, L-2000AFlour) e a captura de imagens foi realizada com uma câmera digital acoplada (Leica EC3). As fotomicrografias foram analisadas usando o software UTHSCSA-Imagetool® versão 3.0 calibrado com régua microscópica. Para as secções transversais das folhas e das raízes, e as secções paradérmicas das folhas foram fotografadas duas secções por lâminas, em seis repetições diferentes por tratamento (n=6).

Para as raízes, foram mensurados o número de vasos de metaxilema, o diâmetro da raiz (μm), a espessura da parede celular da exoderme (μm) e da endoderme (μm). Para as folhas foram determinadas a densidade (0.01 mm^{-2}) e o tamanho (μm^2) de células epidérmicas estomáticas, a espessura do clorênquima (μm) e da face abaxial e adaxial da epiderme (μm), a área de esclerênquima (μm^2) e do floema (μm^2), bem como o número e o diâmetro de vasos do xilema (μm). A densidade estomática foi calculada contando o número de estômatos em uma área conhecida.

Conteúdo de pigmentos fotossintéticos

O conteúdo de clorofila *a* (Chl *a*), clorofila *b* (Chl *b*) e carotenóides (Car) foi quantificado por meio de fragmentos de dez amostras por tratamento (n=10) selecionadas aleatoriamente seguindo a metodologia descrita por Martins *et al.* (2019). A absorbância foi

medida usando um dispositivo Genesys ™ 10S UV-Vis espectrofotômetro (Thermo Fisher Scientific, West Palm Beach, FL, EUA), realizadas em λ = 470, 645 e 663 nm para Car, Chl *b* e Chl *a*, respectivamente. O conteúdo dos pigmentos foi calculado de acordo com método descrito por Arnon (1949) e Wellburn (1994) e expresso em μg g^{-1} FW (peso fresco).

Análise da fluorescência Modulada da Clorofila *a*

Análises da eficiência fotoquímica foram obtidas por meio de medições da Fluorescência Modulada da clorofila entre 8:00 h e 10:00 horas, utilizando a terceira folha totalmente expandida a partir da base da roseta em 15 plantas por tratamento (n=15). As medições foram realizadas com um fluorômetro portátil o MINI-PAM II (Heinz Walz GmbH, Effeltrich, Germany), seguindo a metodologia de Ögren e Baker (1985) e Schreiber (1986) Kramer *et al.* (2004), descrita em Cipriano et al. (2021b). Foram obtidas do relatório medidas dos parâmetros ΦPSII, ETR, qN, qP, qL, NPQ, ΦNPQ, ΦNO e F_V/F_M.

Análise de características de crescimento

Foram realizadas as medições da massa fresca total da planta (parte aérea + raiz) (g $planta^{-1}$). As amostras consistiram em 25 plantas no total por tratamento, com cinco repetição por tratamentos, de modo que cada repetição consistiu de 5 plantas (cinco repetições; n = 5).

Análise estatística

O delineamento experimental foi inteiramente casualizado em esquema fatorial 3 x 3: três fontes de Si ($CaSiO_3$, MgO_3Si e K_2O_3Si) e três concentrações das fontes (8, 16 e 32 μM) e com um tratamento controle adicional (0 μM). A comparação entre os tratamentos com Si e o controle foi realizado usando o teste de normalidade dos resíduos Shapiro-Wilk a 5% de probabilidade. Os dados obtidos foram submetidos a análise de variância (ANOVA) e as médias foram comparadas pelo teste de Tukey ($p<0.05$). Todas as análises e cálculos foram feitas com R CRAN versão 4.0.5 (R Core Team 2021). Para análise fatorial com tratamento adicional foi utilizado o pacote "ExpDes.pt" versão 1.2.2 (Ferreira *et al.* 2014). Para análises adicionais, foi realizada uma matriz de correlação. Matrizes de correlação foram criadas usando o método de Pearson no pacote corrplot da versão 0.84 R (Le *et al.* 2008; Wei e Simko 2017; Kassambara e Mundt 2020).

Resultados

Análise do controle (0 µM de Si) comparado aos demais tratamentos (fontes de Si)

A presença de Si independente da fonte e da concentração influenciou características anatômicas e o crescimento das plantas de *A. blanchetiana in vitro* (Figura 1). Em relação a anatomia da raiz, o Si reduziu o número de vasos do metaxilema e a espessura da parede celular da exoderme. O Si também reduziu a densidade estomática e aumentou o tamanho dos estômatos. Nas secções transversais das folhas, a presença de Si, aumentou a espessura do clorênquima, da área do esclerênquima, do diâmetro dos vasos do xilema, da área do floema e reduziu a espessura da epiderme adaxial. A presença de Si não alterou de forma significativa o conteúdo de pigmentos fotossintéticos e os parâmetros da fluorescência modulada. A presença de Si aumentou a massa fresca total da planta.

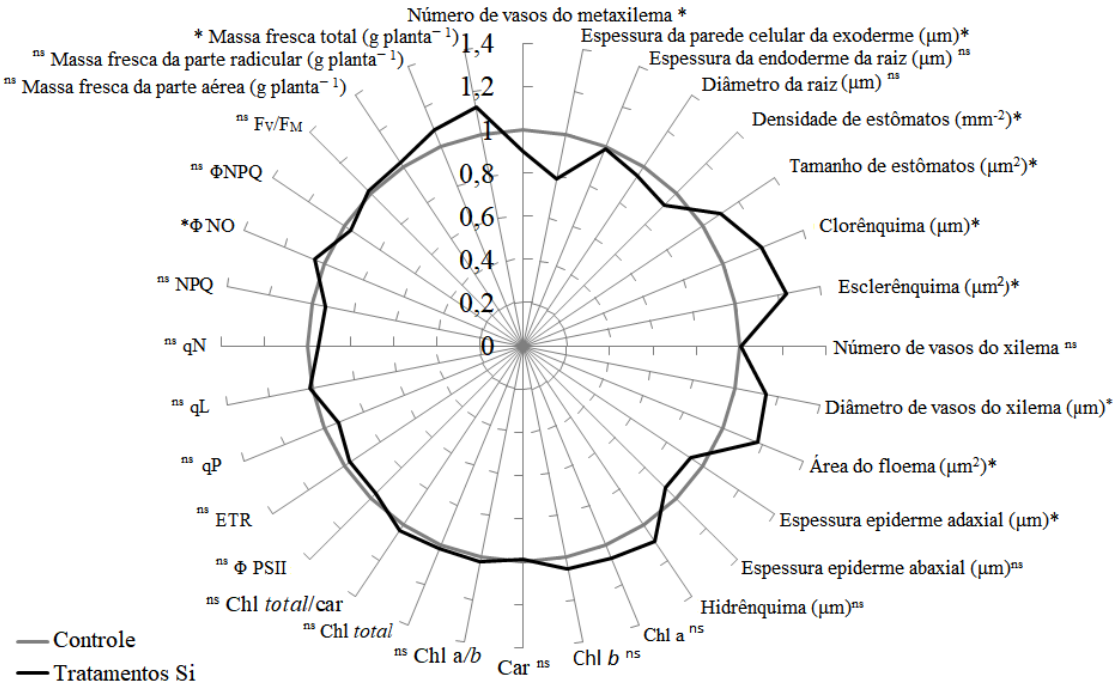

Figura 1 Análise do controle (0 µM de Si) comparado aos demais tratamentos com Si ($CaSiO_3$, MgO_3Si, K_2O_3Si). Médias (± erro padrão) seguidas por um asterisco (*) são significativamente diferentes de acordo com o teste de Tukey ($p<0.05$). ns – diferença não significativa. Os dados foram normalizados com o controle (0 µM Si) igual a 1.

Análise anatômica em função das fontes e concentrações de Si

Nas raízes foram verificadas diferenças significativas na espessura da parede da exoderme e no diâmetro, sendo influenciados apenas pelas fontes de Si (Figura 2; Figura 3). A espessura da parede da exoderme teve maiores médias na presença do $CaSiO_3$ e de MgO_3Si. O diâmetro das raízes aumentou na presença de $CaSiO_3$. O número de vasos de metaxilema da raiz não apresentou diferença entre os tratamentos (5,44 ± 0,15).

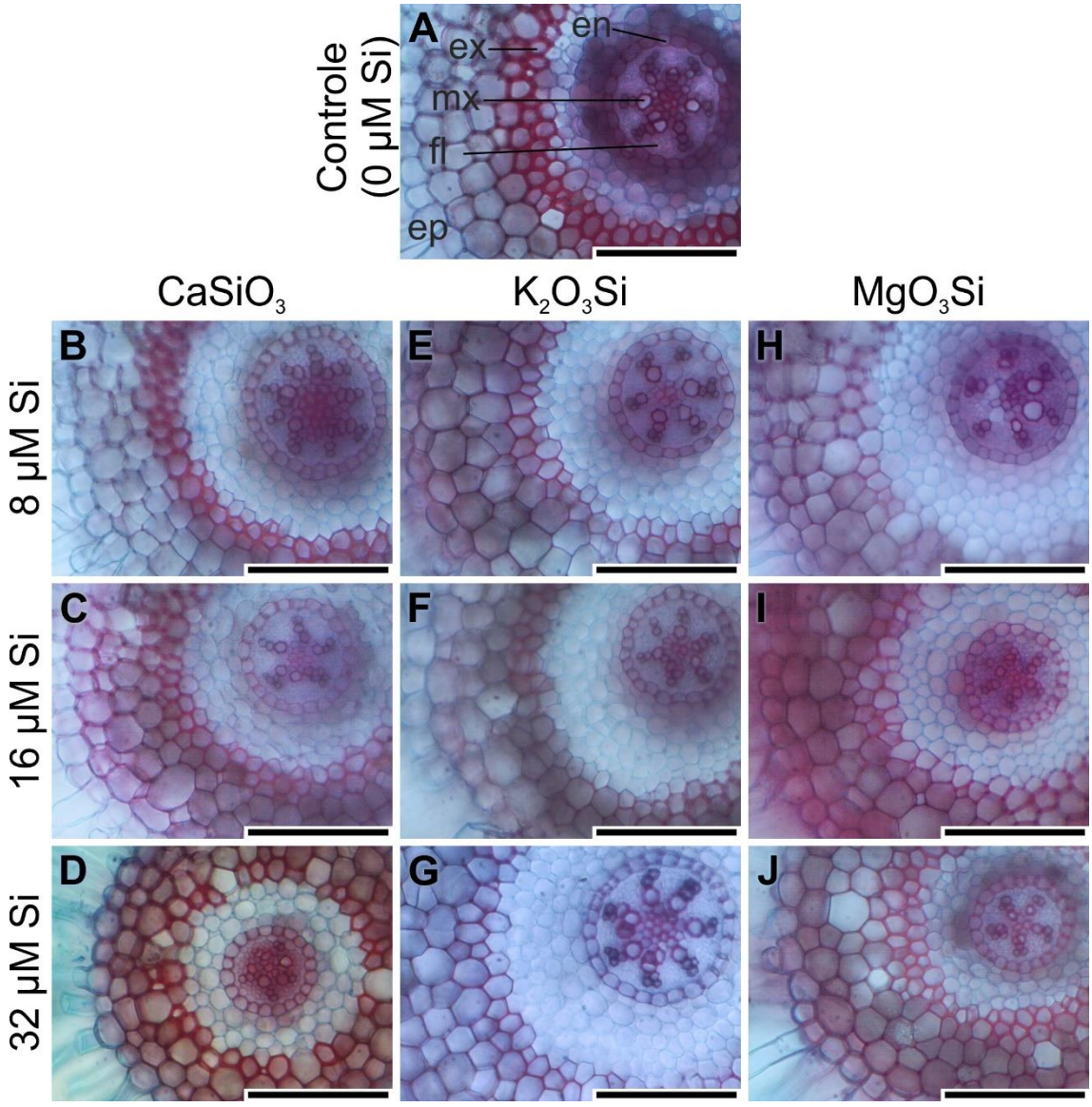

Figura 2 Cortes transversais de raízes de plantas de *Aechmea blanchetiana* cultivadas *in vitro* em função de diferentes fontes de Si ($CaSiO_3$, MgO_3Si, K_2O_3Si) e concentrações (8, 16 e 32 µM). A) Controle (0 µM Si). en-endoderme, ex-exoderme, ep- epiderme, mx- vasos de metaxilema, fl-floema. Barras = 100 µm

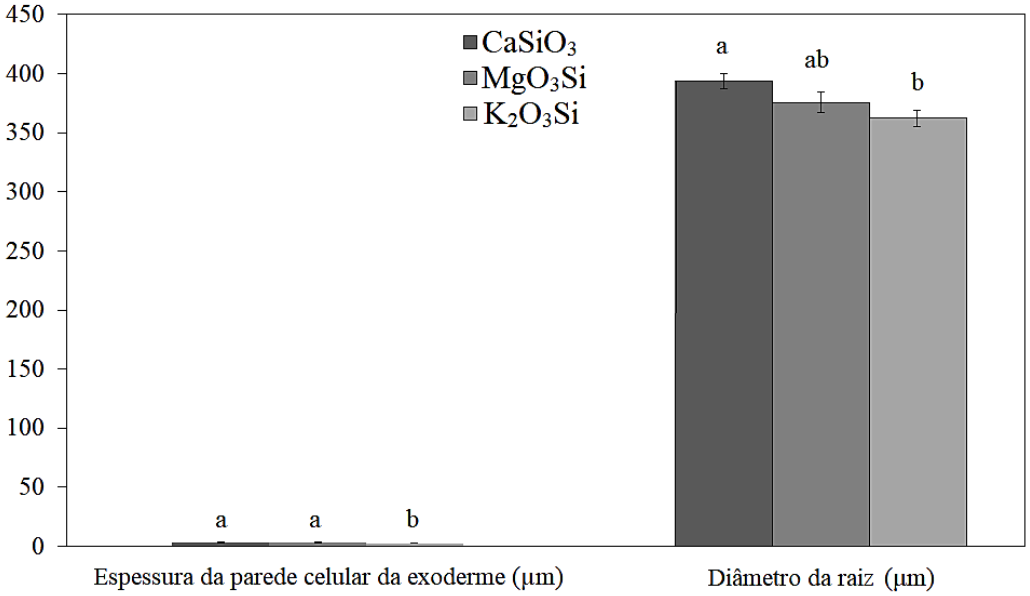

Figura 3 Espessura da parede celular da exoderme (µm) e diâmetro das raízes (µm) de *Aechmea blanchetiana* em função de fontes de Si ($CaSiO_3$, MgO_3Si, K_2O_3Si). Médias (± erro padrão) seguidos pela mesma letra não diferem de acordo com o teste de Tukey ($p<0.05$).

Nas secções paradérmicas das folhas, a densidade estomática foi influenciada por ambos os fatores de variação, com as maiores médias obtidas em plantas cultivadas com 8 µM de MgO_3Si (Figura 4; Figura 5A). Comparadas as concentrações dentro de cada fonte, apenas o K_2O_3Si apresentou diferença significativa, com aumento dos valores em 16 e 32 µM. O tamanho dos estômatos foi influenciado apenas pelas fontes de Si, com as maiores médias apresentadas nas plantas cultivadas com 8 µM de $CaSiO_3$ (Figura 5 B).

Nas secções transversais das folhas (Figura 4), a espessura da face adaxial da epiderme sofreu influência de ambos os fatores de variação, porém atuaram de forma independente. Menores valores foram obtidos em 8 e 16 µM de MgO_3Si (Figura 5 F-G). A espessura da epiderme abaxial sofreu interferência das concentrações, cujo maior valor foi em 32 µM (Figura 5 F-G). Diferenças significativas foram verificadas entre as fontes e concentrações na área do esclerênquima, no diâmetro dos vasos do xilema e na área do floema, com interação significativa entre eles (Figura 5 C-E). Avaliando as fontes de Si em cada concentração, a maior média de área do esclerênquima, foi obtida em plantas cultivadas com 8 µM de $CaSiO_3$ e de

MgO_3Si. O diâmetro dos vasos do xilema teve valores maiores em 8 µM de MgO_3Si. Quando analisada as concentrações em cada fonte maior área do floema foi verificada em 8 µM de MgO_3Si e em 16 µM de $CaSiO_3$. A espessura do hidrênquima sofreu interferência das fontes de Si, com maiores valores nas plantas cultivadas com K_2O_3Si (Figura 5 F). O número de vasos do xilema (3,83 ± 0,07), assim como a espessura do clorênquima (322,08 µm ± 3,05), não apresentaram diferença entre os tratamentos.

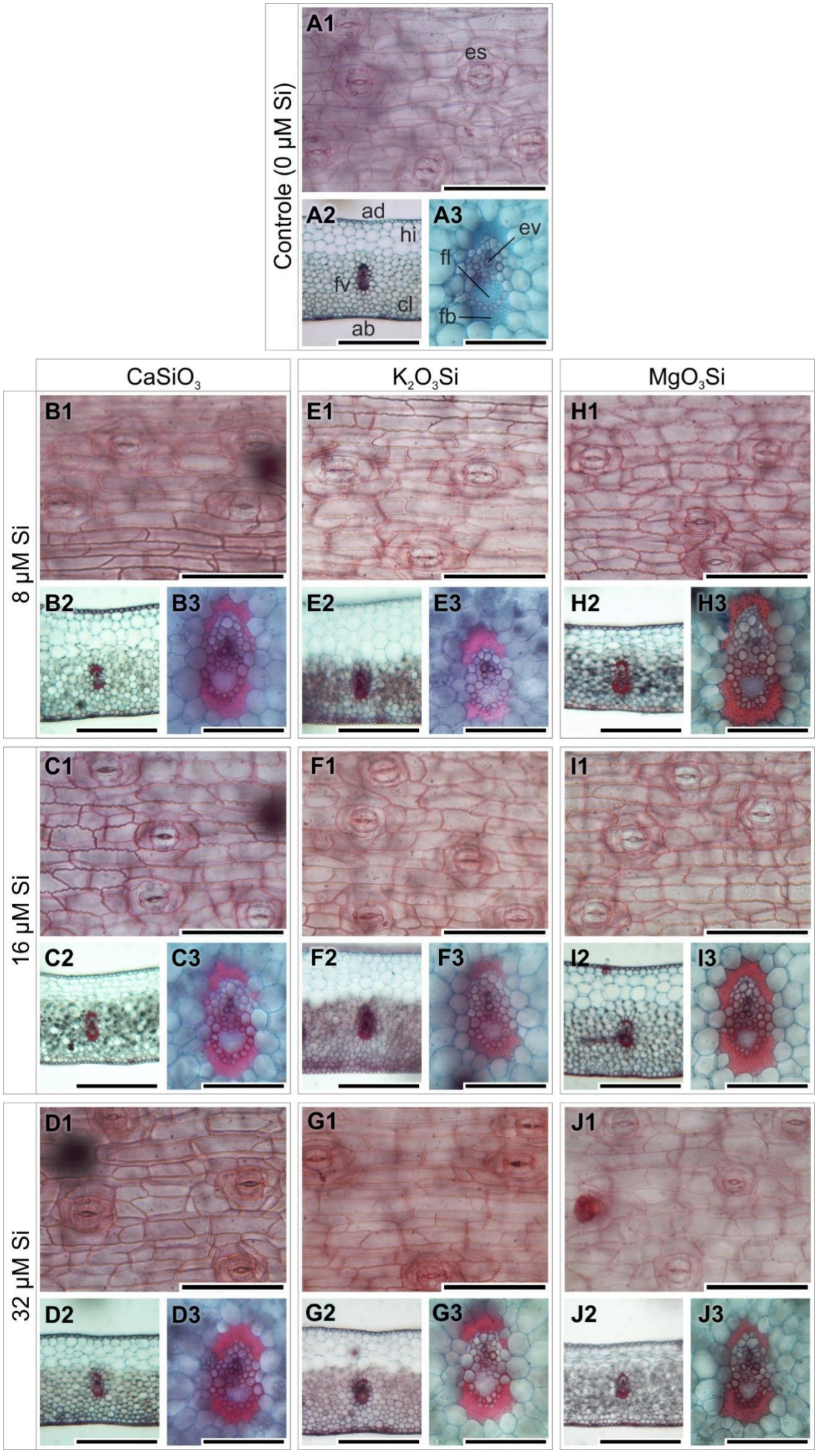
Controle (0 µM Si)
A1
es
A2
ad
hi
fv
cl
ab
A3
ev
fl
fb
CaSiO3
K2O3Si
MgO3Si
8 µM Si
B1
B2
B3
E1
E2
E3
H1
H2
H3
16 µM Si
C1
C2
C3
F1
F2
F3
I1
I2
I3
32 µM Si
D1
D2
D3
G1
G2
G3
J1
J2
J3

Figura 4 Secções paradérmicas e secções transversais de folhas de plantas de *Aechmea blanchetiana* cultivadas *in vitro* em função de diferentes fontes de Si ($CaSiO_3$, MgO_3Si, K_2O_3Si) e concentrações (0, 8, 16 e 32 µM). ad, epiderme adaxial; ab, epiderme abaxial; cl, clorênquima; hi, hidrênquima; ev, elementos de vasos (vasos do xilema); fl, floema; fb-fibras do esclerênquima; fv- feixes vasculares; es, estômatos. Barras = 100 µm. Secções paradérmicas (A1) Controle (0 µM Si); (B1, C1, D1; E1, F1, G1, H1; I1, J1) e secções transversais (A2, A3) Controle (B2; B3; C2, C3; D2, D3; E2, E3; F2, F3; G2; G3; H2, H3; I2, I3; J2, J3).

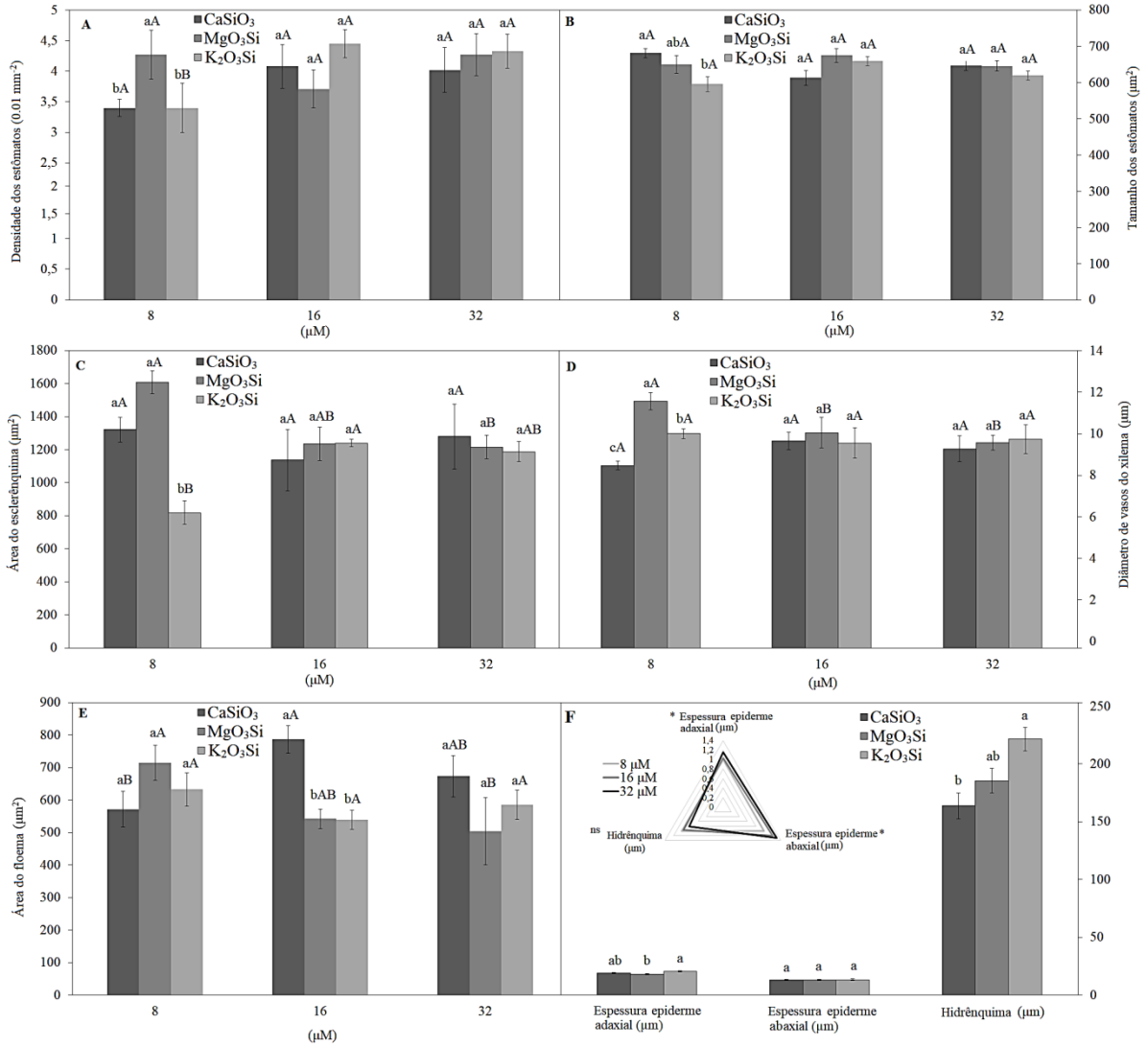

Figura 5 Densidade dos estômatos (0.01 mm^{-2}) (A), tamanho dos estômatos (μm^2) (B), área do esclerênquima (C), diâmetro de vasos do xilema (D), área do floema (E), espessura da epiderme adaxial e abaxial e do hidrênquima (F) de folhas de *Aechmea blanchetiana* em função das fontes de Si ($CaSiO_3$, MgO_3Si, K_2O_3Si) e das concentrações (8, 16, 32µM). (A – E) Médias (± erro padrão) seguidas da mesma letra (minúscula em função das fontes em cada concentração e maiúscula em função das concentrações em cada fonte), não diferem pelo teste de Tukey ($p<0.05$). (F) Valores (± erro padrão) seguidos da mesma letra em função das fontes não diferem de acordo com o teste de Tukey ($p<0.05$). Médias (± erro padrão) em função das concentrações

seguidas por um asterisco (*) são significativamente diferentes de acordo com o teste de Tukey ($p<0.05$). ns – diferença não significativa. Os dados foram normalizados com o tratamento 8 µM Si igual a 1.

Conteúdo de pigmentos fotossintéticos em função das fontes e concentrações de Si

Os tratamentos com as diferentes fontes e concentrações de Si tiveram uma clara influência no conteúdo de pigmentos fotossintéticos (Figura 6). O conteúdo de Chl *a*, Chl *b*, Car, Chl a*/b* e Chl *total* tiveram interferência de ambos os fatores, porém atuaram de forma independente. O conteúdo de Chl *total*/car sofreu atuação das fontes de Si. O crescimento das plantas em meio com $CaSiO_3$ e MgO_3Si induziu o aumento do conteúdo de Chl *a*, Car e Chl *total*. O conteúdo de Chl *b* e de Chl *total*/car foram maiores em plantas com o $CaSiO_3$. Enquanto que a razão Chl a*/b* foi maior com o MgO_3Si e K_2O_3Si. Plantas submetidas a concentração de 8 µM aumentaram o conteúdo de Chl *a*, Chl *b* e de Chl *total*. Nas plantas cultivadas nas concentrações de 8 e 16 µM aumentaram o conteúdo de Car e em 32 µM tiveram aumento da razão Chl a*/b*.

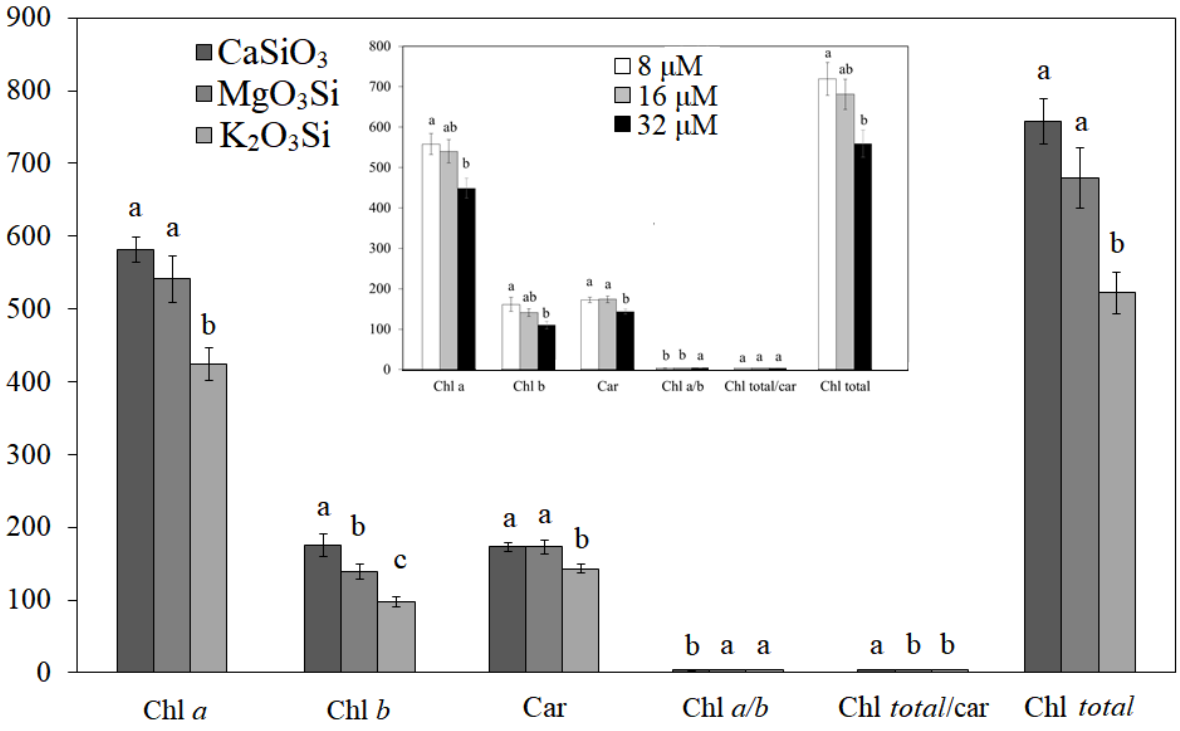

Figura 6 Conteúdo de pigmentos fotossintéticos clorofila *a* (Chl *a*), clorofila b (Chl *b*), carotenoides (Car), razão clorofila *a/b* (Chl *a/b*), clorofila *total*/car e clorofila *total* em plantas de *Aechmea blanchetiana* em função de fontes de Si ($CaSiO_3$, MgO_3Si, K_2O_3Si) e de

concentrações (8, 16, 32 µM) em *Aechmea blanchetiana*. Valores (± erro padrão) seguidos pela mesma letra em cada pigmento fotossintético não diferem de acordo com o teste de Tukey ($p<0.05$).

Análise da Fluorescência modulada da clorofila *a* em função das fontes e concentrações de Si

Os parâmetros ΦPSII, ETR, qP e qL foram influenciados por ambos os fatores de variação, porém atuaram de forma independente (Figura 7 A-B). Para o NPQ e ΦNPQ foram observadas diferenças somente das fontes de Si (Figura 7 A). Já o qN, ΦNO e F_V/F_M sofreram alterações significativas em função de ambos os fatores de variação, com interação significativa entre eles (Figura 7 C-E). As plantas cultivadas com 8 e 16 µM de $CaSiO_3$ apresentaram os maiores valores de ΦPSII, ETR, qP e qL. Para o NPQ e o ΦNPQ as maiores médias foram observadas com o K_2O_3Si. Para o qN as maiores médias foram observadas em 8 e 32 µM de K_2O_3Si. Aumento em ΦNO foi obtido em plantas com 32 µM de MgO_3Si. Para o F_V/F_M valores mais elevados foram obtidos em plantas crescidas com 16 µM de MgO_3Si e de K_2O_3Si. Já em 32 µM os maiores valores foram alcançados para $CaSiO_3$ e K_2O_3Si. Avaliando as concentrações dentro de cada fonte, aumento de F_V/F_M foi obtido em 32 µM de $CaSiO_3$.

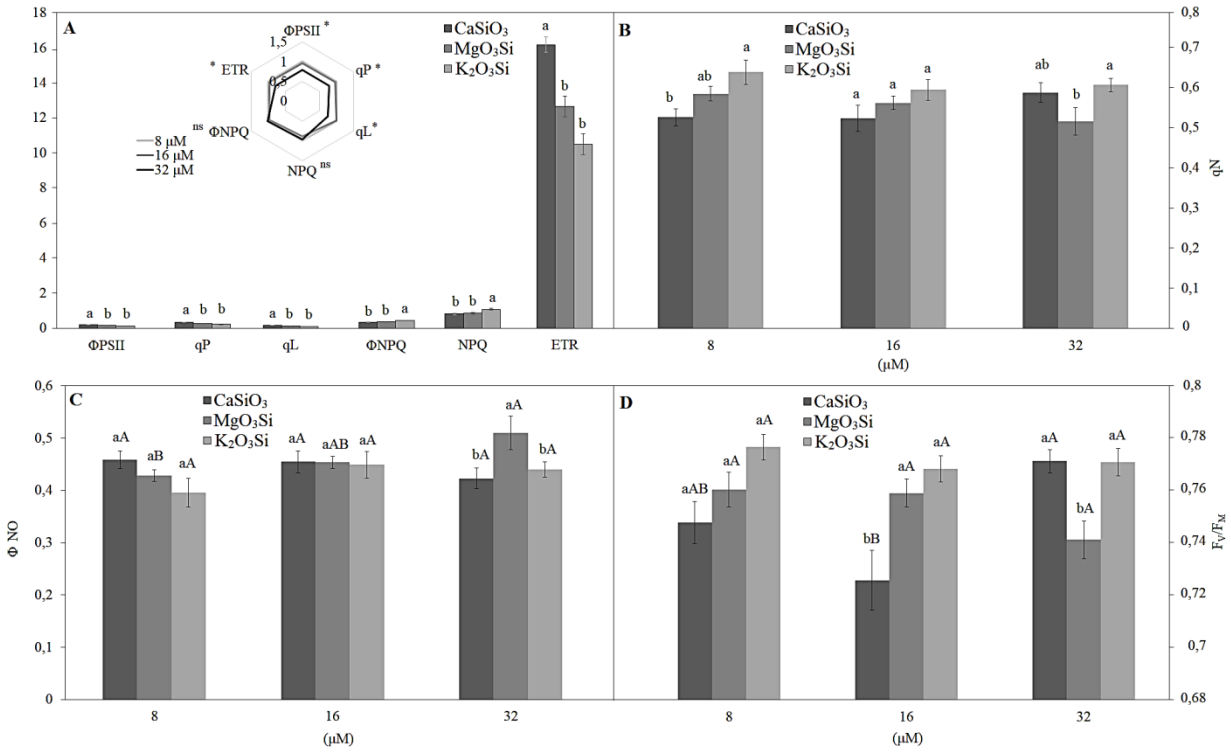

Figura 7 Parâmetros da fluorescência modulada de plantas de *Aechmea blanchetiana* em função das fontes de Si ($CaSiO_3$, MgO_3Si, K_2O_3Si) e das concentrações (8, 16, 32 µM). (A - C)

Valores (± erro padrão) seguidos da mesma letra em cada parâmetro não diferem de acordo com o teste de Tukey ($p<0.05$). (A) Médias (± erro padrão) em função das concentrações seguidas por um asterisco (*) são significativamente diferentes de acordo com o teste de Tukey ($p<0.05$). ns – diferença não significativa. Os dados foram normalizados com o tratamento 8 µM Si igual a 1. (D) Valores (± erro padrão) seguidos da mesma letra para cada parâmetro (minúsculas em função das fontes em cada concentração e maiúsculas em função das concentrações em cada fonte), não diferem de acordo com o teste de Tukey ($p<0.05$).

Análise de crescimento em função das fontes e concentrações de Si

As fontes de Si atuaram significativamente na massa fresca total das plantas de *A. blanchetiana* cultivadas *in vitro*, com os maiores valores observados nas plantas com $CaSiO_3$ e MgO_3Si (Figura 8). As concentrações de Si não atuaram de forma significativa.

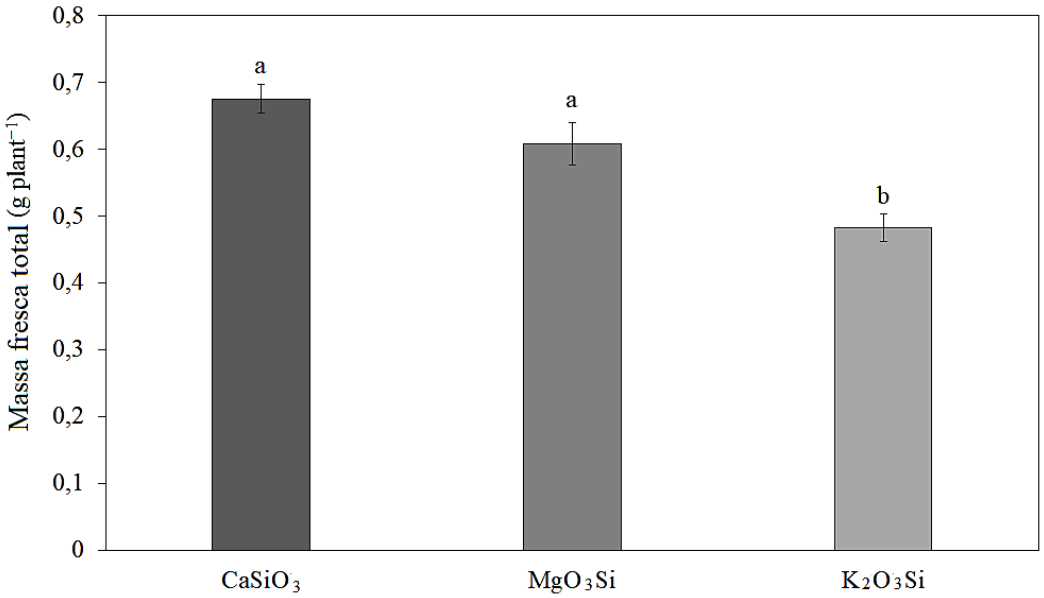

Figura 8 Massa fresca total (parte aérea + raiz) (g $plant^{-1}$) de plantas de *Aechmea blanchetiana* em função das fontes de Si ($CaSiO_3$, MgO_3Si, K_2O_3Si). Valores (± erro padrão) seguidos pela mesma letra não diferem de acordo com o teste de Tukey ($p<0.05$).

Análise de Correlação

Foi realizada análise de correlação entre todos os parâmetros medidos (Figura 9). A característica de crescimento massa fresca total mostrou relação positiva com qL, qP, ΦPSII e ETR e relação negativa com a razão de Chl *a/b*. A razão de Chl *a/b* se mostrou negativamente

correlacionada com a Chl *a*, Chl *b*, Chl *total* e Chl *total*/car. Os parâmetros qL, qP, ΦPSII e ETR possuem relação positiva com a espessura da parede celular da exoderme, conteúdo de Chl *a*, Car e de Chl *total*. No entanto, os mesmos possuem relação negativa com ΦNO e Chl *a/b*. Já ΦNPQ, qN e NPQ se mostraram negativamente relacionados com ΦNO e ETR.

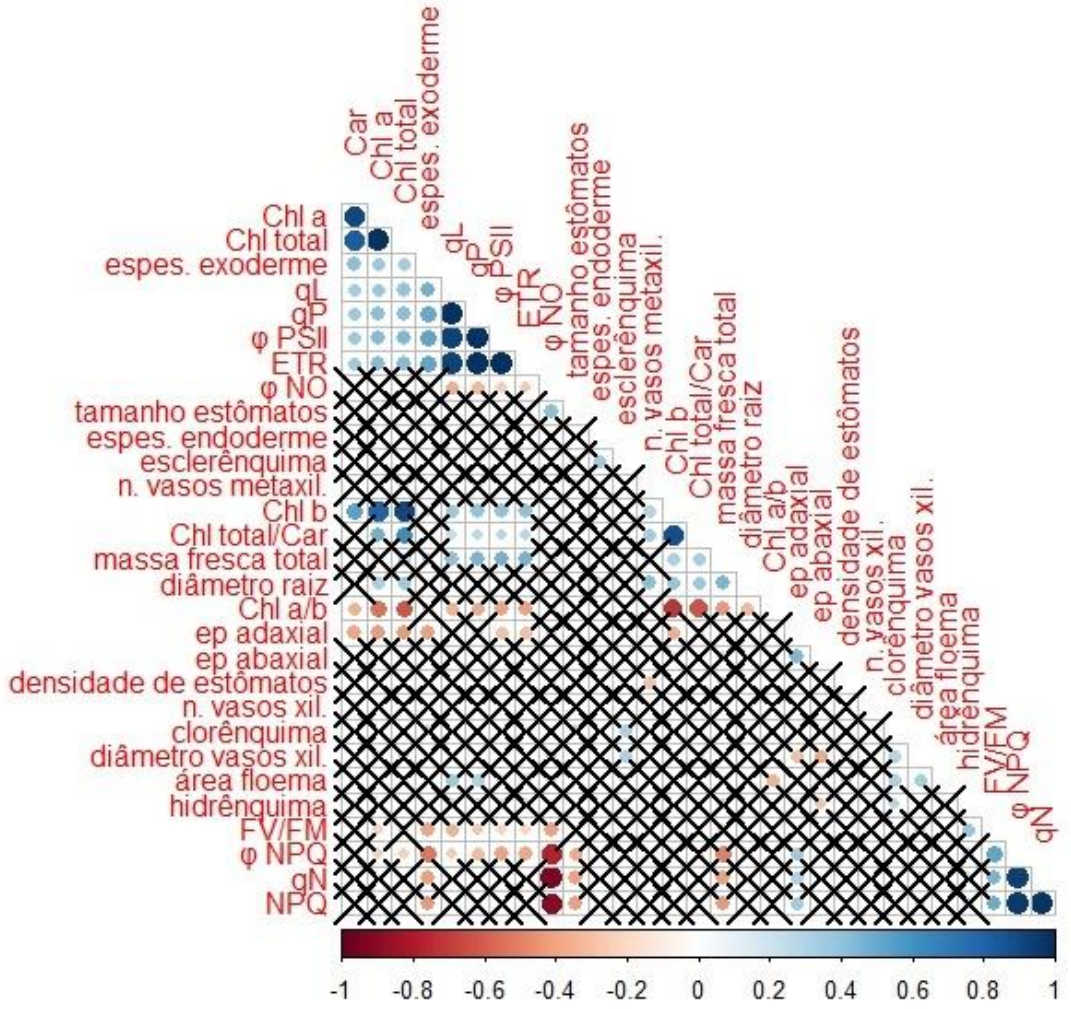

Figura 9 Coeficiente de Correlação de Pearson de plantas de *Aechmea blanchetiana* em função das fontes de Si ($CaSiO_3$, MgO_3Si, K_2O_3Si) e de concentrações (8, 16, 32 μM). Símbolos em vermelho indicam correlação negativa; símbolos em azul indicam correlação positiva.

Discussão

As modificações anatômicas promovidas pela presença de Si no meio de cultura podem impactar diretamente no status nutricional de plantas *in vitro* de *A. blanchetiana.* Na anatomia das raízes, a espessura mais fina da parede celular da exoderme em plantas crescidas com o Si pode permitir maior absorção de nutrientes do meio de cultura e translocação para a parte aérea

(Asmar *et al.* 2013). Essa resposta pode contribuir para o aumento de biomassa da planta, tal como observado para o aumento da massa fresca total das plantas cultivadas com o Si. O espessamento das paredes celulares em bromélias, ocorre por um processo natural e pode ser um dos mecanismos para regular a absorção e translocação de nutrientes minerais por toda a planta (Martins *et al.* 2019). Uma modulação na anatomia das raízes promovida por fontes de Si foi o aumento no diâmetro em plantas cultivadas com o $CaSiO_3$. Este pode ser um dos fatores que contribuiu no aumento da massa fresca total das plantas, cuja relação positiva foi mostrada na análise de correlação.

Nas folhas, a presença de Si reduziu a densidade e aumentou o tamanho dos estômatos, o que pode influenciar na fotossíntese e na condutividade estomática das plantas. Estas duas características são importantes nas respostas de longo prazo aos estímulos ambientais e na determinação da velocidade de reações estomáticas (Kubarsepp *et al.* 2020). A redução na densidade estomática pode caracterizar um meio pelo qual as plantas podem otimizar a eficiência do uso da água já que esta característica pode reduzir a condutância estomática (Kiani-Pouya *et al.* 2019). Em relação ao tamanho dos estômatos, a capacidade limitada de influxo de água pode reduzir a taxa de movimentos estomáticos em folhas com células-guarda maiores, reduzindo a eficiência do uso da água (Kubarsepp *et al.* 2020). Pode-se sugerir que o aumento no tamanho dos estômatos seja uma estratégia de compensação (tradeoff) para a redução da densidade estomática, que pode manter um equilíbrio adequado entre a assimilação de CO_2 e a perda de água (Martins *et al.* 2021). Estômatos maiores podem permitir um aumento na transpiração, e consequentemente, na translocação e assimilação de água e nutrientes por fluxo de massa, que são absorvidos pelas raízes (Bertolino *et al.* 2019). Essas modulações em plantas de *A. blanchetiana* cultivadas com o Si contribuíram para aumentar o crescimento das plantas *in vitro*. Essa resposta dos estômatos, podem beneficiar as plantas em fases iniciais de aclimatização (Camargo *et al.* 2007).

Ainda relacionado à anatomia foliar, o aumento promovido pelo Si na espessura do clorênquima, na área do esclerênquima e do floema e no diâmetro dos vasos do xilema contribuem em conjunto com o aumento do crescimento da planta. Fato esse comprovado pela maior massa fresca total da planta em presença de Si. Esses mecanismos garantem benefícios a planta como maior translocação de água e nutrientes possibilitada pelo aumento do diâmetro dos vasos do xilema. Diâmetros maiores dos vasos estão relacionados a maior condutância hidráulica que pode aumentar o potencial hídrico, e consequentemente o crescimento da parte aérea (Tombesi *et al.* 2010). A maior área do floema também é uma modificação que permite maior translocação de carboidratos, hormônios, nutrientes e água (Hu *et al.* 2019; Cao *et al.*

2020). O aumento da área do esclerênquima nas folhas desempenha papel fundamental na conservação de água e dá força e proteção aos tecidos vegetais (Rafique *et al.* 2021). Esse aumento da área do esclerênquima possui relação positiva com o aumento no crescimento dessas plantas. O aumento do clorênquima está associado a maior atividade fotoquímica das plantas (Freschi *et al.* 2010). O Si também promoveu redução da espessura da epiderme adaxial das plantas, o que pode contribuir com a absorção de nutrientes via foliar. Considerando que as plantas podem absorver os nutrientes também a partir das folhas, uma redução da espessura da epiderme poderia funcionar como um mecanismo para aumentar a absorção de nutrientes (Mahmood *et al.* 2019). Além de poder aumentar a transpiração cuticular (Trejo-Téllez *et al.* 2020).

Analisando o efeito das fontes ainda na anatomia foliar, o maior aumento na área do floema com 8 µM de MgO_3Si e 16 µM de $CaSiO_3$, possibilita o maior transporte de carboidratos, hormônios, nutrientes e água. Já o menor aumento da área do floema em 16 µM de K_2O_3Si, pode ser um dos fatores responsáveis pela redução do crescimento das plantas nesse meio de cultura. Suprimento suficiente de K nas plantas pode estabelecer o potencial osmótico no floema e ajudar no transporte e distribuição de carboidratos de órgãos fonte para os drenos (Cakmak 2005; Pettigrew 2008). No entanto, a carga de carboidratos no floema de plantas tanto com deficiência quanto com excesso de K é inibida e o transporte para as raízes é significativamente reduzido (Gerardeaux *et al.* 2010). Assim, tanto a deficiência quanto o excesso de K podem inibir o crescimento (Xu *et al*. 2020).

Alterações fisiológicas relacionadas ao conteúdo de pigmentos fotossintéticos foram observadas entre as fontes de Si em plantas de *A. blanchetiana*. O incremento de Chl *a*, Car e Chl *total* na presença de 8 µM de $CaSiO_3$ e MgO_3Si, pode estar relacionado a maior atividade do sistema de defesa antioxidante. Maior atividade das enzimas do sistema antioxidante leva a uma menor degradação da clorofila (Gong et al. 2018). Conteúdos maiores de Chl *a* e de Chl *total* contribuem para o aumento da absorção de energia da radiação e do processo fotoquímico da fotossíntese (Martins *et al.* 2018). Isso está de acordo com nossos resultados já que plantas cultivadas com o $CaSiO_3$ apresentaram maiores valores de $\Phi PSII$, qP, qL e ETR, confirmando a relação positiva entre esses parâmetros. A redução do conteúdo de pigmentos nas plantas em meio com 32 µM de K_2O_3Si, pode refletir no funcionamento do aparato fotossintético e no crescimento das plantas. O suprimento adequado de K contribui para aumentar o transporte de fotoassimilados das folhas para as raízes e a eficiência do uso do nitrogênio (NUE) (Xu *et al.* 2020). O maior conteúdo de Car e de Chl *total*/car, indicam um maior potencial dessas plantas para atuar em mecanismos de defesa contra estresse oxidativo (Mostofa *et al.* 2017). Os Car

são capazes de capturar diretamente espécies reativas de oxigênio (ERO), protegendo as células contra a degradação e destruição mediada pelas ERO (Gill e Tuteja 2010). Os Car também fazem parte das estruturas essenciais do aparelho fotossintético, no qual tem papel direto na fotossíntese (Yaroshevich *et al.* 2015).

O aumento dos valores da razão Chl *a/b* juntamente com a redução do conteúdo de Chl *total*, observados nas plantas cultivadas com 32 μM de K_2O_3Si, evidencia a relação negativa entre esses parâmetros. A razão Chl *a/b* está associada ao grau de empilhamento da membrana dos tilacóides e na eficiência do complexo coletor de luz do FSII (LHCII) (Sil *et al.* 2019). Assim, poderia ser sugerido que concentrações mais altas de K_2O_3Si podem causar alterações na integridade da membrana dos tilacóides e na eficácia do LHCII (Jeong *et al.* 2017). A hormese é uma relação dose-resposta bifásica com baixas doses induzindo efeitos estimulatórios, ativando mecanismos adaptativos que aumentam a resiliência, enquanto doses mais altas podem induzir respostas inibitórias que, em doses ainda mais altas, muitas vezes se tornam tóxicas (Agathokleous e Calabrese 2019a, 2019b, 2020). É importante ressaltar que o Si pode afetar diferencialmente o crescimento e o metabolismo das plantas, dependendo da fonte e da concentração aplicada, o que pode ser atribuído à hormese induzida quimicamente (Calabrese *et al.* 2019; Agathokleous e Calabrese 2020).

As modulações morfofisiológicas promovidas pelas fontes e concentrações de Si favoreceram alterações no funcionamento do aparato fotossintético, como evidenciado pela análise da fluorescência modulada da clorofila *a*. Os maiores valores de ΦPSII, ETR, qP e qL induzidos em 8 e 16 μM de $CaSiO_3$ implicam em uma maior capacidade de conversão fotoquímica e de transferência de elétrons do FSII (Wang *et al.* 2018). Valores mais elevados desses parâmetros indicam que as plantas aumentaram o fluxo de elétrons entre o FSII e FSI (fotossistema I) e a atividade fotoquímica efetiva do FSII (Bączek-Kwinta *et al.* 2019; Xin *et al.* 2019; Cipriano *et al.* 2021). Aumento no crescimento das plantas induzido por $CaSiO_3$ e MgO_3Si, visto como o acúmulo de biomassa total, pode ser associado ao aumento da atividade fotoquímica, eliminação de ERO, melhor atividade de enzimas do sistema antioxidantes e consequentemente menor nível de estresse (Zhang *et al.* 2019). Redução de F_V/F_M e aumento nos valores de ΦNO foram obtidos em plantas cultivadas com 32 μM de MgO_3Si, evidência a relação negativa entre estes e indica que essas plantas sofreram fotoinibição e danos. De acordo com Bolhar-Nordenkampf *et al.* (1989), plantas cultivadas sob condições sem estresse geralmente apresentam valores de $F_V/F_M \geq 0{,}75$. ΦNO é um importante índice de fotodano aos centros de reação (RC) do FSII (Shu *et al.* 2019; Martins *et al.* 2020). De fato, níveis excessivos de Si podem afetar o metabolismo e fisiologia da planta (Trejo-Téllez *et al.* 2020).

A redução de ΦPSII, ETR, qP e qL em plantas cultivadas com K_2O_3Si e MgO_3Si na maior concentração, sugere que menos energia luminosa foi utilizada por reações fotoquímicas. Visto que a diminuição de ETR indica um bloqueio parcial de transporte de elétrons do FSII para o FSI (Cao *et al.* 2018; Xin *et al.* 2019). A menor atividade fotoquímica efetiva e aumento de parâmetros não fotoquímicos em plantas de *A. blanchetiana* tratadas com K_2O_3Si refletiram na redução do crescimento total dessas plantas. O aumento em qN, NPQ e ΦNPQ em plantas cultivadas com K_2O_3Si, reflete a ativação dos processos não fotoquímicos, indicando que mecanismos de dissipação do excesso de energia de excitação, na forma de calor, foram mais eficientes nesse tratamento (Shu *et al.* 2019). O ΦNPQ refere-se à dissipação regulada por indução dos pigmentos do ciclo das xantofilas e por gradiente de prótons nas membranas dos tilacóides (Dias *et al.* 2018; Cipriano *et al.* 2021). Esses mecanismos de proteção em conjunto possibilitaram com que as plantas cultivadas com o K_2O_3Si mantivessem o transporte de elétrons no FSII. Fato esse evidenciado pelo $F_V/F_M \geq 0,75$, o que indica aumento na atividade fotoquímica potencial do FSII (Lotfi *et al.* 2018). Porém, essas respostas não foram o suficiente para promover o crescimento das plantas de *A. blanchetiana.* Uma tendência de redução de características de crescimento com aumento da concentração de K_2O_3Si também foi visto em estudo de Kadlecová *et al.* (2020).

Conclusão

A suplementação com o Si induziu respostas anatômicas das raízes e de folhas em *A. blanchetiana* que possibilitaram maior absorção de nutrientes minerais e maior conservação de água. Essas características podem ter contribuído para o maior crescimento total das plantas. Em relação as fontes de Si, respostas em conjunto promovidas pelo $CaSiO_3$, como o aumento de ΦPSII, ETR e qP, contribuíram para aumentar o crescimento das plantas. Plantas crescidas com MgO_3Si promoveram respostas como o aumento no diâmetro dos vasos do xilema e da área de esclerênquima que permitiram o aumento da massa fresca total das plantas *in vitro*. No entanto, plantas cultivadas com K_2O_3Si apresentaram modulações anatômicas e fisiológicas que reduziram a atividade fotoquímica efetiva do FSII e o crescimento de plantas de *A. blanchetiana*. As concentrações 8 e 16 µM foram as que possuíram maior contribuição com a atividade fotoquímica efetiva do FSII. O presente estudo comprovou que as respostas induzidas pelo Si contribuem para a anatomia, fisiologia e crescimento de plantas de *A. blanchetiana* cultivadas *in vitro*. Dentre as fontes de Si testadas, o $CaSiO_3$ foi o que apresentou maior contribuição para o aumento do funcionamento efetivo do FSII e do crescimento das plantas.

Referências

Agathokleous E., Calabrese E.J. Hormesis: the dose response for the 21st Century: the future has arrived. – Toxicology **425**:152249, 2019a.

Agathokleous E., Calabrese E.J. Hormesis can enhance agricultural sustainability in a changing world. – Global Food Security **20**:150–155, 2019b.

Agathokleous E., Calabrese E.J. A global environmental health perspective and optimisation of stress. – Science of the Total Environment **704**: 135263, 2020.

Asmar S.A., Castro E.M., Pasqual M., Pereira F.J., Soares, J.D.R. Changes in leaf anatomy and photosynthesis of micropropagated banana plantlets under different silicon sources. – Scientia Horticulturae, **161**: 328–332, 2013.

Asmar A.S., Soares J.D.R., Silva R.A.L., Pasqual M., Pio L.A.S., Castro E.M. Anatomical and structural changes in response to application of silicon (Si) *in vitro* during the acclimatization of banana cv. 'Grand Naine'. – Aust J Crop Sci **9:** 1236–1241, 2015.

Arnon D.I. Copper enzymes in isolated chloroplasts. Polyphenoloxidase in *Beta vulgaris*. – Plant Physiol **24**: 1–15, 1949.

Bączek-Kwinta R., Juzoń K., Borek M., Antonkiewicz J. Photosynthetic response of cabbage 480 in cadmium-spiked soil. – Photosynthetica **57**, 731-739, 2019.

Bhagooli R., Mattan-Moorgawa S., Kaullysing D., Louis Y.D., Gopeechund A., Ramah S., Baker A.C. Chlorophyll fluorescence – A tool to assess photosynthetic performance and stress photophysiology in symbiotic marine invertebrates and seaplants. – Marine Pollution Bulletin **165**: 112059, 2021.

Bertolino L.T., Caine R.S., Gray J.E. Impact of stomatal density and morphology on water-use eefficiency in a changing world. – Front Plant Sci **10**: 225, 2019.

Cao Y., Ma C., Chen H., Zhang J., White J., Chen G., Xing B. Xylem-based long-distance transport and phloem remobilization of copper in Salix integra Thunb. – J. Hazard. Mater. **392**: 122428, 2020.

Cuong T.X., Ullah H., Datta A., Hanh T.C. Effects of Silicon-Based Fertilizer on Growth, Yield and Nutrient Uptake of Rice in Tropical Zone of Vietnam. – Rice Science **24**: 283–290, 2017.

Cipriano R., Martins J.P.R., Conde L.T., Moreira S.W., Clairvil E., Braga P.C.S., Gontijo A.B.P.L., Falqueto A.R. Anatomical, physiological, and biochemical modulations of silicon in *Aechmea blanchetiana* (Bromeliaceae) cultivated *in vitro* in response to cadmium. – Plant Cell Tissue Organ Cult **147**:271-285, 2021.

Crooks R., Prentice P. Extensive investigation into field based responses to a silica fertilizer. *Silicon* **9**: 301–304, 2017.

Dias C.S., Araujo L., Alves Chaves J.A., DaMatta F.M., Rodrigues F.A. Water relation, leaf gas exchange and chlorophyll a fluorescence imaging of soybean leaves infected with *Colletotrichum truncatum*. – Plant Physiology and Biochemistry **127**: 119–128, 2018.

Ferreira E.B., Cavalcanti P.P; Nogueira D.A. ExpDes: An R Package for ANOVA and Experimental Designs. – Applied Mathematics **5**: 2952-2958, 2014.

Gill S.S., Tuteja N. Reactive oxygen species and antioxidant machinery in abiotic stress tolerance in crop plants. – Plant Physiol Biochem **48**: 909-930, 2010.

Gong D.H., Wang G.Z., Si W.T., Zhou Y., Liu Z., Jia J. Effects of salt stress on photosynthetic pigments and activity of ribulose-1,5-bisphosphate carboxylase/oxygenase in *Kalidium foliatum*. – Russ J Plant Physiol **65**:98–103, 2018.

Hafez E.M., Osman H.S., El-Razek U.A.A., Elbagory M., Omara A.E.-D., Eid M.A., Gowayed S.M. Foliar-Applied Potassium Silicate Coupled with Plant Growth-Promoting Rhizobacteria Improves Growth, Physiology, Nutrient Uptake and Productivity of Faba Bean (*Vicia faba* L.) Irrigated with Saline Water in Salt-Affected Soil. – Plants **10**: 894, 2021.

Hu A.Y., Che J., Shao J.F., Yokosho K., Zhao X.Q., Shen R.F., Ma J.F. Silicon accumulated in the shoots results in down-regulation of phosphorus transporter gene expression and decrease of phosphorus uptake in rice. – Plant and Soil **423**: 317–325, 2017.

Hu Y., Tian S.K., Foyer C.H., Hou D.D., Wang H.X., Zhou W.W., Liu T., Ge J., Lu L.L., Lin X.Y. Efficient phloem transport significantly remobilizes cadmium from old to young organs in a hyperaccumulator Sedum alfredii. – J. Hazard. Mater. **365**, 421–429, 2019.

Jeong J., Baek K., Kirst H., Melis A., Jin E. Loss of CpSRP54 function leads to a truncated light-harvesting antenna size in *Chlamydomonas reinhardtii*. – BBA-Bioenergetics **1858**: 45–55, 2017.

Kadlecová E., Baránek M., Magnús S., Gazdík F. The Effects of Potassium Silicate as a Component of Nutrient Medium for Selected *in Vitro* Cultures of Prunus and *Corylus Genera*. – Acta Universitatis Agriculturae et Silviculturae Mendelianae Brunensis **68**: 851–857, 2020.

Kalaji H.M., Rastogi A., Živčak M. *et al.*: Prompt chlorophyll fluorescence as a tool for crop phenotyping: an example of barley landraces exposed to various abiotic stress factors. – Photosynthetica **56**: 953–961, 2018.

Kiani-Pouya A., Rasouli F., Bazihizina N. *et al.*: A large-scale screening of quinoa accessions reveals an important role of epidermal bladder cells and stomatal patterning in salinity tolerance. – Environ. Exp. Bot. **168**: 103885, 2019.

Kübarsepp L., Laanisto L., Niinemets Ü., Talts E., Tosens T. Are stomata in ferns and allies sluggish? Stomatal responses to CO_2, humidity and light and their scaling with size and density. – New Phytologist, **225**: 183-95, 2020.

Lotfi R., Kalaji H.M., Valizadeh G.R., Khalilvand Behrozyar E., Hemati A., Gharavi-Kochebagh P., Ghassemi A. Effects of humic acid on photosynthetic efficiency of rapeseed plants growing under different watering conditions. – Photosynthetica **56**: 962–970, 2018.

Ma J.F., Yamaji N. A cooperative system of silicon transport in plants. – Trends Plant Sci. **20**: 435–442, 2015.

Mahmood Y.A., Ahmed F.W., Juma S.S., Al-Arazah A.A. Effect of solid and liquid organic fertilizer and spray with humic acid and nutrient uptake of nitrogen, phosphorus and potassium on growth, yield of cauliflower. – Plant Archives **19**: 1504-1509, 2019.

Manivannan A., Soundararajan P., Cho Y.S., Park J.E., Jeong B.R. Sources of silicon influence photosystem and redox homeostasis- related proteins during the axillary shoot multiplication of *Dianthus caryophyllus*. – Plant Biosyst **152**: 704–710, 2017.

Mantovani C., Pivetta K.F.L., Mello Prado R.; Souza J.P., Nascimento C.S, Nascimento C.S., Gratão P.L. Silicon toxicity induced by different concentrations and sources added to *in vitro* culture of epiphytic orchids. – Scientia Horticulturae **265**: 109272, 2020.

Martins A.D., Martins J.P.R., Batista L.A., DIAS G.M.G., Almeida M.O., Pasqual M., Santos H.O. Morpho-physiological changes in *Billbergia zebrina* due to the use of silicates *in vitro*. – An Acad Bras Ciênc **90**:3449–3462, 2018.

Martins J.P.R., Rodrigues L.C.A., Silva T.S., Santos E.R., Falqueto A.R., Gontijo A.B.P.L. Sources and concentrations of silicon modulate the physiological and anatomical responses of *Aechmea blanchetiana* (Bromeliaceae) during in vitro culture. – Plant Cell Tissue Organ Cult **137**: 397–410, 2019.

Martins J.P.R., Vasconcelos L.L., Braga P.d.d. *et al.*: Morphophysiological responses, bioaccumulation and tolerance of *Alternanthera tenella Colla* (Amaranthaceae) to excess copper under *in vitro* conditions. – Plant Cell Tiss Organ Cult **143**: 303–318, 2020.

Martins J.P.R., Moreira S.W., Braga P.C.S., Conde L.T., Cipriano, R., Falqueto, A.R., Gontijo A.B.P.L. Photosynthetic apparatus performance and anatomical modulations of *Alcantarea imperialis* (Bromeliaceae) exposed to selenium during *in vitro* growth. – Photosynthetica, **59**: 529-537, 2021.

Moradi F., Ismail A.M. Responses of photosynthesis, chlorophyll fluorescence and ROS-scavenging systems to salt stress during seedling and reproductive stages in rice. – Ann Bot. **99**: 1161–1173, 2007.

Mostofa M.G., Hossain M.A., Siddiqui M.N., Fujita M., Tran L.S.P. Phenotypical, physiological and biochemical analyses provide insight into selenium-induced phytotoxicity in rice plants. – Chemosphere. **178**: 212-223, 2017.

R Core Team. R: A language and environment for statistical computing. R Foundation for Statistical Computing, Vienna, Austria. URL https://www.R-project.org/, 2021.

Rafique T., Hameed M., Naseer M., Rafique R., Sadiq R., Zikreae A., Sajjad M.R. Comparative Leaf Anatomy of Grasses (Poaceae) in Faisalabad Region of Pakistan. – Polish Journal of Environmental Studies **30**: 5701-5709, 2021.

Rodrigues F.A. *et al.*: Application of silicon sources in yam (*Dioscorea* spp.) micropropagation. – Australian Journal of Crop Science, [S.l.], **11**: 1469-1473, 2017.

Rosa W.S., Martins J.P.R., Santos E.R., Rodrigues L.C.A., Gontijo A.B.P.L., Falqueto A.R. Photosynthetic apparatus performance in function of the cytokinins used during the in vitro multiplication of *Aechmea blanchetiana* (Bromeliaceae). – Plant Cell Tissue Organ Cul **133**:339–350, 2018.

Sahebi M., Hanafi M.M., Parisa A. Application of silicon in plant tissue culture. – In Vitro Cell Dev Biol – Plant. **52**: 226–232, 2016.

Seal P., Das P., Biswas A.K. Versatile potentiality of silicon in mitigation of biotic and abiotic stresses in plants: a review. – Am J Plant Sci **9**: 1433–1454, 2018.

Shu S., Yuan R., Shen J., Chen J., Wang L., Wu J., Sun J., Wang Y., Shirong G. The positive regulation of putrescine on light-harvesting complex II and excitation energy dissipation in salt-stressed cucumber seedlings. – Environ Exp Bot **162**:283–294, 2019.

Sil P., Das P., Biswas S., Mazumdar A., Biswas A.K. Modulation of photosynthetic parameters, sugar metabolism, polyamine and ion contents by silicon amendments in wheat *(Triticum aestivum L.)* seedlings exposed to arsenic. – Environmental Science and Pollution Research **26**: 13630-13648, 2019.

Sipahutar I.A. *et al.:* IOP Conf. Ser.: Earth Environ. Sci. **648**: 012064, 2021.

Sivanesan I., Jeong B.R. Silicon promotes adventitious shoot regeneration and enhances salinity tolerance of *Ajuga multiflora* Bunge by altering activity of antioxidant enzyme. – Sci World J, **2014**: 1-10, 2014.

Sivanesan I., Park S.W. The role of silicon in plant tissue culture. – Front Plant Sci **5**: 571, 2014.

Trejo-Téllez L.I., García-Jiménez A., Escobar-Sepúlveda H.F., Ramírez-Olvera S.M., Bello-Bello J.J., Gómez-Merino F.C. Silicon induces hormetic dose-response effects on growth and concentrations of chlorophylls, amino acids and sugars in pepper plants during the early developmental stage. – PeerJ **8**:e9224, 2020.

Xin J., Zhao X.H., Tan Q.L., Sun X.C., Zhao Y.Y., Hu C.X. Effects of cadmium exposure on the growth, photosynthesis, and antioxidante defense system in two radish (*Raphanus sativus* L.) cultivars. – Photosynthetica **57**: 967–973, 2019.

Xu X., Du X., Wang F., Sha J., Chen Q., Tian G., Zhu Z., Ge S., Jiang Y. Effects of Potassium Levels on Plant Growth, Accumulation and Distribution of Carbon, and Nitrate Metabolism in Apple Dwarf Rootstock Seedlings. – Frontiers in Plant Science **11**, 2020.

Wang Z., Li G., Sun H., Ma L., Guo Y., Zhao Z., Gao H., Mei L. Effects of drought stress on photosynthesis and photosynthetic electron transport chain in young apple tree leaves. – Biol Open **7**: bio035279, 2018.

Wellburn A.R. The spectral determination of chlorophylls *a* and *b*, as well as total carotenoids, using various solvents with spectrophotometers of different resolution. – J Plant Physiol **144**: 307–313, 1994.

Yao J., Sun D., Cen H., Xu H., Weng H., Yuan F., He Y. Phenotyping of Arabidopsis drought stress response using Kinetic Chlorophyll Fluorescence and Multicolor Fluorescence Imaging. – Front Plant Sci **9**: 603, 2018.

Yaroshevich I.A., Krasilnikov P.M., Rubin A.B. Functional interpretation of the role of cyclic carotenoids in photosynthetic antennas via quantum chemical calculations. – Comput. theor. Chem. **1070**: 27-32, 2015.

Zhang Y., Liang Y., Zhao X., Jin X., Hou L., Shi Y., Ahammed G.J. Silicon Compensates Phosphorus Deficit-Induced Growth Inhibition by Improving Photosynthetic Capacity, Antioxidant Potential, and Nutrient Homeostasis in Tomato. – Agronomy **9**: 733, 2019.

Zhang Z., Wu P., Zhang W., Yang Z., Liu H., Ahammed G.J., Cui J. Calcium is involved in exogenous NO-induced enhancement of photosynthesis in cucumber (*Cucumis sativus* L.) seedlings under low temperature. – Scientia Horticulturae **261**: 108953, 2020.

CAPÍTULO 2

Anatomical and physiological responses of *Aechmea blanchetiana* (Bromeliaceae) induced by silicon and salt stress during *in vitro* culture

Rosiane Cipriano[1,4], João Paulo Rodrigues Martins[2*], Lorenzo Toscano Conde[1], Mariela Mattos da Silva[3], Diolina Moura Silva[3], Andreia Barcelos Passos Lima Gontijo[1], Antelmo Ralph Falqueto[4]

[1] Plant Tissue Culture Laboratory, Federal University of Espírito Santo, Litorâneo, São Mateus, ES 29932-540, Brazil

[2] Institute of Dendrology, Polish Academy of Sciences, Parkowa 5, 62-035 Kórnik, Poland

[3] Center for the Study of Photosynthesis, Federal University of Espírito Santo, Av. Fernando Ferrari, Vitória, ES 29075-910, Brazil

[4] Plant Ecophysiology Laboratory, Federal University of Espírito Santo, Litorâneo, São Mateus, ES 29932-540, Brazil

* Corresponding author: E-mail address: jprmartinss@yahoo.com.br (J.P.R. Martins)

Abstract

Salt stress is one of the most severe abiotic stresses affecting plant growth and development. The application of silicon (Si) is an alternative that can increase the tolerance of plants to various types of biotic and abiotic stresses. The objective was to evaluate salt stress's effect *in vitro* and Si's mitigation potential on *Aechmea blanchetiana* plants. For this purpose, plants already established in vitro were transferred to a culture medium with 0 or 14 µM of Si ($CaSiO_3$). After growth for 30 days, a stationary liquid medium containing different concentrations of NaCl (0, 100, 200, or 300 µM) was added to the flasks. Anatomical and physiological analyses were performed after growth for 45 days. The plants cultivated with excess NaCl presented reduced root diameter and effective photochemical quantum yield of photosystem II (PSII) (ΦPSII) and increased non-photochemical dissipation of fluorescence (qN). Plants that grew with the presence of Si also had greater content of photosynthetic pigments and activity of the enzymes of the antioxidant system, as well as higher values of maximum quantum yield of PSII (F_V/F_M), photochemical dissipation coefficient of fluorescence (qP) and fresh weight bioaccumulation of roots and shoots. The anatomical, physiological and biochemical responses, and growth induced by Si mitigated the effect of

salt stress on the *A. blanchetiana* plants cultivated *in vitro*, which can be partly explained by the tolerance of this species to grow in sandbank (*Restinga*) areas.

Keywords: Bromeliads, Modulated Fluorescence, Plant Tissue Culture, Salinity, Tolerance.

Abbreviations: ΦPSII = Y(II) = Φ(II) – Effective photochemical quantum yield of PSII; ETR – Rate of linear electron flow; F_V/F_M – maximum quantum yield of PSII; NPQ – non-photochemical fluorescence dissipation; PSII – photosystem II; qP – photochemical quenching; qL – photochemical fluorescence quenching assuming interconnected PSII antennae; qN – non-photochemical quenching; ΦNPQ – quantum yield induced light (ΔpH and zeaxanthin-dependent) from non-photochemical fluorescence dissipation; ΦNO – quantum yield of non-regulated energy dissipation.

Introduction

Salinity is responsible for multiple effects that reduce the growth, development, and survival of plants, by means of various mechanisms, including alteration of their hydric relations, deficiency or toxicity of ions, and oxidative stress (*Carillo, 2018; Hniličková et al., 2019; Morton et al., 2019; Zhu, Gong & Yin, 2019; Chung et al., 2020*).

During prolonged exposure to high salinity, plants suffer ionic stress, mainly due to sodium chloride, which negatively affects the synthesis of proteins, enzyme activities, and photosynthesis (*Munns & Tester, 2008; Zhu, Gong & Yin, 2019*). Salt stress is accompanied by oxidative stress, leading to the production of reactive oxygen species (ROS). These factors contribute to the deleterious effects of salinity on plants (*Acosta- Motos et al., 2015; Zhu, Gong & Yin, 2019*). ROS can alter normal cell metabolism through oxidative damage to the organelles and membranes by lipid peroxidation. Plants' antioxidant systems can be stimulated to combat the oxidative injuries induced by salt stress. These responses include the removal of ROS by enzymes such as ascorbate peroxidase (APX), superoxide dismutase (SOD), and catalase (CAT) (*Zhu, Gong & Yin, 2019; Jabeen et al., 2022*).

The physiological mechanisms used by plants to minimize the damages caused by stress and reestablish normal growth include processes such as detection and signaling of stress; regulation of metabolism; reduction of stomatal opening, transpiration, and photosynthesis; inhibition of cell division and expansion; and changes in plants' morphology,

phenology, and allocation of resources (*Negrão, Schmöckel & Tester, 2017; Morton et al., 2019*). In particular, the regulation of ionic homeostasis involves the sequestration of toxic ions, along with the production and accumulation of organic osmolytes in the cytosol, enabling rapid osmotic adjustment and preventing toxicity (*Nikalje et al., 2017; Carillo, 2018; Hniličková et al., 2019; Larbi et al., 2020*).

Physiological studies of salt stress *in vitro* are considered a feasible alternative to represent adverse conditions of the external environment (*Claeys et al., 2014*). Moreover, this method allows for controlling the stress level and reducing the variability of *in vivo* studies (*Lawlor, 2013*). Studies of salt stress have also been conducted under *in vitro* conditions (*Harter et al., 2014; Pandey & Chikara, 2015; Cantabella et al., 2017; Zushi & Matsuzoe, 2017; Rezende et al., 2018; Javed & Gürel, 2019*), which have demonstrated the advantages of these techniques for the study of plant physiology.

One alternative to reduce the effects of salt stress on plants is the application of silicon (Si) (*Sahebi, Hanafi & Azizi, 2016*). Si is a beneficial element due to its possibly favorable effects on monocots and eudicots (*Martins et al., 2019; Zhu, Gong & Yin, 2019; Trejo-Téllez et al., 2020; Cipriano et al., 2021b*). Although Si is the majority element in the sand (SiO2) (> 90%) (*Costa et al., 2020*), its Si availability for plants is low. Many researchers have reported that Si has attenuating effects on abiotic stresses, such as salinity, drought, and toxicity of heavy metals (*Wu et al., 2015; Coskun et al., 2016; Manivannan & Ahn, 2017; Rios et al., 2017; Zhu, Gong & Yin, 2019; Cipriano et al., 2021b*).

In vitro cultivation allows for studying the physiological functions of Si in plants (*Sivanesan & Park, 2014; Rezende et al., 2018; Martins et al., 2019; Cipriano et al., 2021a; Cipriano et al., 2021b*). Using Si in the culture medium of plants grown *in vitro* can increase the growth rate and content of photosynthetic pigments (*Asmar et al., 2015; Dias et al., 2017; Rezende et al., 2018; Martins et al., 2019; Cipriano et al., 2021b*). The addition of Si can also favor the increased activity of photosynthesis and the antioxidant system (*Rodrigues et al., 2017; Manivannan et al., 2018; Ribera-Fonseca et al., 2018; Cipriano et al., 2021b*). The positive effects of Si in the culture medium of plants can be related to increased absorption of nutrients and higher photosynthetic activity, besides enhancing the morphogenetic potential of plants' cells, tissues, and organs (*Sivanesan & Park, 2014; Zhu, Gong & Yin, 2019; Liu, Soundararajan & Manivannan, 2019; Liu et al., 2020*).

Among the techniques for detecting physiological disturbances, pulse-amplitude modulation (PAM) chlorophyll fluorescence is frequently used since it can detect stress by alterations in the performance of photosynthetic apparatus (*Yao et al., 2018*). Besides these,

studies of the leaf and root anatomy can be important to evaluate the morphological adjustments of plants in response to stressors (*Paez-Garcia et al., 2015; Martins et al., 2019*).

In most studies, only the roots are exposed to salt stress. However, for some plant species, such as bromeliads, the leaves are the primary organ for nutrient uptake. This way, abiotic stress agents, such as salt, can cause different responses compared to those species that face exposure only in the roots. In the present study, we chose the species *Aechmea blanchetiana* (Baker) L.B. Smith (Bromeliaceae). The plants of this bromeliad species grow naturally in sandbank (*Restinga*) areas characterized by high salinity. This species contains a central tank (formed of leaves) that accumulates water, detritus, and salt (sea-salt aerosol generated from ocean−wind). In this context, it is crucial to understand which morphophysiological mechanisms allow mitigating the damages induced by salt stress. It is not yet clear how the co-exposure to Si and NaCl can influence the anatomy, performance of the photosynthetic apparatus, and antioxidant enzymes of plants native to sandbank areas. Therefore, the objective of this study was to evaluate the effect of salt stress *in vitro* induced by NaCl and the mitigation potential of Si in *A. blanchetiana* plants.

Materials and Methods

In vitro culture conditions

Side buds of *A. blanchetiana* with a shoot length of approximately 2.5 cm (previously established *in vitro*) were transferred to glass flasks containing 30 mL MS culture medium (*Murashige & Skoog, 1962*), supplemented with 30 g L^{-1} sucrose and 4 µM 1-naphthaleneacetic acid, and solidified with 7 g L^{-1} agar. The initial treatments consisted of two Si levels (0 or 14 µM $CaSiO_3$) added to the culture medium, and the concentrations were chosen following *Martins et al. (2019)*. After 30 days of *in vitro* culture with both Si levels, the next step was performed. This involved adding 30 mL stationary liquid MS medium (at 25% strength) to the flasks, supplemented with different concentrations of NaCl (0, 100, 200, or 300 µM), forming a solid/liquid medium (two phases) and constituting eight treatments (2 Si x 4 NaCl). The NaCl concentrations were chosen through previous tests, in which plants' highest concentration did not induce death. The treatments with two phases were adapted from the methodology of *Cipriano et al. (2021b)*. The experiment was carried out with five explants per flask, and the treatments involving co-exposure (Si and NaCl) occurred for 45

days (75 total days). The pH of all the media was adjusted to 5.8 before autoclaving at 120º C during 20 minutes. The plant material was kept in a growth room with a 16-hour photoperiod under LED lamps (Luminaria LED Slim 36W Bi-Volt 2800 lm) at a temperature of 26 ± 2 ºC.

Analysis of the leaf and root anatomy

After culture for 45 days with Si-NaCl co-exposure, anatomical analyses were performed on the first and second fully expanded leaf and on roots (at 0.5 cm from the plant's base) of six different samples per treatment (n = 6). The samples were collected randomly and fixed in an FAA solution (formaldehyde, acetic acid, and 50% ethanol in a proportion of 0.5:0.5:9.0) for 72 hours and conserved in 50% ethanol (*Johansen, 1940*). All the microtechnique procedures concerning sectioning, cleaning, and staining of the paradermal and cross-sections were according to *Martins et al. (2018)* and *Martins et al. (2020)*. The sections were then observed under an optical microscope (Leica DM5000 B) coupled with a digital camera (Leica EC3) to capture images. The photomicrographs were analyzed using the UTHSCSA-Imagetool® version 3.0 software, calibrated with a microscopic ruler.

Analysis of the mineral nutrient levels

The tissue samples were prepared by drying the entire plants in a forced-air oven for 72 hours at a temperature between 68 and 72 ºC. The analyses were conducted with 1 g dry plant material per sample and three repetitions per treatment (n = 3). The samples were ground with a Wiley mill and placed in glass jars. To determine the concentrations of potassium (K), calcium (Ca), magnesium (Mg), sulfur (S), boron (B), zinc (Zn), manganese (Mn), iron (Fe), and sodium (Na), the samples were digested in a nitric-perchloric acid solution in 4:1 proportion (*Sarruge & Haag, 1974*). The minerals were quantified using inductively coupled plasma-optical emission spectrometry (ICP-OES; PerkinElmer model Optima 8300 DV). The nitrogen (N) content was measured by digestion in sulfuric acid according to the Kjeldahl method (*Sarruge & Haag, 1974*).

Analysis of enzymatic activity

To determine the antioxidant enzyme activities, plants were collected after 45 days of growth. The samples were immediately frozen in liquid nitrogen and stored at -80 ºC until

analysis. The activities of superoxide dismutase (SOD; EC 1.15.1.1), ascorbate peroxidase (APX; EC 1.11.1.11), and catalase (CAT; EC 1.11.1.6) were determined in fully expanded leaves and roots from 5 different samples (n = 5). Approximately 0.200 g of fresh-frozen leaf or root samples was ground in a mortar and pestle with liquid nitrogen, potassium phosphate buffer (pH 7.8), EDTA 0.1 mM, ascorbic acid 10 mM, and PVPP 2% w/v. The homogenate was centrifuged at 13,000 g at 4 °C for 10 min. Aliquots of the supernatant were used for the enzymatic assays described below.

SOD activity was determined by forming blue formazan, resulting from nitrotetrazolium blue chloride (NBT) photoreduction following *Giannopolitis & Ries (1977)*. SOD activity was detected after incubation under a 15 W fluorescent light for 10 min at 560 nm and expressed as U min^{-1} mg^{-1} protein. CAT activity was determined according to *Havir & McHale (1987)* by the decay of absorbance at 240 nm, using a 36 mM^{-1} cm^{-1} extinction coefficient and expressed as μmol H_2O_2 min^{-1} mg^{-1} protein. APX activity was determined by the initial ascorbate oxidation by H_2O_2 at 290 nm using a 2.8 mM^{-1} cm^{-1} extinction coefficient and expressed as nmol of ascorbate min^{-1} mg^{-1} protein according to *Nakano & Asada (1981)*. Soluble protein was estimated using Bradford's reagent (Sigma-Aldrich, B6916), by the Coomassie blue dye-binding protein assay, with bovine serum albumin as the standard, according to *Bradford (1976)*, to calculate specific enzyme activity.

Contents of photosynthetic pigments

The contents of photosynthetic pigments were quantified by analyzing 8 randomly chosen fragments (n = 8) according to the method described by *Martins et al. (2019)*. The absorbance was measured using a Genesys™ 10S UV-Vis spectrophotometer (Thermo Fisher Scientific, West Palm Beach, FL, USA), conducted at λ = 470, 645, and 663 nm for carotenoids (Car), chlorophyll *b* (Chl *b*), and chlorophyll *a* (Chl *a*), respectively.

Measurement of modulated chlorophyll *a* fluorescence

The analyses of photosynthetic efficiency were carried out between 8:00 and 10:00 a.m. by measuring the modulated chlorophyll *a* fluorescence with a PAM-2500 Walz portable chlorophyll fluorometer. The measurements were carried out on the third leaf from the plant's rosette center of 12 plants per treatment (n = 12), according to the method *Kramer et al.*

(2004) and described further in *Martins et al. (2020)*. The following variables were obtained: F_V/F_M, ETR, ΦPSII, qN, qP, qL, NPQ, ΦNPQ, and ΦNO.

Analysis of the growth traits

After 45 days of co-exposure to Si-NaCl, the fresh weight was evaluated of the shoots and roots (g plant^{-1}) with 5 repetitions per treatment (n = 5), with each repetition consisting of 5 plants.

Statistical analysis

The experimental design was completely randomized in a 4x2 factorial scheme: 4 NaCl concentrations (0, 100, 200, or 300 µM) and 2 Si concentrations (0 or 14 µM). The data obtained were submitted to analysis of variance (ANOVA), and the means were compared by the Tukey test at 5% probability using the SISVAR 5.4 software *(Ferreira, 2011)*.

Results

Anatomical analysis

Significant differences were observed in the anatomical traits of the roots. The root diameter was influenced only by the saline concentration, being largest at 100 µM and smallest at 0 µM and 300 µM NaCl (Figs. 1A-I). The thickness of the cell walls of the exodermis was influenced by both factors evaluated. In the absence of Si, the exodermal cell wall thickness was smaller with all NaCl concentrations compared to the control. In turn, in the presence of Si, the values were similar regardless of the concentration of NaCl applied. However, the cell walls were thinner in relation to those of the roots in the control treatment (Figs. 1A-H and 1I). The number of metaxylem vessels did not differ among the treatments (5.94 ± 0.55).

In the paradermal leaf sections, the stomatal density of the basal region was influenced only by the NaCl concentration. In this region, there was a decrease in the number of stomata with increasing NaCl concentration (Fig. 2A-H and 2R). However, the density and size of the stomata of the middle region of the leaves were influenced only by exposure to Si. When

cultivated with 14 µM Si, the plants presented a reduction of 14% in the stomatal density and 3% in the stomatal size (Fig. 2I-P and 2S-T).

In the leaf cross-sections, the thickness of the adaxial and abaxial faces of the leaf epidermis (µm) was influenced only by the NaCl concentration, being largest at the concentration of 300 µM NaCl (Figs. 3 and 4A-B). Plants cultivated in NaCl presence had thicker chlorenchyma, mainly at the concentration of 200 µM NaCl (Figs. 3 and 4C). The area of the sclerenchyma (1007.5 μm^2 ± 59.86), area of the phloem (587.08 μm^2 ± 26.01), and diameter of the xylem vessels (9.90 ± 0.36) did not differ significantly among the treatments (Fig. 3).

Contents of nutrients

The contents of Mg, S, Na, and B were influenced by both variation factors, with a significant interaction between them. Plants grown in a medium with Si and NaCl, irrespective of the concentration, had lower content of S. On the other hand, higher NaCl concentration promoted increased Mg, Na, and B contents (Figs. 5A-D). The contents of Fe, Zn, Mn, and Ca, and the Na/K ratio, were influenced by both variation factors, but Si and NaCl acted independently. Lower contents of Fe, Zn, Mn, and Ca were observed in NaCl presence. A higher Na/K ratio was associated with greater salt concentration. The content of K did not differ significantly between the different concentrations of NaCl (2.027 ± 0.098), nor did the content of N (1.75 ± 0.073). The presence of Si increased the contents of Zn, Mn, Ca, and N and the Na/ K ratio. Finally, the content of Fe (179.97 ± 8.77) did not differ in function of the Si concentration (Figs. 6A-B).

Antioxidant enzyme activity

The activity of SOD and CAT, both shoots and roots, was influenced by both variation factors. The activity of SOD was higher in the plants cultured with Si and increased in the function of rising NaCl concentration. The greatest activity of SOD occurred in the presence of 300 µM NaCl, both in the leaves and roots (Figs. 7A-B). The activity of CAT was greatest in the plants grown with Si and increased with rising concentrations of NaCl (200 and 300 µM NaCl) (Figs. 7C-D). Both factors influenced the activity of APX, but they acted separately. The activity of APX was highest with greater concentrations of NaCl in the plants cultivated in a medium supplemented with Si, both in the leaves and roots (Figs. 7E-F).

Contents of photosynthetic pigments

Only the treatment with Si influenced the contents of photosynthetic pigments. Plants cultivated with Si had higher contents of Chl *a*, Car, and Chl total, but there was no alteration in Chl *b* and Chl *a/b* in the leaves of *A. blanchetiana* plants cultured *in vitro* (Fig. 8).

Analysis of modulated chlorophyll *a* fluorescence

The variables ΦPSII and ETR were influenced only by NaCl, with lower values associated with rising NaCl concentration (Figs. 9A-B). In turn, NPQ and F_V/F_M were influenced by Si, presenting lower NPQ and higher F_V/F_M in the plants grown in a medium supplemented with Si (Figs. 9C-D). qP, qL, qN, ΦNPQ, and ΦNO were all influenced by both variation factors. No significant differences were observed among the plants cultivated without Si for qP and qL. However, at the highest concentration of NaCl, there were increases in qN and ΦNPQ. The highest values of ΦNO were obtained in the control plants and those grown with 100 μM NaCl and the lowest at 200 μM NaCl. Among the plants cultivated in the presence of Si, the lowest values of qP and qL were observed in those grown with 200 μM NaCl, as was the case for qN. However, the greatest values of qN were obtained in the plants cultivated in a medium containing 300 μM NaCl. The absence of NaCl was associated with the highest values of qP and qL. No changes in ΦNO and ΦNPQ were observed between treatments (Fig. 10).

Analysis of growth

The fresh weights of the roots and shoots were influenced by both variation factors. Among the plants grown without Si, the shoot and root weights declined with increasing NaCl concentration. However, among the plants cultivated in a medium with Si, the shoot's fresh weight increased in the presence of 200 μM NaCl, while the root's fresh weight increased in the plants receiving 100 μM NaCl. Overall, the fresh weights of the shoots and roots were greater in the plants cultivated in Si and higher concentrations of NaCl than in those grown without Si (Fig. 11).

Discussion

The *A. blanchetiana* plants cultivated under the *in vitro* conditions imposed showed different anatomical and physiological responses due to the presence or absence of Si and the variation in concentrations of NaCl. The morphophysiological responses induced by Si had an attenuating effect on salt stress, through anatomical alterations, increased content of photosynthetic pigments, and greater activity of the enzymes of the antioxidant system, besides their contribution to enhance the performance of the photosynthetic apparatus.

The root and leaf anatomy of the plants was in accordance with the previous description by *Martins et al. (2018)*. The reduction of the diameter of the root cross-sections under salt stress conditions found in this study might have resulted from reductions in the size and number of cells, especially in the internal cortex. The alterations of the cell size can be related to resistance to salt stress since smaller cells can indicate an essential response to increase the water potential, possibly contributing to more effective maintenance of turgor under water deficit *(Munns & Tester, 2008; Terletskaya et al., 2019)*. Reduced root diameters can be a sign of adaptation to the high pressure of the water column on the conductor system *(Rewald et al., 2013; Terletskaya et al., 2019)*.

The induction of a thinner exodermis observed in this study in response to excess NaCl in the shoots may have been the key to the NaCl tolerance. It may induce a greater flow of nutrients from the culture medium to the shoots, improving the nutritional balance. This thickening occurs naturally by the deposition of lignin and/or suberin, and the degree of thickening can moderate the uptake and translocation of mineral nutrients to the entire plant (*Martins et al., 2019*). Thus, the reduction in the thickness of the exodermis cell walls caused by Si shows that this element acted positively, facilitating the uptake of nutrients from the culture medium.

In the leaves, the direct exposure to NaCl at the leaf base reduced the stomatal density. Besides this, the epidermis was thicker in the plants exposed to salt. These responses together suggest a morphological adjustment to control the entry of NaCl through the symplastic and transcellular veins *(Morton et al., 2019)*. Considering that plants can also uptake nutrients through the leaves, an increase in the thickness of the epidermis can act as a mechanism to control the absorption of excessive NaCl *(Mahmood et al., 2019)*. It has been suggested that the movement of nutrients to the interior of plants can involve diffusion through the cuticle and absorbed by leaf cells. Absorption through the stomatal pore can also occur since the

stomata act as potential pathways for the movement of nutrients applied to the leaves *(Li et al., 2019)*.

In the middle region of the leaves, the stomatal density was greater than in the base region, as previously observed by *Santos et al. (2020)*. However, a comparison of the treatments revealed that Si could influence the morphology of the stomata of other leaf regions. The morphophysiological modulations in the middle leaf region in plants grown with Si, such as smaller stomatal density and size, might have occurred to reduce the osmotic stress *(Mahmoudi et al., 2019; Morton et al., 2019)*. This reduction resulting from the action of Si might be a mechanism to maintain the prompt functioning of the stomata for osmotic control. The size of the stomata is related to their functionality because smaller guard cells respond (open/close) faster than larger ones, and consequently maintain the stomatal conductance *(Rouphael et al., 2017)*. Another alteration observed in this study was an increase in the thickness of the chlorenchyma, apparently related to a tradeoff mechanism in which the smaller leaf area is offset by the greater thickness of this tissue *(Pereira et al., 2016)*. This capacity for protecting the photosynthetic tissues permits the maintenance of the plant's biomass production *(Pereira et al., 2016; Ribeiro et al., 2019)*.

The excess of NaCl altered the content of mineral nutrients in *A. blanchetiana*, reducing the contents of the macronutrients S and Ca and the micronutrients Fe, Zn, and Mn. The excessive accumulation of Na^+ competitively inhibits the absorption of other cations, including K^+, Ca^{2+}, and Fe^{2+}, leading to an imbalance in cell homeostasis, oxidative stress, and interference in the functions of Ca^{2+} and K^+ *(Kim et al., 2021)*. We suggest that reducing the contents of S, Ca, Fe, Zn, and Mn reduced the stress tolerance of the plants, generating oxidative stress and affecting the performance of the photosynthetic apparatus. Limited availability of Ca can reduce the tolerance of plants to salt stress since this is involved in the gene induction of tolerance to salt stress and regulation of the antioxidant defense *(Liu, Soundararajan & Manivannan, 2019)*. K plays a fundamental role in synthesizing proteins, photosynthesis, and the activity of glycolytic enzymes in plants *(Liu, Soundararajan & Manivannan, 2019)*.

The modulations of the contents of mineral nutrients in *A. blanchetiana* promoted by Si contributed to improve the nutritional balance and mitigated the damages caused by the toxicity of NaCl in the leaf cells. The increase promoted by Si in the contents of the nutrients Ca, B, Zn, Mn, N, and Mg was probably due to the thinner exodermis in the roots, modulated by Si, which allowed greater absorption of these nutrients. Higher B content may also increase the antioxidant system's defense and diminishes oxidative stress *(Rahman et al.,*

2021). These responses resulted in a better nutritional balance contributing to an increase in the content of photosynthetic pigments and the activity of the enzymes of the antioxidant system (SOD, APX, and CAT). This promoted the protection of the plants' tissues against oxidative damage to the membrane under salt stress, thus alleviating the toxicity of salt and increasing the growth of *A. blanchetiana* plants. The increase in the activity of antioxidant enzymes is also responsible for reducing oxidative stress and eliminating the ROS produced during salt stress *(Tewari, Kumar & Sharma, 2019; Zhang et al., 2019; Chung et al., 2020; Kim et al., 2021)*. These nutrients are structural components of the chlorophyll molecule and play a role in forming the amino acids necessary for the processes of the antioxidant defense system, acting as enzymatic cofactors, for example *(Rahman et al., 2016; Tewari, Kumar & Sharma, 2019; Santos et al., 2021)*. Besides this, the greater activity of the antioxidant system enzymes leads to lower degradation of chlorophyll *(Gong et al., 2018)*. Alterations in the antioxidant system enzymes evidenced the physiological stress caused by NaCl exposure. In this study, the activity of the antioxidant enzymes was greater in the leaves than in the roots of the plants. This result indicates that the direct exposure to NaCl on the leaves had an impact, generating oxidative stress. However, the higher activity of enzymes of plants cultivated in a medium supplemented with Si showed the benefits of this element.

Even though the presence of Na caused stress, as indicated by the biochemical alterations described, this element also appears to play a fundamental role in the metabolism of *A. blanchetiana* plants, and its absorption in minimum quantities seems to have occurred. Plants grown in the 0 µM NaCl + 14 µM Si condition had greater content of Na than in the control plants (Na added only in the form of Na-EDTA in the MS medium). Other studies have shown that *A. blanchetiana* has crassulacean acid metabolism (CAM) for carbon fixation under adverse conditions *(Chaves, Leal & Lemos-Filho, 2015; Krause et al., 2016)*. We suggest that even in *in vitro* conditions, *A. blanchetiana* plants can have some CAM behavior level, such as reducing leaf area and making the leaves more compact. Plants that use CAM metabolism can require sodium ions (Na^+) *(Scholl et al., 2020)*. In this species, Na^+ seems to be fundamental for the regeneration of phosphoenolpyruvate, the substrate for initial carboxylation in plants with C_4 and CAM metabolism *(Scholl et al., 2020)*. CAM metabolism is a mechanism that protects against increased salinity, but the most critical tolerance mechanism can be the accumulation of ions in leaf vacuoles for osmotic adjustment *(Montero et al., 2018)*. In halophytes, the accumulation of Na and its compartmentalization in vacuoles modulate the osmotic potential and help guarantee water absorption under salt stress conditions *(Zeng et al., 2015)*. The Na ions stimulate growth by promoting cell expansion and

partially substitute K ions as an osmotically active solute *(Hussain et al., 2010)*. This modulation of the content of Na^+ can partly explain the salt tolerance and, thus, the existence of *A. blanchetiana* in the sandbank (*Restinga*) region studied here. Furthermore, this can also explain the increase in the Na/K ratio with higher salt concentration and the presence of Si observed in this study, which has been confirmed to be one of the main determinants of resistance to salts *(Liu et al., 2020)*. Despite this increase in the Na/ K ratio, Si was responsible for modulating the competitive absorption between Na and K and maintaining the balance in the intercellular distribution of K in the *A. blanchetiana* plants since the content of K was not different among the treatments.

The morphophysiological modulations promoted by Si, such as the greater activity of the enzymes SOD, APX, and CAT, reduced the stress on the photosynthetic apparatus, as demonstrated by the analysis of the chlorophyll *a* fluorescence. The plants grown in the medium supplemented with Si had the highest values of qP and qL, implying a more remarkable ability for photochemical conversion and transfer of electrons from PSII *(Wang et al., 2018)*. This suggests that even though the plants grown with high NaCl suffered photodamage, the Si was able to ameliorate this damage by maintaining a proper balance of nutrients, as well as enhancing the activity of the antioxidant system, impeding oxidative damage to the photosystems *(Liu et al., 2020)*. The Si also contributed to maintain the electron transport, as evidenced by the higher F_V/F_M ratio, indicating greater potential photochemical activity of PSII *(Lotfi et al., 2018)*. Factors for the photosynthetic apparatus's functioning were also evidenced by the lower values of the parameters of non-photochemical quenching, such as qN, ΦNPQ, and NPQ, compared with the plants grown without Si. These responses helped reduce the damage to the plants caused by the stress, which in turn helped maintain the plants' growth since they had greater fresh weight when cultivated with higher concentrations of NaCl. The excess of NaCl in plants grown without Si caused increases of qN, ΦNPQ, and ΦNO, leading to over-reduction of the photosynthetic electron transport chain, excess excitation energy, and consequently, reduction of the photochemical step and biochemical processes. Furthermore, the increase of ΦNO indicates that this energy loss did not involve the action of trans-thylakoid ΔpH and zeaxanthin, meaning the excess flow of energy was out of control *(Yao et al., 2018; Wang et al., 2018)*.

The increased stress level caused by NaCl affected the functioning of the photosynthetic apparatus by reducing the values of ΦPSII and ETR. The decrease might have partly inhibited the transport of electrons and effective photochemical activity of PSII and increased the formation of ROS since the activity of the antioxidant system was affected. This

reduction indicates a smaller density of the flow of photons absorbed by PSII *(Wang et al., 2018)*. These responses induced by excess NaCl in the absence of Si caused a reduction in the plants' growth. The decline of the fresh and dry weights of the leaves and roots, and thus the reduction in growth, are symptoms commonly observed in plants under salt stress *(Dias et al., 2017)*. This result can be attributed to the osmotic effect of the salt solution beyond the roots, as well as an imbalance in the absorption and assimilation of nutrients *(Dias et al., 2017; Rezende et al., 2018)*.

Conclusion

In *in vitro* conditions, NaCl acted to stunt the growth of the *A. blanchetiana* plants since it affected the plants' anatomy, uptake of nutrients, and physiology. These plants presented tolerance responses by implementing various mechanisms to deal with salt stress, such as thinner walls of the exodermis, reduced stomatal density, and increased non-photochemical dissipation of fluorescence. The application of Si reduced the damages generated by stress through modulation of the root anatomy, enabling greater uptake of nutrients essential for the antioxidant system's activity. The greater enzymatic activity reduced oxidative stress and enabled alterations in the functioning of the photosynthetic apparatus. These modulations contributed to minimizing the damage to the plants caused by the stress, as proved by the chlorophyll *a* fluorescence.

CRediT authorship contribution statement

Rosiane Cipriano, João Paulo Rodrigues Martins, and Lorenzo Toscano Conde performed experiments. Mariela Mattos da Silva and Diolina Moura Silva performed the analysis of enzymatic activity. Rosiane Cipriano and João Paulo Rodrigues Martins wrote the manuscript and performed the statistical analysis. Andreia Barcelos Passos Lima Gontijo and Antelmo Ralph Falqueto provided the structure and contributed to the design and interpretation of the results. All the authors have read and approved the manuscript.

Declaration of Competing Interest

The authors declare that they do not have competing interests.

Acknowledgments: The authors acknowledge the scholarship granted by CAPES (Coordination for the Improvement of Higher Education Personnel). The authors also

acknowledge Luiz Carlos de Almeida Rodrigues for technical assistance in making the figures.

References

Acosta-Motos JR, Díaz-Vivancos P, Álvarez S, Fernández-García N, Sánchez- Blanco MJ, Hernández JA. 2015. NaCl-induced physiological and biochemical adaptative mechanisms in the ornamental *Myrtus communis* L. plants. *Journal Plant Physiology* 183:41-51 DOI: 10.1016/j.jplph.2015.05.005.

Asmar AS, Soares JDR, Silva RAL, Pasqual M, Pio LAS, Castro EM. 2015. Anatomical and structural changes in response to application of silicon (Si) *in vitro* during the acclimatization of banana cv. 'Grand Naine'. *Australian Journal of Crop Science* 9:1236–1241.

Bradford MM. 1976. A rapid and sensitive method for the quantitation of microgram quantities of protein utilizing the principle of protein–dye binding. *Analytical Biochemistry* 72:248–254 DOI: 10.1016/0003-2697(76)90527-3.

Cantabella D, Piqueras A, Acosta-Motos JR, Bernal-Vicente A, Hernández JA, Díaz-Vivancos P. 2017. Salt-tolerance mechanisms induced in *Stevia rebaudiana* Bertoni: Effects on mineral nutrition, antioxidative metabolism and steviol glycoside content. *Plant Physiology and Biochemistry* 115:484–496 DOI: 10.1016/j.plaphy.2017.04.023.

Carillo P. 2018. GABA Shunt in Durum Wheat. *Frontiers in Plant Science* 9:100 DOI: 10.3389/fpls.2018.00100.

Chaves CJN, Leal BSS, Lemos-Filho JP. 2015. Temperature modulation of thermal tolerance of a CAM-tank bromeliad and the relationship with acid accumulation in different leaf regions. *Physiologia Plantarum 154:*500-510 DOI: 10.1111/ppl.12295.

Chung YS, Kim K-S, Hamayun M, Kim Y. 2020. Silicon Confers Soybean Resistance to Salinity Stress Through Regulation of Reactive Oxygen and Reactive Nitrogen Species. *Frontiers in Plant Science* 10:1725 DOI: 10.3389/fpls.2019.01725.

Cipriano R, Martins JPR, Rodrigues LCA, Falqueto AR, Gontijo ABPL. 2021a. Impact of saline solution on growth and photosystem II during *in vitro* cultivation of *Bromelia antiacantha* (Bromeliaceae). *Rodriguésia* 72 DOI: 10.1590/2175-7860202172018.

Cipriano R, Martins JPR, Conde LT, Moreira SW, Clairvil E, Braga PCS, Gontijo ABPL, Falqueto AR. 2021b. Anatomical, physiological, and biochemical modulations of silicon in *Aechmea blanchetiana* (Bromeliaceae) cultivated *in vitro* in response to cadmium. *Plant Cell, Tissue and Organ Culture* 147:271-285 DOI: 10.1007/s11240-021-02122-2.

Claeys H, Landeghen SV, Dubois M, Maleux K, Inzé D. 2014. What is stress? Dose-response effects in commonly used *in vitro* stress assays. *Plant Physiology* 165:519-527 DOI: 10.1104/pp.113.234641.

Coskun D, Britto DT, Huynh WQ, Kronzucker HJ. 2016. The role of silicon in higher plants under salinity and drought stress. *Frontiers in Plant Science* 7:1072 DOI: 10.3389/fpls.2016.01072.

Costa WS, Yamamura RHR, Morcelli CPR, Sígolo JB. 2020. Adição de resíduo de marmoraria em pastas cimentícias, avaliação de suas propriedades mecânicas e caracterização química. INOVAE - Journal of Engineering, Architecture and Technology Innovation 8:1-18.

Dias GMG, Soares JDR, Ribeiro SF, Martins AD, Paqual M, Alves E. 2017. Morphological and physiological characteristics *in vitro* anthurium plantlets exposed to silicon. *Crop Breeding and Applied Biotechnology* 17:18–24 DOI: 10.1590/1984-70332017v17n1a3.

Ferreira DF. 2011. Sisvar: a computer statistical analysis system. *Ciência e Agrotecnologia* 35:1039–1042 DOI: 10.1590/S1413-70542011000600001.

Giannopolitis CN, Ries SK. 1977. Superoxide dismutases: I. Occurrence in higher plants. *Plant Physiology* 59:309-314 DOI: 10.1104/pp.59.2.309.

Gong DH, Wang GZ, Si WT, Zhou Y, Liu Z, Jia J. 2018. Effects of salt stress on photosynthetic pigments and activity of ribulose-1,5-bisphosphate carboxylase/oxygenase in *Kalidium foliatum*. *Russian Journal of Plant Physiology* 65:98–103 DOI: 10.1134/S1021443718010144.

Harter LSH, Harter FS, Deuner C, Meneghello GE, Villela FA. 2014. Effect of salinity on physiological performance of mogango seeds and seedlings. *Horticultura Brasileira* 32:80-85 DOI: 10.1590/S0102- 5362014000100013.

Havir EA, McHale NN. 1987. Biochemical and developmental characterization of multiple forms of catalase in tobacco leaves. *Plant Physiology* 84:450-455 DOI: 10.1104/pp.84.2.450.

Hniličková H, Hnilička F, Orsák M, Hejnák V. 2019. Effect of salt stress on growth, electrolyte leakage, Na^+ and K^+ content in selected plant species. *Plant, Soil and Environment* 65:90–96 DOI: 10.17221/620/2018-PSE.

Hussain K, Nisar MF, Majeed A, Nawaz K, Bhatti KH, Afghan S, Shahazad A, Zia-ul-Hussnian S. 2010. What molecular mechanism is adapted by plants during salt stress tolerance?. *African Journal of Biotechnology* 9:416-422.

Jabeen Z, Irshad F, Habib A, Hussain N, Sajjad M, Mumtaz S, Rehman S, Haider W, Hassan MN. 2022. Alleviation of cadmium stress in rice by inoculation of *Bacillus cereus*. *PeerJ* 10:e13131 DOI: 10.7717/peerj.13131.

Javed R, Gurel E. 2019. Salt stress by NaCl alters the physiology and biochemistry of tissue culture-grown *Stevia rebaudiana* Bertoni. *Turkish Journal of Agriculture and Forestry* 43:11-20 DOI: 10.3906/tar-1711-71.

Johansen DA. 1940. Plant microtechnique. *Nature* 147:222 DOI: 10.1038/147222b0.

Kim B, Lee H, Song YH, Kim H. 2021. Effect of salt stress on the growth, mineral contents, and metabolite profiles of spinach. *Journal of Science of Food and Agriculture* 101:3787-3794 DOI: 10.1002/jsfa.11011.

Krause GH, Winter K, Krause B, Virgo A. 2016. Protection by light against heat stress in leaves of tropical crassulacean acid metabolism plants containing high acid levels. *Functional Plant Biology* 43:1061-1069 DOI: 10.1071/fp16093.

Lawlor DW. 2013. Genetic engineering to improve plant performance under drought: physiological evaluation of achievements, limitations, and possibilities. *Journal of Experimental Botany* 64:83-108 DOI: 10.1093/jxb/ers326.

Larbi A, Kchaoub H, Gaaliche B, Gargouri K, Boulal H, Morales F. 2020. Supplementary potassium and calcium improves salt tolerance in olive plants. *Scientia Horticulturae* 260:108912 DOI: 10.1016/J.SCIENTA.2019.108912.

Li C, Wang P, Van der Ent A, Cheng M, Jiang H, Lund Read T, Lombi E, Tang C, Jonge MD, Menzies NW, Kopittke PM. 2019. Absorption of foliar-applied Zn in sunflower (*Helianthus annuus*): importance of the cuticle, stomata and trichomes. *Annals of Botany* 123:57-68 DOI: 10.1093/aob/mcy135.

Liu B, Soundararajan P, Manivannan A. 2019. Mechanisms of Silicon-Mediated Amelioration of Salt Stress in Plants. *Plants* 8:307 DOI: 10.3390/plants8090307.

Liu C, Zhao X, Yan J, Yuan Z, Gu M. 2020. Effects of Salt Stress on Growth, Photosynthesis, and Mineral Nutrients of 18 Pomegranate (*Punica granatum*) Cultivars. *Agronomy 10:*27 DOI: 10.3390/agronomy10010027.

Lotfi R, Kalaji HM, Valizadeh GR, Khalilvand Behrozyar E, Hemati A, Gharavi-Kochebagh P, Ghassemi A. 2018. Effects of humic acid on photosynthetic efficiency of rapeseed plants growing under different watering conditions. *Photosynthetica* 56:962–970. DOI: 10.1007/s11099-017-0745-9.

Mahmood YA, Ahmed FW, Juma SS, Al-Arazah AA. 2019. Effect of solid and liquid organic fertilizer and spray with humic acid and nutrient uptake of nitrogen, phosphorus and potassium on growth, yield of cauliflower. *Plant Archives* 19:1504-1509.

Mahmoudi H, Salah IB, Zaouali W, Hamrouni L, Gruber M, Ouerghi Z, Hosni K. 2020. Priming-induced changes in germination, morpho-physiological and leaf biochemical responses of fenugreek (*Trigonella foenum-graecum*) under salt stress. *Plant Biosystems* 154:601-614 DOI: 10.1080/11263504.2019.1651785.

Manivannan A, Ahn YK. 2017. Silicon regulates potential genes involved in major physiological processes in plants to combat stress. *Frontiers in Plant Science* 8:1346 DOI: 10.3389/fpls.2017.01346.

Manivannan A, Soundararajan P, Cho YS, Park JE, Jeong BR. 2018. Sources of silicon influence photosystem and redox homeostasis- related proteins during the axillary shoot multiplication of *Dianthus caryophyllus*. *Plant Biosystems* 152:704–710 DOI: 10.1080/11263504.2017.1320312.

Martins JPR, Rodrigues LCA, Santos ER, Batista BG, Gontijo A, Falqueto AR. 2018. Anatomy and photosystem II activity of *in vitro* grown *Aechmea blanchetiana* as affected by 1-naphthaleneacetic acid. *Biologia Plantarum* 62:211–221 DOI: 10.1007/s10535-018-0781-8.

Martins JPR, Rodrigues LCA, Silva TS, Santos ER, Falqueto AR, Gontijo ABPL. 2019. Sources and concentrations of silicon modulate the physiological and anatomical responses of *Aechmea blanchetiana* (Bromeliaceae) during *in vitro* culture. *Plant Cell, Tissue and Organ Culture* 137:397-410 DOI: 10.1007/s11240-019-01579-6.

Martins JPR, Vasconcelos LL, Braga PCS, Rossini FP, Conde LT, Rodrigues LCA, Falqueto AR, Gontijo ABPL. 2020. Morphophysiological responses, bioaccumulation and tolerance of *Alternanthera tenella* Colla (Amaranthaceae) to excess copper under *in vitro* conditions. *Plant Cell, Tissue and Organ Culture* 143:303-318 DOI: 10.1007/s11240-020-01917-z.

Montero E, Francisco AM, Montes E, Herrera A. 2018. Salinity induction of recycling Crassulacean acid metabolism and salt tolerance in plants of *Talinum triangulare*. *Annals of Botany* 121:1333–1342 DOI: 10.1093/aob/mcy030.

Morton MJL, Awlia M, Al-Tamimi N, Saade S, Pailles Y, Negrão S, Tester M. 2019. Salt stress under the scalpel–dissecting the genetics of salt tolerance. *Plant J* 97:148–163 DOI: 10.1111/tpj.14189.

Munns R, Tester M. 2008. Mechanisms of salinity tolerance. *Annual Review of Plant Biology* 59:651–681 DOI: 10.1146/annurev.arplant.59.032607.092911.

Murashige T, Skoog F. 1962. A revised medium for rapid growth and bioassays with tobacco tissue cultures. *Physiologia Plantarum* 15:473–497 DOI: 10.1111/j.1399-3054.1962.tb08052.x.

Nakano Y, Asada K. 1981. Hydrogen peroxide is scavenged by ascorbate specific peroxidase in spinach chloroplasts. *Plant and Cell Physiology* 22:867-880 DOI: 10.1093/oxfordjournals.pcp.a076232.

Negrão S, Schmöckel SM, Tester M. 2017. Evaluating physiological responses of plants to salinity stress. *Annals of Botany* 119:1–11 DOI: 10.1093/aob/mcw191.

Nikalje GC, Srivastava AK, Pandey GK, Suprasanna P. 2017 Halophytes in biosaline agriculture: Mechanism, utilization, and value addition. Land Degradation & Developmental 29:1081–1095 DOI: 10.1002/ldr.2819.

Paez-Garcia A, Motes CM, Scheible W, Chen R, Blancaflor EB, Monteros MJ. 2015. Root traits and phenotyping strategies for plant improvement. Plants 4:334–355 DOI: 10.3390/plants4020334.

Pandey M, Chikara SK. 2015. Effect of salinity and drought stress on growth parameters, glycoside content and expression level of vital genes in steviol glycosides biosynthesis pathway of *Stevia rebaudiana* (Bertoni). *International Journal of Human Genetics* 7:153-160.

Pereira MP, Rodrigues LCA, Corrêa FF, Castro CM, Ribeiro VE, Pereira FJ. 2016. Cadmium tolerance in *Schinus molle* trees is modulated by enhanced leaf anatomy and photosynthesis. *Trees* 30:807-814 DOI: 10.1007/s00468-015-1322-0.

Rahman A, Hossain MS, Mahmud JA, Nahar K, Hasanuzzaman M, Fujita M. 2016. Manganese induced salt stress tolerance in rice seedlings: regulation of ion homeostasis, antioxidant defense and glyoxalase systems. *Physiology and Molecular Biology of Plants* 22:291-306 DOI: 10.1007/s12298-016-0371-1.

Rahman M, Rahman K, Sathi KS, Alam MM, Nahar K, Fujita M, Hasanuzzaman M. 2021. Supplemental Selenium and Boron Mitigate Salt-Induced Oxidative Damages in *Glycine max* L. *Plants 10*:2224 DOI: 10.3390/plants10102224.

Rewald B, Shelef O, Ephrath JE, Rachmilevitch S. 2013. Adaptive plasticity of salt-stressed root systems. In: Ahmad P, Azooz MM, Prasad MNV (eds) Ecophysiology and responses of plants under salt stress, *Springer, New York*, pp 169–202 DOI: 10.1007/978-1-4614-4747-4_6.

Rezende RALS, Rodrigues FA, Soares JDR, Silveira HRO, Pasqual M, Dias GMG. 2018. Salt stress and exogenous silicon influence physiological and anatomical features of *in vitro*-grown cape gooseberry. *Ciência Rural* 48 DOI: 10.1590/0103-8478cr20170176.

Ribera-Fonseca A, Rumpel C, Mora ML, Nikolic M, Cartes P. 2018. Sodium silicate and calcium silicate differentially affect silicone and aluminium uptake, antioxidant performance and phenolics metabolism of ryegrass in an acid Andisol. *Crop and Pasture Science* 69:205–215 DOI: 10.1071/CP17202.

Ribeiro VE, Pereira MP, De Castro EM, Corrêa FF, Cardoso MG, Pereira FJ. 2019. Enhanced essential oil and leaf anatomy of *Schinus molle* plants under lead contamination. *Industrial Crops and Products* 132:92-98 DOI: 10.1016/j.indcrop.2019.02.014.

Rios JJ, Martínez-Ballesta MC, Ruiz JM, Blasco B, Carvajal M. 2017. Silicon- mediated improvement in plant salinity tolerance: The role of aquaporins. *Frontiers in Plant Science* 8:948 DOI: 10.3389/fpls.2017.00948.

Rodrigues FA, Rezende RALS, Soares JDR, Rodrigues VA, Pasqual M, Silva SO. 2017. Application of silicon sources in yam (*Dioscorea* spp.) micropropagation. *Australian Journal of Crop Science* 11:1469–1473 DOI: 10.21475/ajcs.17.11.11.pne685.

Rouphael Y, Micco V, Arena C, Raimondi G, Colla G, Pascale S. 2017. Effect of *Ecklonia maxima* seaweed extract on yield, mineral composition, gas exchange, and leaf anatomy of zucchini squash grown under saline conditions. *Journal of Applied Phycology* 29:459–470 DOI: 10.1007/s10811-016-0937-x.

Sahebi M, Hanafi MM, Azizi P. 2016. Application of silicon in plant tissue culture. *In Vitro Cellular & Developmental Biology - Plant* 52:226-232 DOI: 10.1007/s11627-016-9757-6.

Santos ER, Martins JPR, Rodrigues LCA, Gontijo ABPL, Falqueto AR. 2020. Morphophysiological responses of *Billbergia zebrina* Lindl. (Bromeliaceae) in function of types and concentrations of carbohydrates during conventional *in vitro* culture. *Ornamental Horticulture* 26:18–34 DOI: 10.1590/2447-536X.v26i1.2092.

Santos LR, Paula LS, Pereira YC, Silva BRS, Batista BL, Alsahli AA, Lobato AKS. 2021. Brassinosteroids- Mediated Amelioration of Iron Deficiency in Soybean Plants: Beneficial Effects on the Nutritional Status, Photosynthetic Pigments and Chlorophyll Fluorescence. *Journal of Plant Growth Regulation* 40:1803–1823 DOI: 10.1007/s00344-020-10232-y.

Sarruge JR; Haag HP. 1974. Análise química de plantas. Piracicaba: Departamento de Química- Escola Superior de Agricultura Luiz de Queiroz 56p.

Scholl J, Dengler L, Bader L, Forchhammer K. 2020. Phosphoenolpyruvate Carboxylase from the cyanobacterium *Synechocystis* sp. PCC 6803 is under global metabolic control by P_{II} signaling. *Molecular Microbiology* 114:1–16 DOI: 10.1111/mmi.14512.

Schreiber U. 1986. Detection of rapid induction kinetics with a new type of high-frequency modulated chlorophyll fluorometer. *Photosynthesis Research* 9: 261–272 DOI: 10.1007/BF00029749.

Sivanesan I, Park SW. 2014. The role of silicon in plant tissue culture. *Frontiers in Plant Science* 5:1-4 DOI: 10.3389/fpls.2014.00571.

Terletskaya N, Duisenbayeva U, Rysbekova A, Kurmanbayeva M, Blavachinskaya I. 2019. Architectural traits in response to salinity of wheat primary roots. *Acta Physiologiae Plantarum* 41:157 DOI: 10.1007/s11738-019-2948-0.

Tewari RK, Kumar P, Sharma PN. 2019. An effective antioxidante defense provides protection against zinc deficiency-induced oxidative stress in Zn-efficient maize plants. *Journal of Plant Nutrition and Soil Science* 182:701–707 DOI: 10.1002/jpln.20180 0622.

Trejo-Téllez LI, García-Jiménez A, Escobar-Sepúlveda HF, Ramírez-Olvera SM, Bello-Bello JJ, Gómez-Merino FC. 2020. Silicon induces hormetic dose-response effects on growth and concentrations of chlorophylls, amino acids and sugars in pepper plants during the early developmental stage. *PeerJ* 8:e9224 DOI: 10.7717/peerj.9224.

Wang Z, Li G, Sun H, Ma L, Guo Y, Zhao Z, Gao H, Mei L. 2018. Effects of drought stress on photosynthesis and photosynthetic electron transport chain in young apple tree leaves. *Biology Open* 7: bio035279 DOI: 10.1242/bio.035279.

Wellburn AR. 1994. The spectral determination of chlorophylls *a* and *b*, as well as total carotenoids, using various solvents with spectrophotometers of different resolution. *Journal of Plant Physiology* 144:307–313 DOI: 10.1016/S0176-1617(11)81192-2.

Wu J, Guo J, Hu Y, Gong H. 2015. Distinct physiological responses of tomato and cucumber plants in silicon-mediated alleviation of cadmium stress. *Frontiers in Plant Science* 6:453 DOI: 10.3389/fpls.2015.00453.

Yao J, Sun D, Cen H, Xu H, Weng H, Yuan F, He Y. 2018. Phenotyping of Arabidopsis drought stress response using Kinetic Chlorophyll Fluorescence and Multicolor Fluorescence Imaging. *Frontiers in Plant Science* 9: 603 DOI: 10.3389/fpls.2018.00603.

Zeng Y, Li L, Yang R, Yi X, Zhang B. 2015. Contribution and distribution of inorganic ions and organic compounds to the osmotic adjustment in *Halostachys caspica* response to salt stress. *Scientific Reports* 5:13639 DOI: 10.1038/srep13639.

Zushi K, Matsuzoe N. 2017. Using of chlorophyll a fluorescence OJIP transients for sensing salt stress in the leaves and fruits of tomato. *Scientia Horticulturae* 219:216–221 DOI: 10.1016/j.scienta.2017.03.016.

Zhang Y, Liang Y, Zhao X, Jin X, Hou L, Shi Y, Ahammed GJ. 2019. Silicon Compensates Phosphorus Deficit-Induced Growth Inhibition by Improving Photosynthetic Capacity, Antioxidant Potential, and Nutrient Homeostasis in Tomato. *Agronomy* 9:733 DOI: 10.3390/agronomia9110733.

Zhu YX, Gong HJ, Yin JL. 2019. Role of Silicon in Mediating Salt Tolerance in Plants: A Review. *Plants* 8:147 DOI: 10.3390/plants8060147.

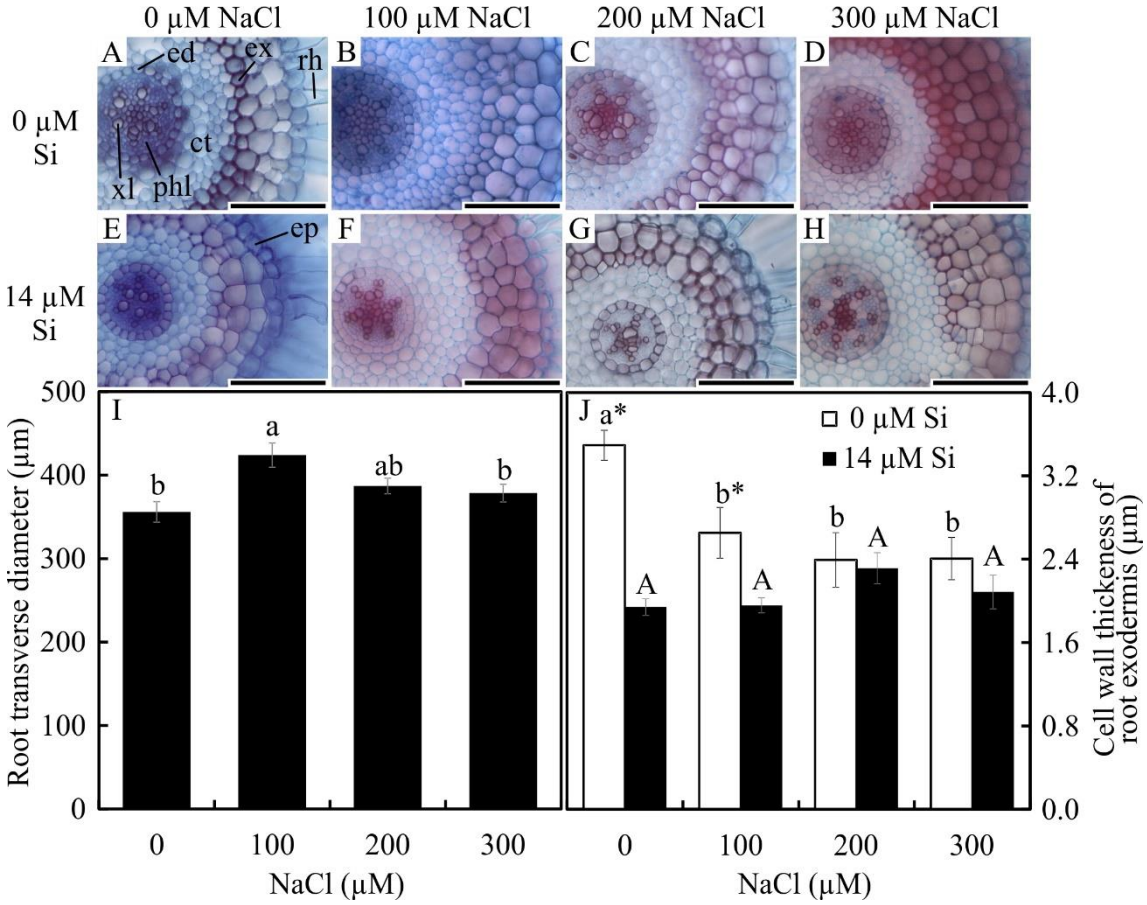

Fig. 1. Cross-sections (A–H) and anatomical traits (I–J) of roots of *Aechmea blanchetiana* plants in the function of different concentrations of sodium chloride (NaCl) in the absence and presence of silicon (Si) during *in vitro* culture. Root transverse diameter (I) and cell wall thickness of root exodermis (J) of *Aechmea blanchetiana* in the function of the NaCl concentration (µM) and in the absence and presence of silicon (Si) during *in vitro* culture. (I) Means (± SE), *n* = 6, followed by the same letter do not differ according to the Tukey test at 5% significance. (J) Means (± SE), *n* = 6, followed by the same letter (lowercase for 0 µM Si and uppercase for 14 µM Si), at each NaCl concentration, do not differ according to the Tukey test at 5% significance. For each Si concentration analyzed (0 and 14 µM Si), the means followed by an asterisk are significantly different according to the Tukey test at 5% significance. ct – cortex, ed – endodermis, ep – epidermis, ex – exodermis, rh – root hair, xl – xylem, and phl – phloem. Bars =100 µm.

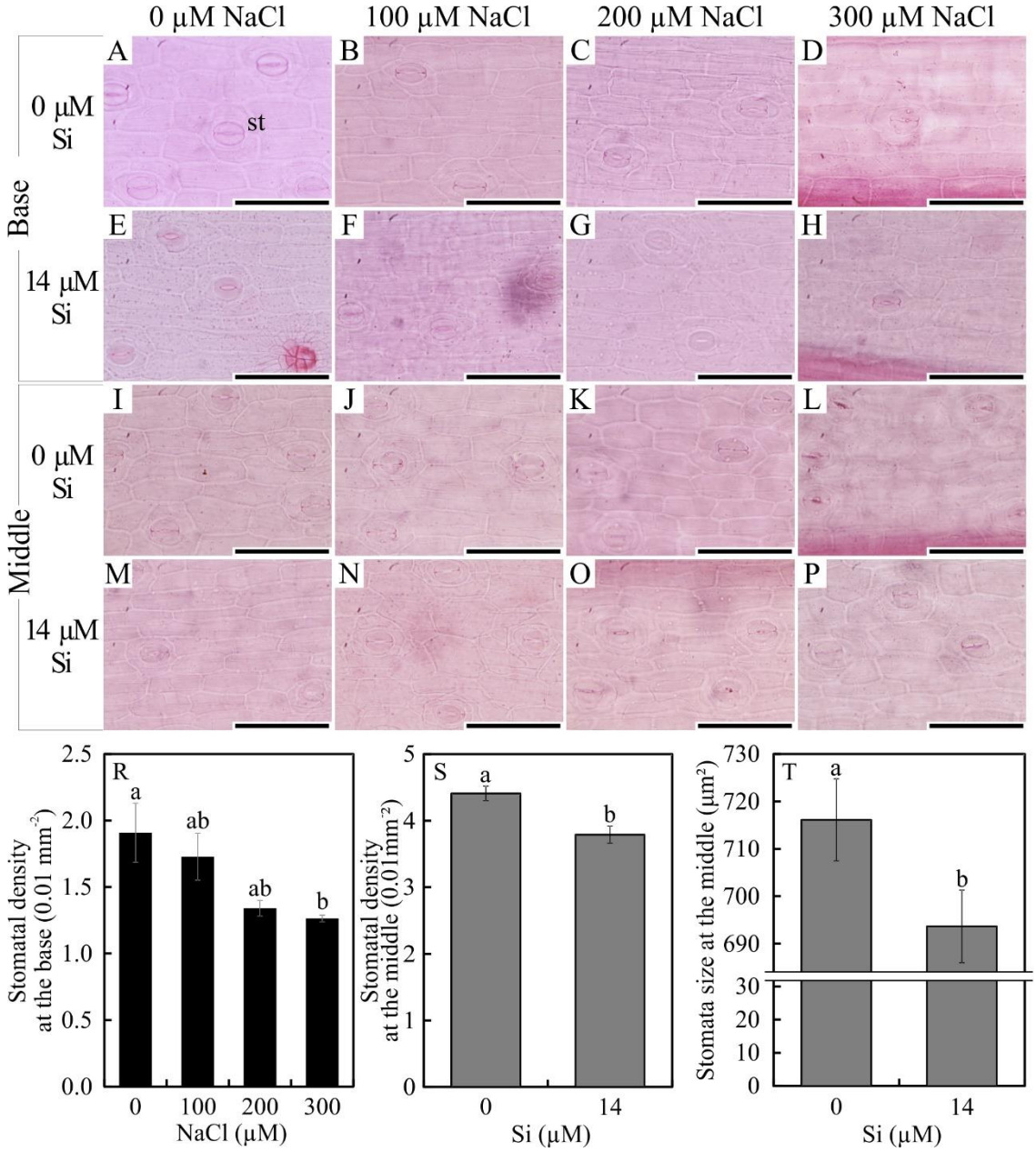

Fig. 2. Paradermal sections (A – P) and stomatal traits of leaves of *Aechmea blanchetiana* plants in the function of different concentrations of sodium chloride (NaCl) in the absence and presence of silicon (Si) during *in vitro* culture. Means (± SE), *n* = 6, followed by the same letter, do not differ according to the Tukey test at 5% significance. st – stomata. Bars = 100 µm.

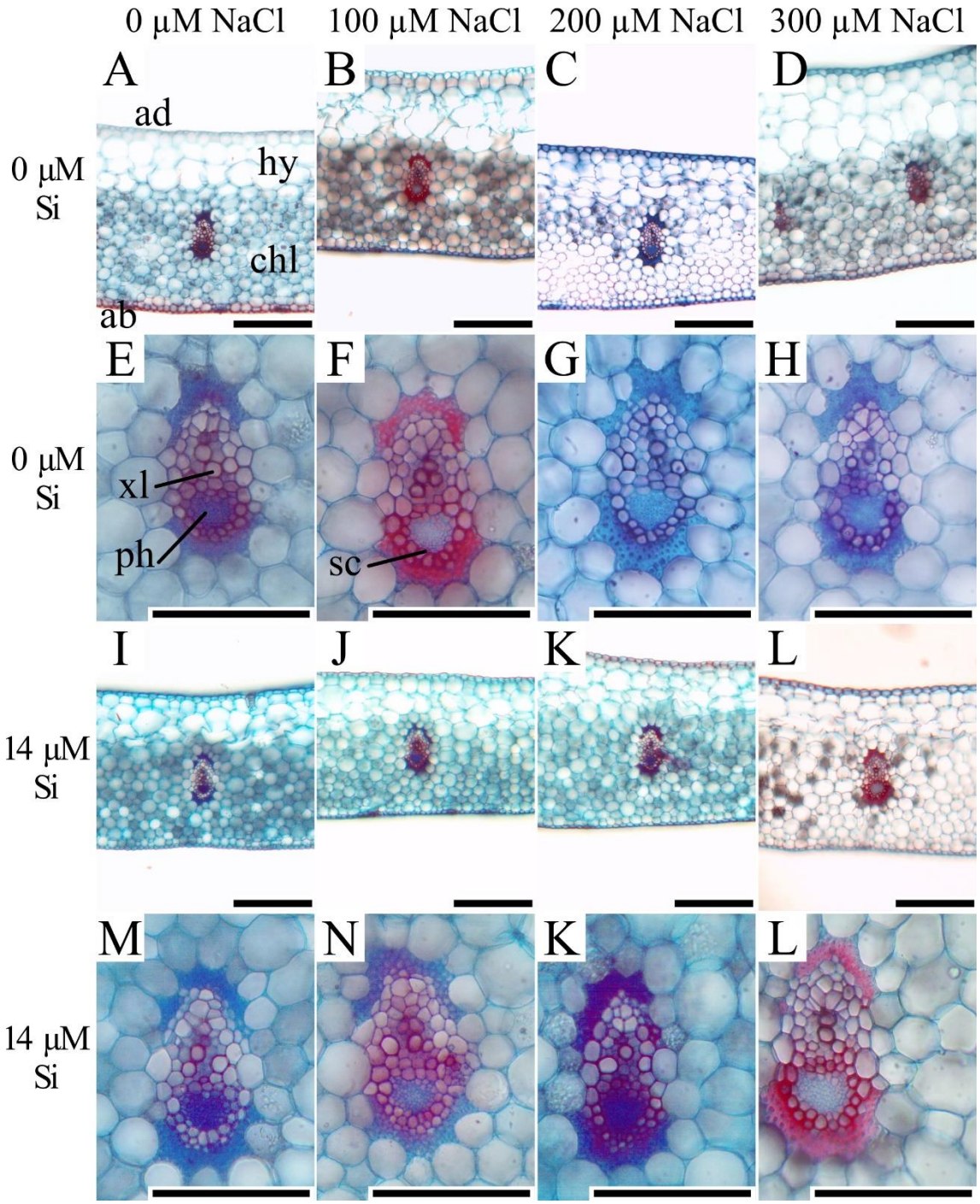

Fig. 3. Cross-sections of leaves of *Aechmea blanchetiana* plants in the function of different concentrations of sodium chloride (NaCl) in the absence and presence of silicon (Si) during *in vitro* culture. ad – adaxial epidermis, ab – abaxial epidermis, chl – chlorenchyma, hy – hydrenchyma, ph – phloem, sc – sclerenchyma, xl – xylem. Bars = 100 µm.

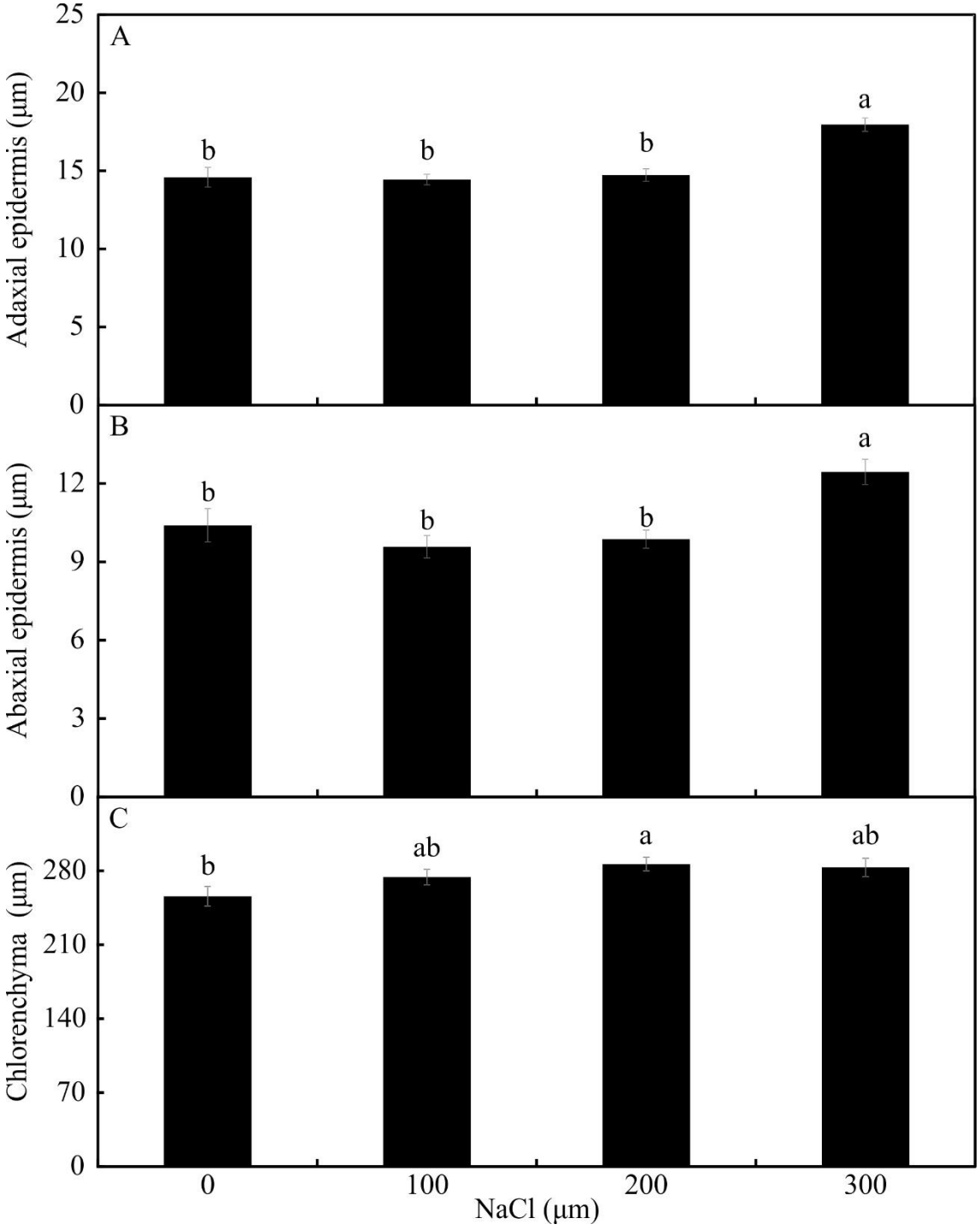

Fig. 4. The thickness of the adaxial and abaxial faces of the epidermis (µm) (A – B) and the chlorenchyma (C) of leaves of *Aechmea blanchetiana* in the function of the concentrations of NaCl (0, 100, 200, 300 µM). Means (± SE), *n* = 6, followed by the same letter, do not differ according to the Tukey test at 5% significance.

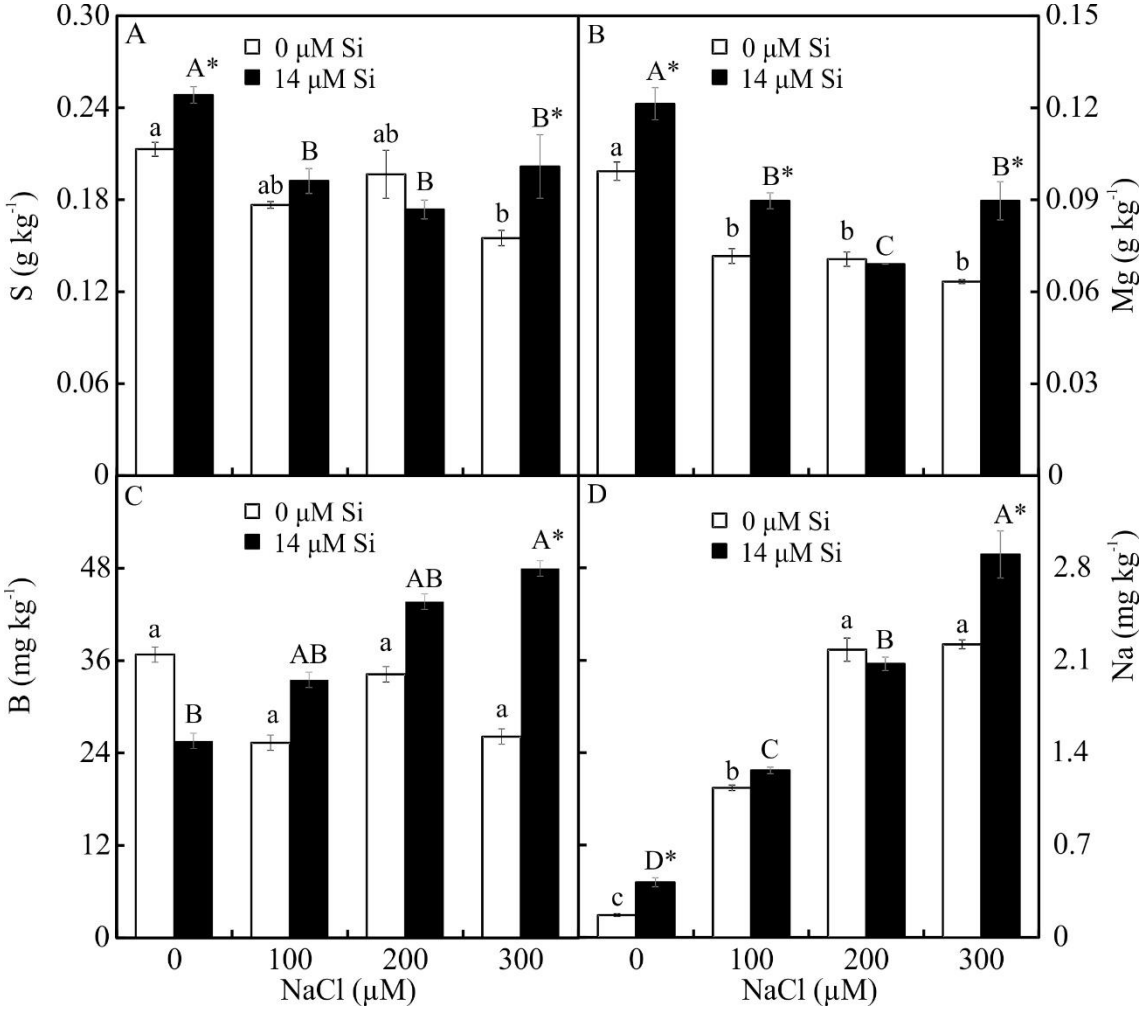

Fig. 5. Contents of macronutrients and micronutrients in *Aechmea blanchetiana* plants in the function of NaCl concentrations (0, 100, 200, 300 µM) combined with 0 or 14 µM Si. For each nutrient, the means (± SE), $n = 3$, followed by the same letter (lowercase for 0 µM Si and uppercase for 14 µM Si), at each NaCl concentration, do not differ according to the Tukey test at 5% significance. For each Si concentration analyzed (0 and 14 µM Si), the means followed by an asterisk are significantly different according to the Tukey test at 5% significance. S = sulfur, Mg = magnesium, B = boron, Na = sodium.

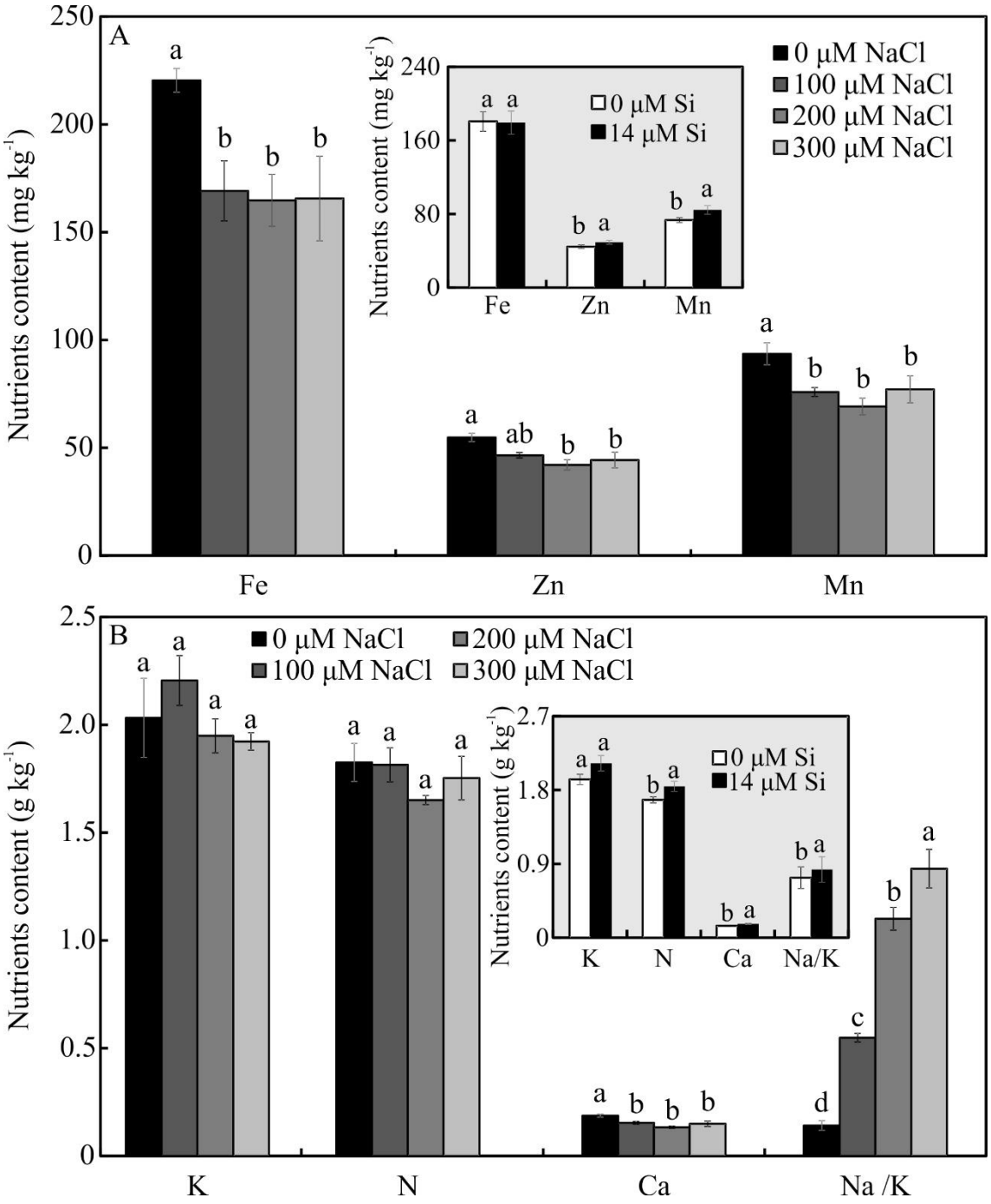

Fig. 6. Contents of nutrients in *Aechmea blanchetiana* plants in the function of the concentrations of NaCl (0, 100, 200, 300 µM) or concentration of Si (0 or 14 µM Si). For each content of nutrients, the means (± SE), *n* = 3, followed by the same letter do not differ according to the Tukey test at 5% significance. Fe = iron, Zn = zinc, Mn = manganese, Ca = calcium, N = nitrogen, K = potassium, Na = sodium.

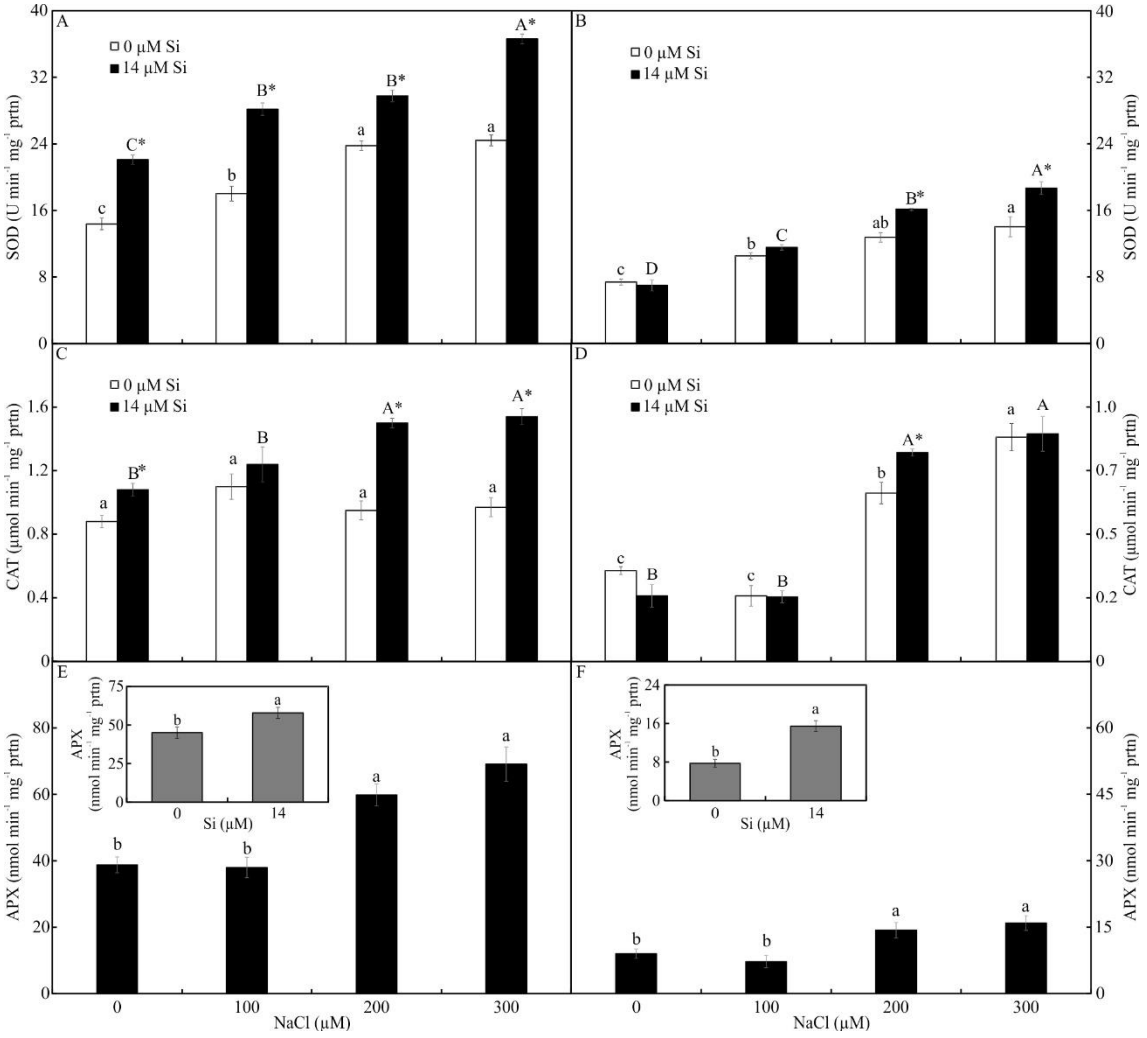

Fig. 7. The activity of superoxide dismutase (SOD), catalase (CAT), and ascorbate peroxidase (APX), respectively, in the leaves (A-C-E) and roots (B-D-F) of *Aechmea blanchetiana* plants cultivated *in vitro* in the function of the concentrations of NaCl (0, 100, 200, 300 µM) and concentration of Si (0 or 14 µM Si). Means (± SE), $n = 5$, followed by the same letter (lowercase for 0 µM Si and uppercase for 14 µM Si), at each NaCl concentration, do not differ according to the Tukey test at 5% significance. For each Si concentration analyzed (0 and 14 µM Si), the means followed by an asterisk are significantly different according to the Tukey test at 5% significance (A-D). Means (± SE), $n = 5$ followed by the same letter at each NaCl concentration, do not differ between Si content according to the Tukey test at 5% significance.

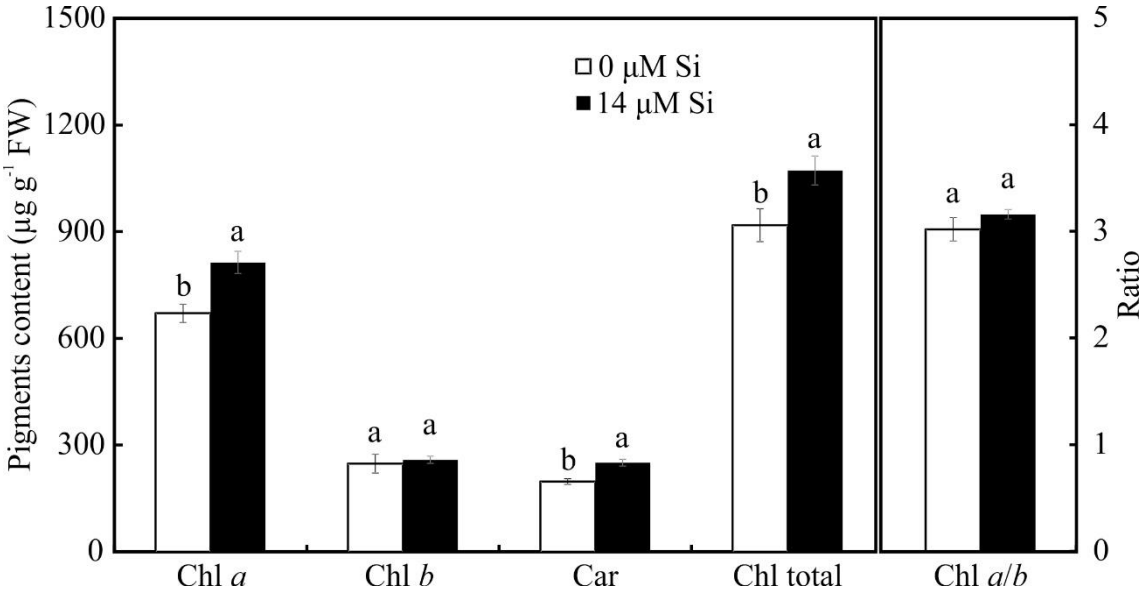

Fig. 8. Contents of the photosynthetic pigments in *Aechmea blanchetiana* plants in the function of the presence or absence of Si (0 or 14 μM Si). Means (± SE), n = 8, followed by the same letter in each photosynthetic pigment, do not differ according to the Tukey test at 5% significance.

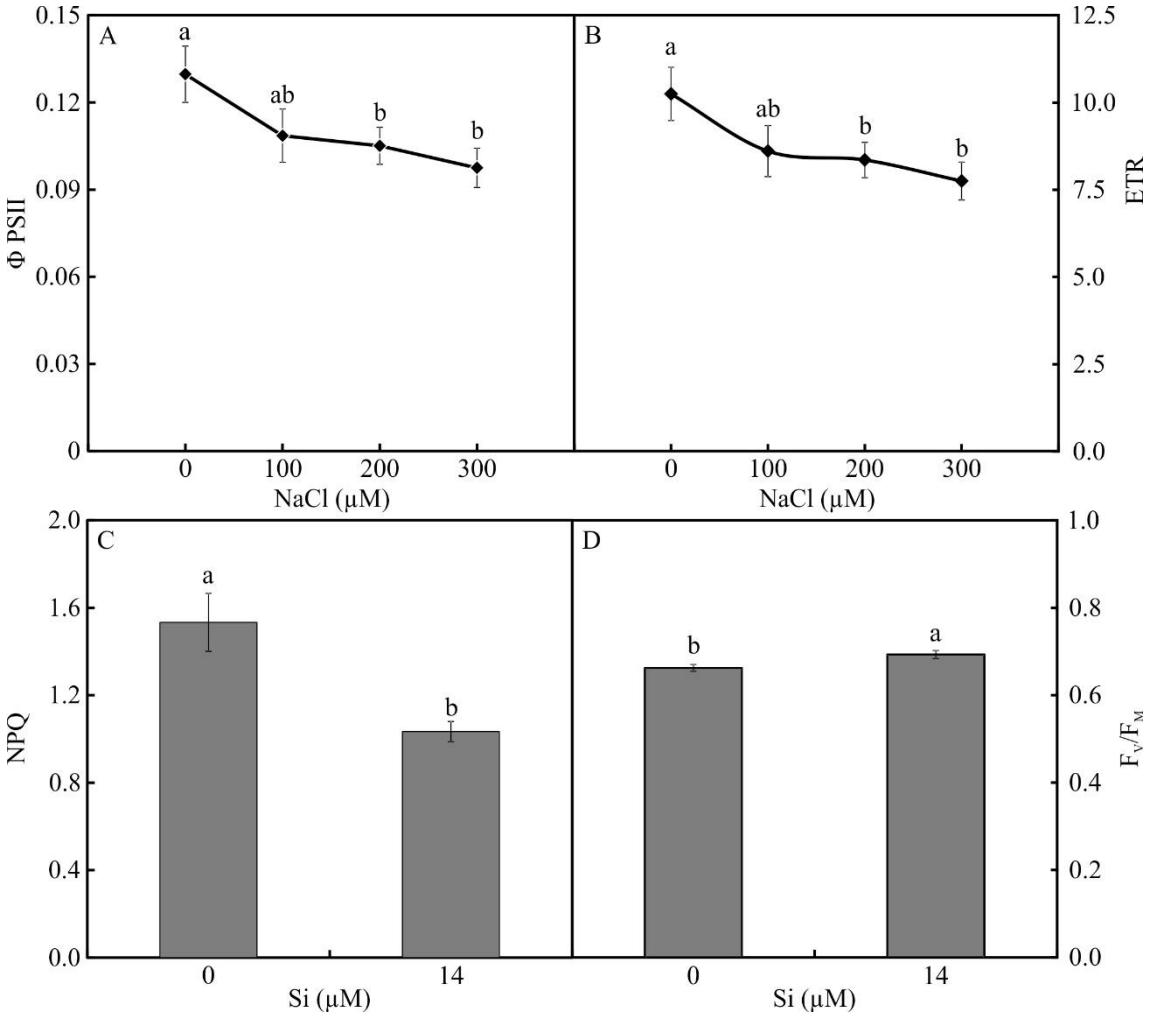

Fig. 9. The effective photochemical quantum yield of PSII (ΦPSII) (A) and electron transport rate (ETR) (B) in the function of the concentrations of NaCl (0, 100, 200, 300 μM). Non-photochemical dissipation of fluorescence (non-photochemical quenching) (NPQ) (C) and maximum quantum yield of PSII (F_V/F_M) (D) in *Aechmea blanchetiana* plants in the function of the presence or absence of Si (0 or 14 μM Si). Means (± SE), n = 12, followed by the same letter for each parameter, do not differ according to the Tukey test at 5% significance.

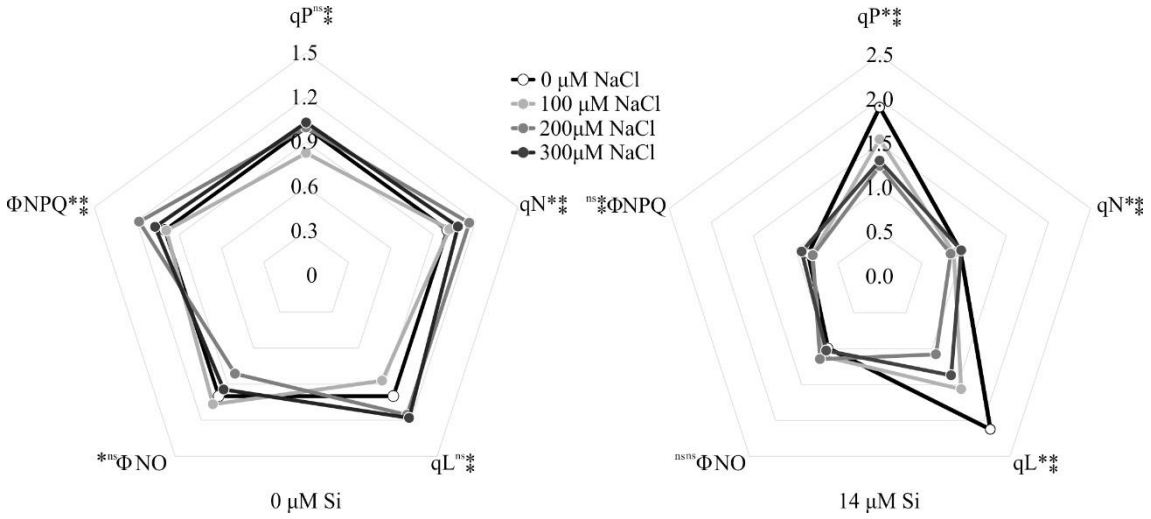

Fig. 10. Modulated fluorescence parameters of *Aechmea blanchetiana* plants in the function of the concentrations of NaCl (0, 100, 200, 300 µM) combined with 0 µM Si (A) or 14 µM Si (B). For each parameter, means (n = 12) followed by an asterisk (*) denote significant differences between the concentrations of NaCl at each level of Si, while two asterisks (‡) denote significant differences between the presence and absence of Si according to the Tukey test at 5% probability. ns = no significant.

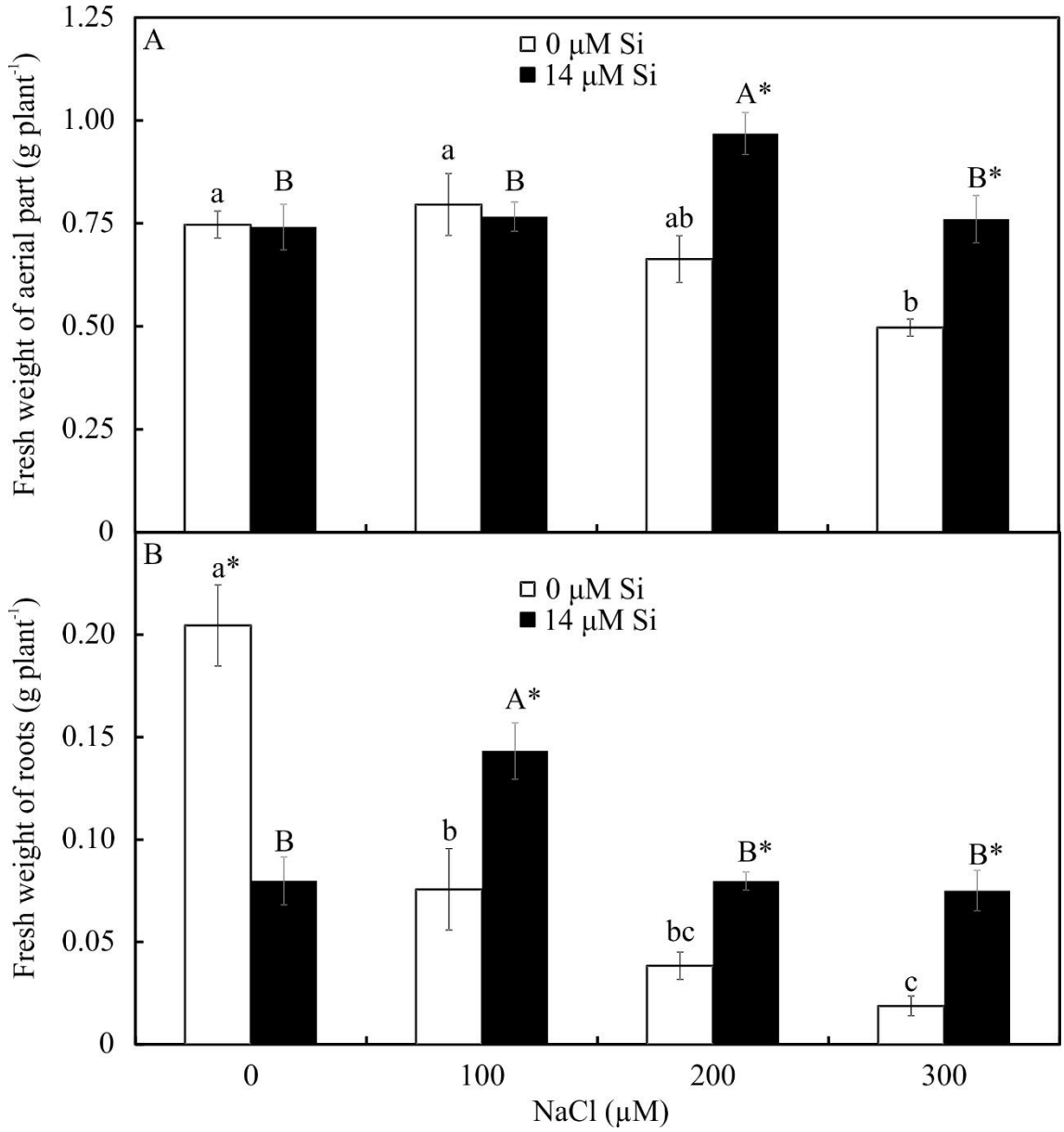

Fig. 11. Shoot (A) and root (B) fresh weights of *Aechmea blanchetiana* plants in the function of the concentrations of NaCl combined with 0 or 14 µM Si. Means (± SE), *n* = 5, followed by the same letters (lowercase for 0 µM Si and uppercase for 14 µM Si) at each NaCl concentration, do not differ according to the Tukey test at 5% significance. For each Si concentration analyzed (0 and 14 µM Si), the means followed by an asterisk are significantly different according to the Tukey test at 5% significance

CAPÍTULO 3

Plant Cell, Tissue and Organ Culture (PCTOC)
https://doi.org/10.1007/s11240-021-02122-2

ORIGINAL ARTICLE

Anatomical, physiological, and biochemical modulations of silicon in Aechmea blanchetiana (Bromeliaceae) cultivated in vitro in response to cadmium

Rosiane Cipriano[1,2] · João Paulo Rodrigues Martins[1,2] · Lorenzo Toscano Conde[2] · Samuel Werner Moreira[2] · Evens Clairvil[2] · Priscila da Conceição de Souza Braga[1] · Andreia Barcelos Passos Lima Gontijo[2] · Antelmo Ralph Falqueto[1]

Received: 28 March 2021 / Accepted: 5 June 2021

Abstract
Cadmium (Cd) has no known biological role in plants but shows high toxicity. A viable alternative to alleviate the deleterious effects of plants under heavy metal stress is with the use of silicon (Si). The objective was to investigate the anatomical, physiological, and biochemical modulations of *Aechmea blanchetiana* exposed to Cd in vitro and the Cd and Si co-exposure. Plants previously established under in vitro culture conditions were transferred to MS culture medium with 0 or 14 µM Si and solidified with agar. After 30 days of growth, a stationary liquid MS medium containing increasing concentrations of Cd (0, 50, 100 or 200 µM) was added to the containers, forming a biphasic medium. After 45 days, anatomical and physiological analyses were performed. Plants cultivated with 14 µM Si showed a thinner exodermis, a decrease in the Chl *a*/*b* ratio and a higher *total* Chl/Car ratio. The positive L- and K-bands were verified at all applied Cd concentrations. Cd induced damage to the oxygen-evolving complex (W_K) and altered the quantum yield of non-regulated energy dissipation (ΦNO). In the presence of Si there was an increase in the photochemical activity of photosystem II and electron transport, even when the plants were exposed to Cd. The plants were able to withstand exposure to Cd, although exhibiting physiological disturbances. The anatomical, physiological, and biochemical responses induced by Si were effective in easing the stress of *A. blanchetiana* plants grown in vitro with Cd.

Key Message
A. blanchetiana plants were able to withstand exposure to Cd, although exhibiting physiological disorders. The responses induced by Si were effective in easing the stress of *A. blanchetiana* grown in vitro with Cd.

Keywords Chlorophyll *a* fluorescence · Modulated fluorescence · Plant physiology · Plant tissue culture · Heavy metal

Introduction

Heavy metal contamination is a global environmental problem. It is mainly caused by anthropogenic, industrial, and agricultural activities, such as dispersion of mining waste, phosphate fertilizers, and metal-based pesticides (Malčovská et al. 2014; Paunov et al. 2018; Kaya et al. 2020). Heavy metals are highly stable, non-biodegradable and, therefore, easily transported and accumulated through the food chain, which can significantly threaten living beings (Younis et al. 2016; Feng et al. 2018b).

Cadmium (Cd) is one of the most dangerous heavy metals due to its high mobility in the soil–plant system (Feng et al.

Communicated by Mohammad Faisal.

✉ João Paulo Rodrigues Martins
jprmartinss@yahoo.com.br

[1] Plant Ecophysiology Laboratory, Federal University of Espírito Santo, Litorâneo, São Mateus, ES 29932-540, Brazil

[2] Plant Tissue Culture Laboratory, Federal University of Espírito Santo, Litorâneo, São Mateus, ES 29932-540, Brazil

Published online: 11 June 2021

CAPÍTULO 3

Anatomical, physiological, and biochemical modulations of silicon in *Aechmea blanchetiana* (Bromeliaceae) cultivated in vitro in response to cadmium

Rosiane Cipriano [1,2], João Paulo Rodrigues Martins[1,2]*, Lorenzo Toscano Conde[2], Samuel Werner Moreira[2], Evens Clairvil[2], Priscila da Conceição de Souza Braga[1], Andreia Barcelos Passos Lima Gontijo[2], Antelmo Ralph Falqueto[1]

[1] Plant Ecophysiology Laboratory, Federal University of Espírito Santo, Litorâneo, São Mateus, ES 29932-540, Brazil

[2] Plant Tissue Culture Laboratory, Federal University of Espírito Santo, Litorâneo, São Mateus, ES 29932- 540, Brazil

*Author for correspondence: jprmartinss@yahoo.com.br

Manuscript published in the journal: *Plant Cell, Tissue and Organ Culture (PCTOC)*

Abstract

Cadmium (Cd) has no known biological role in plants but shows high toxicity. A viable alternative to alleviate the deleterious effects of plants under heavy metal stress is with the use of silicon (Si). The objective was to investigate the anatomical, physiological, and biochemical modulations of *Aechmea blanchetiana* exposed to Cd in vitro and the Cd and Si co-exposure. Plants previously established under in vitro culture conditions were transferred to MS culture medium with 0 or 14 µM Si and solidified with agar. After 30 days of growth, a stationary liquid MS medium containing increasing concentrations of Cd (0, 50, 100 or 200 µM) was added to the containers, forming a biphasic medium. After 45 days, anatomical and physiological analyses were performed. Plants cultivated with 14 µM Si showed a thinner exodermis, a decrease in the Chl *a/b* ratio and a higher *total* Chl/Car ratio. The positive L- and K-bands were verified at all applied Cd concentrations. Cd induced damage to the oxygen-evolving complex (W_K) and altered the quantum yield of non-regulated energy dissipation (ΦNO). In the presence of Si there was an increase in the photochemical activity of photosystem II and electron transport, even when the plants were exposed to Cd. The plants were able to withstand exposure to Cd, although exhibiting physiological disturbances. The anatomical, physiological, and biochemical responses induced by Si were effective in easing the stress of *A. blanchetiana* plants grown in vitro with Cd.

Keywords: chlorophyll *a* fluorescence; modulated fluorescence; plant physiology; plant tissue culture; heavy metal

Introduction

Heavy metal contamination is a global environmental problem. It is mainly caused by anthropogenic, industrial, and agricultural activities, such as dispersion of mining waste, phosphate fertilizers, and metal-based pesticides (Malčovská et al. 2014; Paunov et al. 2018; Kaya et al. 2020). Heavy metals are highly stable, non-biodegradable and, therefore, easily transported and accumulated through the food chain, which can significantly threaten living beings (Younis et al. 2016; Feng et al. 2018b).

Cadmium (Cd) is one of the most dangerous heavy metals due to its high mobility in the soil-plant system (Feng et al. 2018a). It is found naturally in soils due to the decomposition of rocks, but its concentration increases with anthropic activities. It is also common in water and the atmosphere. Critical levels for Cd toxicity in plants range from 6 to 10 μg g^{-1} of the plant dry mass (Oliveira et al. 2017). This element has no biological function known as a nutrient and demonstrates high toxicity, even at low concentrations in plant tissues (Feng et al. 2018a).

Plants that grow in an environment with a high Cd content may present biochemical disturbances and morphophysiological changes. Among the various toxicity symptoms, inhibition of germination, chlorosis, necrosis, growth inhibition, changes in ionic homeostasis, severe disturbances in water relations and nutrient transport have been reported (Malčovská et al. 2014; Oliveira et al. 2017), besides being able to induce changes in pigment content and stomatal conductance, which directly affect the access to CO_2 and photosynthesis rate (Paunov et al. 2018). This metal can also decrease the rate of photosynthetic electron transport chain causing severe photosynthetic disturbances (Oliveira et al. 2017), as well as stimulating oxidative stress by producing reactive oxygen species (ROS), malondialdehyde (MDA), and electrolyte leakage (Nahar et al. 2016; Kaya et al. 2020), which can alter the activities of several key enzymes and even cause cell death (Nahar et al. 2016; Younis et al. 2016).

Different mechanisms have been employed to reduce the toxicity of Cd in plants (Adrees et al. 2015; Rizwan et al. 2016b, 2016c; Younis et al. 2016). Silicon (Si), despite being the second most abundant element in the Earth's crust, its essentiality as a nutrient for plant species is still being discussed. However, the mitigating effect of Si under stress conditions, including pests, diseases, salt stress, drought, radiation and metal toxicity, has already been documented (Malčovská et al. 2014; Adrees et al. 2015; Asmar et al. 2015; Ghassemi-Golezani; Lotfi 2015; Etesami; Jeong 2018; Martins et al. 2019). The use of Si can play positive roles in plants, helping with growth, increasing mineral nutrition and the content of photosynthetic pigments and inducing beneficial morphological changes against heavy metal toxicity. The mitigating effect of Si on Cd-induced toxicity symptoms has been reported in different plant species (Farooq et al. 2013; Malčovská et al. 2014; Ma et al. 2015; Rizwan et al. 2016a; Alzahrani et al. 2018; Khan et al. 2020).

In vitro cultivation is a technique with the potential advantage to isolate the effects of heavy metals on plant metabolism from the effects caused by other types of stress that can interfere with plant response (Giampaoli et al. 2012). This technique allows for anatomical and physiological analysis of plants in controlled microenvironments. Several studies have investigated changes in the physiology and anatomy of plants exposed to Cd in vitro (Son et al. 2014; Anju et al. 2015; Manquián-Cerda et al. 2016; Rodrigues et al. 2017) and other metals (Giampaoli et al 2012; Martins et al. 2016; Martins et al. 2020a). Among the physiological studies, the techniques related to the chlorophyll *a* fluorescence are widely used for characterizing the performance of the photosynthetic apparatus (mainly photosystem II - PSII), providing detailed information about the structure and

function. This analysis is widely used to verify the photochemical performance of plants under stressful conditions (Kalaji et al. 2016, 2017a, 2017b, 2018; Stirbet et al. 2018), as well as exposure to different metals (Zurek et al. 2014; Franić et al. 2017; Paunov et al. 2018; Martins et al. 2020a).

Bromeliads may be helpful in studies within heavy metals due to the formation of a tank system with their leaves at the base of the plant rosette, which can store a large amount of environmental debris and water, resulting in prolonged exposure to metals (Schreck et al. 2016; Martins et al. 2020a). The tank system is a characteristic of many species of bromeliads and it is naturally formed by broad leaves, which overlap basally, forming chambers that store debris and water. Several species of bromeliads show potential as bioindicators of heavy metals, and this potential has already been demonstrated using in vitro conditions (Giampaoli et al. 2012, 2016; Piazzetta et al. 2018; Martins et al. 2016, 2020a). In the present study, the species *Aechmea blanchetiana* (Baker) L.B. Smith (Bromeliaceae) was chosen as a model plant. It is native to sandbank areas of north-eastern Brazil, an environment characterized as saline and containing Si (Kanashiro et al. 2009; Costa et al. 2020). *A. blanchetiana* has been widely used in landscape projects and present tolerance to high concentrations of a heavy metal (Cu), which proposes its potential for use as a bioindicator (Martins et al. 2020a). Therefore, it is suggested that it may also serve as a potential bioindicator for other heavy metals. Despite the existence of several studies that evaluate the effects of high Cd concentrations on plant performance, it is not yet clear how Si would mitigate toxicity to Cd for in vitro conditions based on morphophysiological modulations. Thus, the objective of this study was to investigate the anatomical, physiological, and biochemical modulations of *Aechmea blanchetiana* exposed to Cd in vitro and the potential for stress relief by heavy metal of calcium silicate ($CaSiO_3$).

Material and Methods

Plant material and in vitro culture conditions

Side shoots of 2.5 cm in length of the aerial part of *A. blanchetiana* were obtained as described by Martins et al. (2018). These were transferred to 268 mL glass containers containing 30 mL of MS culture medium (Murashige and Skoog 1962) with 0 or 14 µM Si ($CaSiO_3$), 30 g L^{-1} sucrose, 4 µM 1-naphthalenoacetic acid (NAA) and solidified with 5 g L^{-1} agar. The $CaSiO_3$ concentrations were chosen according to Martins et al. (2019). The media had the pH adjusted to 5.8 before autoclaving at 120ºC for 20 minutes. After inoculation in a laminar flow chamber, the plant material was kept in a growth room for 30 days at 26±2°C and a 16-hour photoperiod (8:00 am to 12:00 am) under LED lamps (Luminaria Slim LED 36W Bi-Volt 2800 lm).

After 30 days of in vitro growth, 30 mL of stationary liquid MS medium were added to the containers, consisting of 25% of the original saline solution (v/v), without addition of sucrose. The medium was supplemented with different concentrations of Cd (0; 50; 100; 200 µM), forming a medium with two phases (biphasic) and eight treatments (2 Si x 4 Cd). The medium was added to the aerial part of the plants. Thus, the biphasic medium consisted of a culture medium solidified with agar (where the roots grew with or without Si) and a stationary liquid medium with Cd that covered only the basal part of the leaves (Fig. 1). The source of Cd was cadmium nitrate [$Cd(NO_3)_2 \cdot 4H_2O$]. Cd concentrations were selected based on previous tests in which the highest concentration did not reduce the survival rate. This stage was carried out with five explants per glass container. The experiment was performed with 12 containers and 60 plants per treatment. The co-exposure treatments of Si-Cd occurred for 45

days (75 days of cultivation in total), and the in vitro plant material was kept under the same environmental conditions of temperature and photoperiod mentioned above.

Analysis of leaf and root anatomy

To analyze the plant anatomy after 45 days of cultivation with co-exposure of Si-Cd, five plants were used per treatment. These were collected at random, fixed for 72 hours, and preserved in 50% ethanol. The cross-sections of leaves and roots, as well as the paradermal sections of leaves were performed by hand, using a razor blade. The leaf cross sections were taken from the median region of the first completely expanded leaf in the rosette central region of the plants. The cross-sections of roots were also made at their base (0.3–0.8 cm from the shoot). The sections were clarified with a commercial sodium hypochlorite 50% (v/v) and stained with safrablau (Bukatsch 1972). The paradermal sections were taken from the middle region of the second completely expanded leaf from the rosette of the plants and stained with safranin (1%). The sections were evaluated using an optical microscope (Bioval, L-2000AFlour) coupled to the digital camera (Leica EC3) to capture images. For the cross-sections of the leaves and roots, two sections per slide were photographed, and five different samples were analyzed (n = 5). For the paradermal sections, the photomicrographs were taken in six different areas for each replicate (five samples). The photomicrographs were analyzed using the UTHSCSA-Imagetool® version 3.0 software calibrated with a microscopic ruler.

The number of metaxylem vessels, root diameter (μm), thickness of cell walls in the exodermis (μm), endodermis thickness (μm) were determined in the roots. In the leaves, the stomatal density (0.01 mm^2), stomatal index (%), size of the stomata (μm^2), the thickness of the chlorenchyma (μm), the area of sclerenchyma (μm^2) and phloem (μm^2), as well as the number and diameter of xylem vessels (μm).

The stomatal index (SI) was calculated SI = number of stomata / (number of epidermal cells + number of stomata) × 100, and stomatal density was calculated by counting the number of stomata in a known area.

Analysis of photosynthetic pigment contents

The contents of photosynthetic pigments were determined based on fragments of eight samples collected randomly from 0.03 g to 0.039 g of fresh weight from each leaf in each treatment. The pigment preparation and extraction procedures followed Martins et al. (2020a). The absorbance was read with a Genesys ™ 10S UV-Vis spectrophotometer (Thermo Fisher Scientific, West Palm Beach, FL, USA), and the readings were performed at λ = 470, 645, and 663 nm for carotenoids (Car), chlorophyll *b* (chl *b*) and chlorophyll *a* (chl *a*), respectively. The pigment content (n = 8) was calculated according to Arnon (1949) and Wellburn (1994), and the Chl *a/b* and *total* Chl / Car ratios were analyzed.

Analysis of chlorophyll *a* fluorescence

The chlorophyll *a* fluorescence readings for each treatment were taken with a fluorometer (Handy PEA, Hansatech Instruments Ltd., King's Lynn, Norfolk, UK), between 7:00 and 9:00 am. The measurements were made in 15 plants per treatment (n = 15), using the third completely expanded leaf in the rosette central region. The

leaves had been previously adapted to the dark for 30 minutes with leaf clips (Hansatech®). Then, a flash of light was emitted, with saturating irradiance of 3000 µmol of photons m^{-2} s^{-1}. The fluorescence kinetics and parameters of the JIP test were recorded (Table 1) and interpreted (Strasser et al. 2004; Wang et al. 2016).

Modulated fluorescence analysis

For a more detailed analysis of the photosynthetic apparatus, measurements were made between 8:00 am and 10:00 am using Modulated Fluorescence measurements with the MINI-PAM II (Heinz Walz GmbH, Effeltrich, Germany), following the methodology of Ögren and Baker (1985) and Schreiber (1986). Readings were performed on 12 plants per treatment (n = 12), using the third completely expanded leaf in the rosette central region. The leaves had been adapted to the dark (30 min) with leaf clip (DCL-8, Walz GmbH). The initial fluorescence (F_0) was obtained using a weak beam of light (<1 µmol (photons) m^{-2} s^{-1}). The actinic light of 619 µmol (photons) m^{-2} s^{-1} leads to photosynthesis and gives F. After about 2 minutes, the steady-state yield of fluorescence (F_s) was subsequently obtained, and a second pulse of white light saturation 6000 µmol (photons) m^{-2} s^{-1} was applied for 0.8s to determine the maximum level of fluorescence (F_M) in the state adapted to light (F_M'). After 5 µmol (photons) m^{-2} s^{-1} of distant red irradiation 720-730 nm, F_0 was determined in the light adapted state (F_0'), which excites photosystem I (PSI) and oxidizes the plastoquinone sets and pools of quinone A (Q_A) associated with PSII (Wang et al. 2018). Measurements for ΦPSII, ETR, qN, NPQ, ΦNPQ, and ΦNO were obtained from the report, described in Table 2.

Analysis of growth traits

At 45 days of Si-Cd co-exposure, the growth factor of the plant total fresh weight (shoot + root) (g $plant^{-1}$) was determined. The samples consisted of five plots (five replicates; n = 5) per treatment, so that each replicate consisted of 5 plants (25 plants in total per treatment).

Statistical Analysis

The experimental design was completely randomized with a factorial scheme: four concentrations of Cd (0, 50, 100 and, 200 µM) and two concentrations of Si (0 and 14 µM). The data obtained were subjected to analysis of variance (ANOVA), and the means were compared using the Tukey test at 5% probability of error. All analyses were performed using the SISVAR software (Ferreira 2011).

Results

ANOVA results for all variables are summarized in Supplement 1.

Root anatomy

Significant differences were found in the anatomical traits of the roots, and Si was the main modulation factor. The thickness of cell walls in the exodermis reduced 9.8% in the presence of Si, while the number of

metaxylem vessels was increased (23.8% higher) (Fig. 2 and Fig. 3). The thickness of the endodermis (9.37 µm ± 0.22) and the diameter of the roots (404.28 µm ± 14.1) did not differ among the treatments (Fig. 3).

Leaf anatomy

In the paradermal sections of the leaves, the stomatal density of the median region had influence of both factors with a significant interaction. Plants grown under Si absence showed a 24.6% reduction in stomatal density at the highest concentration of Cd, compared with control plants (0 µM Si and 0 µM Cd) (Fig. 4 and 5A), while plants grown with Si did not show a significant difference among Cd concentrations. Concerning the Si concentrations, there was a decrease of 35% in stomatal density at the highest concentration of Cd (200 µM) in plants grown without Si, compared with plants grown with 14 µM Si (Fig. 4 and 5A). The size of the stomata in the median leaf region was only influenced by exposure to Si. When grown with 14 µM Si, the plants show a 6% reduction in the size of the stomata (Fig. 4 and 5B). The stomatal index (6.38 ± 0.225) showed no significant difference among the treatments (Fig. 4).

When the cross-sections of the leaves were analyzed, the number of xylem vessels and the sclerenchyma area were influenced only by exposure to Si. The diameter of the xylem vessels was influenced only by Cd concentrations. Plants grown with Si showed a 20% reduction in the number of xylem vessels, regardless of Cd concentrations, and they presented increased sclerenchyma area (14.8% higher) (Fig. 4 and 6A). The diameter of the xylem vessels decreased with increasing Cd concentration (Fig. 4 and 6B). The thickness of the chlorenchyma (323.69 µm ± 3.95) and the phloem area (580.28 μm^2 ± 32.14) did not show any significant difference among the treatments (Fig. 4).

Photosynthetic pigments content

Only Si concentrations influenced the photosynthetic pigment ratios in *A. blanchetiana* leaves grown in vitro. The chl *a/b* ratio was 5.5.% higher in the absence of Si. However, plants grown with Si showed an increase of 5.6% in the *total* chl/Car content (Fig. 7).

Analysis of chlorophyll *a* fluorescence

All plants remained photosynthetically active, regardless of the applied treatment. The kinetic differences were shown between steps O-K and O-J. The positive L- and K-bands were verified at all applied Cd concentrations (Fig. 8). In addition, [$W_L = (F_L - F_0)/(F_K - F_0)$] was 1.96% lower in plants grown with Si (Fig. 8A). On the other hand, W_K [$W_K = (F_K - F_0)/(F_J - F_0)$] did not change in terms of the presence of Si (Fig. 8B).

When the JIP test parameters were analyzed, significant changes were verified due to the variation factors (Cd and Si); however, they acted independently. JIP test parameters were presented in the function of Si levels in Table 3 and Fig. 8, and in the function of Cd concentrations, in which case the data are normalized in relation to the control (0 µM) and presented in Fig. 9. Significant increases in F_0, W_L, W_K, φD_0, and in the fluorescence levels of step K and J (V_K and V_J, respectively) were observed regardless of the Cd concentration. On the other hand, lower values of the parameters F_v/F_0, K_P, RC/CS_M, in the quantum yield parameters φP_0 and φE_0, as well as in the

performance indexes $PI_{(ABS)}$ and $PI_{(TOTAL)}$, were obtained in the presence of Cd. K_N showed no significant difference among the treatments regarding the presence of Cd (Fig. 9).

The JIP test parameters $F_v/F_{0,}$ K_P and $PI_{(ABS)}$, reported as a function of the exposure of Si, were higher in the presence of this element. Likewise, increases in the φP_0 and φE_0, and reduction in φD_0 were obtained in the presence of Si. In contrast, F_0 and V_J obtained the highest values under Si absence; while, V_K, K_N, $PI_{(TOTAL)}$, and RC/CS_M showed no significant difference regarding the presence of Si (Table 3).

Analysis of modulated chlorophyll *a* fluorescence

When examining the modulated fluorescence parameters, significant changes were seen in the parameters qN, NPQ, ΦNPQ, and ΦNO due to the variation factors (Cd and Si); however, they acted independently (Fig. 10; Table 4). When the parameters were analyzed as a function of exposure to Cd, a decrease in ΦPSII, ETR, and qP was observed in the presence of Cd (Table 5). The highest values of qN, NPQ, and ΦNPQ were obtained in both the absence (0 μM) and in 50 μM of Cd (Fig. 10), while the highest values of ΦNO were obtained in the highest concentrations of Cd. As a function of exposure to 14 μM Si, the parameters qN, NPQ, and ΦNPQ obtained the highest values (8.9%, 17,8% and, 10.5% higher, respectively) in the presence of this element. On the other hand, ΦNO obtained the lowest values under 14 μM Si (Table 4).

Analysis of growth traits

There was no plant mortality in any of the treatments with Cd, or any visible sign of physiological disorders, such as necrosis or discoloration of the leaves. However, the total fresh mass (roots and shoot) was influenced by both factors with significant interaction between them. Among plants grown in the absence of Si, the total fresh weight was lower with excess Cd (200 μM Cd); however, in plants grown with Si, the highest values were obtained with 0 and 100 μM Cd (Fig. 11).

Discussion

A. blanchetiana plants simultaneously exposed to Cd-Si during in vitro cultivation showed changes in anatomy and physiology. These responses suggested that the plants were able to adjust to the treatment conditions, which allowed them to withstand the excess Cd. Protection mechanisms such as increased dissipation of excess excitation energy in the form of heat allowed the plants to maintain the stability and function of the photosynthetic apparatus. In addition, the Si-induced anatomical, physiological, and biochemical responses had a mitigating effect on heavy metal stress.

The morphophysiological modulations induced by Si treatments were already verified in the roots, the organ that had direct contact with this element. In this organ, changes in the thickening pattern of cell walls of the exodermis were observed. However, it is worth mentioning that the exodermis cell walls thickening (external cortex) occurs naturally and is expected in the bromeliad roots, even in in vitro conditions (Martins et al. 2020b). The cell walls of the exoderm, as well as the endodermis, are apoplastic barriers due to the formation of Casparian strips. The exodermis can perceive osmotic and ionic stress changes in cells, which can trigger response

mechanisms (Terletskaya et al. 2019); therefore, they regulate the flow of water and mineral elements between cell layers (Silva and Scatena 2011; Martins et al. 2020b). In this work, the roots grown in the presence of Si showed an exodermis with thinner cell walls, which could allow for greater translocation of water and mineral nutrients from the culture medium to the aerial part of the plants. This may explain why plants grown with Si had benefits in growth characteristics. In addition, it should be taken into account that there was direct exposure to Cd in the aerial part of the plant.

Regarding the changes in root anatomy of *A. blanchetiana* plants from treatments, there were differences in the characteristics of the metaxylem vessels, which could suggest changes in the absorption of water and minerals from the culture medium to the aerial part of the plants. Supplementation with Si had a positive impact on the number of metaxylem vessels in the roots, and this suggests that Si may have played an important role in the balance of nutrients, which would allow for it to more efficiently withstand the stress of exposure to heavy metal (Bhat et al. 2019). Plants that have an improved nutritional status are more likely to tolerate excess heavy metals, as several enzymes in the antioxidant system have mineral elements as co-factors (Martins et al. 2020b). According to these same authors, an increased number of metaxylem vessels can improve the translocation of water and nutrients and, consequently, improve growth and increase plant biomass.

Modulations in leaf anatomy may also indicate adjustments to stress conditions. Variations in stomatal density commonly occur in plants under excess salt, water deficit, or exposure to heavy metals (Andrade Júnior et al. 2019; Martins et al. 2020a). This plasticity in the density, as well as the size of the stomata, allows for plants to adjust the area of the stomatal pore in response to the surrounding environment, affecting the maximum leaf capacity to absorb CO_2 (Kübarsepp et al. 2019; Bertolino et al. 2019). Under the cultivation conditions in our study, *A. blanchetiana* plants showed a reduction in stomatal density when exposed to a higher concentration of Cd without Si, indicating a response to heavy metal stress. Conversely, the presence of Si allowed for maintenance of stomatal density in plants when exposed to the highest concentration of Cd, suggesting a lower level of stress. In this work, it was verified that stress induced by heavy metal did not generate a lower investment in stomatal cells as evidenced by the stomatal index. This means that there was a variation in the size of only the epidermal cells (reduction in size) of plants treated with a higher concentration of Cd. This response suggests less transpiration and, consequently, less translocation of mineral elements from the medium (including Cd). The reduction in stoma size observed in plants supplemented with Si consists of an advantageous response to stress, since smaller stomata respond better to functionality and, therefore, are more effective in adapting to prevailing conditions (Kübarsepp et al. 2019).

The reduction in plant leaves xylem vessels grown with Si and/or the diameter induced by the increased concentration of Cd can also interfere in the absorption, distribution, and accumulation of nutrients in the plant tissues (Martins et al. 2019). These xylem vessel characteristics are factors that influence hydraulic conductivity, restricting the flow of water (Bauerle et al. 2011; Martins et al. 2020a). Considering that the direct exposure to Cd was in the aerial part of the plants, a lower translocation of Cd absorbed by the leaf trichomes would mitigate the harmful damages caused by Cd.

In the present study, Si supplementation promoted an increase in the sclerenchyma area. The sclerenchyma cells consist of the set of cell types with thickening of secondary lignified walls when mature (Amri et al. 2019). Considering that the sclerenchyma in the leaves gives rigidity and offers protection of specific structures such as vascular bundles, it can be suggested that the increase in the sclerenchyma area promoted by Si

may strengthen the architecture of the cell walls forming a strong structural support for the transport of water and nutrients (Li et al. 2020b).

When analyzing the photosynthetic pigments content in the leaves, it was found that the plants of *A. blanchetiana* cultivated with Si showed a better balance in the pigments content, which indicated lower stress from Cd. It is suggested that this improved condition could be attributed to the best nutritional balance with greater absorption of macro and micronutrients in the environment (Martins et al. 2020a). The increase in the proportion of *total* Chl/Car in the presence of Si was reflected in the better performance of the photosynthetic apparatus, as can be seen in the higher values of φP_0 and $PI_{(ABS)}$. Adequate levels of the Chl *a/b* ratio and the increase in the proportion of *total* Chl/Car in plants supplemented with Si indicates a lower level of Cd stress. An increase or decrease in the Chl *a/b* ratio indicates physiological disturbances, which is a common response in plants under stress conditions (Zrig et al. 2016; Aydoğan et al. 2017).

Our results clearly demonstrated physiological disturbances caused by Cd in the photosynthetic apparatus, which were verified with the presence of positive L- and K-bands. These bands can be considered as potential indicators of disturbances before the visible appearance of signs in response to stress (Meng et al. 2016). A positive L-band leads to reduced connectivity between RCs (Rosa et al. 2018). These disturbances were even greater in plants grown in the absence of Si, confirmed by the increased W_L values. In contrast, lower W_L values confirm that the negative effects of Cd were mitigated in plants treated with Si. The positive K-band reflects imbalances between electron donation from the OEC to the $P680^+$ and electron acceptors from quinone A (Q_A), besides the inhibition of the water-splitting system (Kalaji et al. 2016; Parmoon et al. 2019; Yin et al. 2019; Gupta 2020; Yang et al. 2020). These disturbances were confirmed by the increased values of the relatively variable fluorescence at point K (V_K) and W_K. The V_K and W_K parameters characterize the photosynthetic performance on the donor side of the PSII (Wang et al. 2016).

The deficiencies in electron transport were notable in plants grown with exposure to Cd. Such effects, observed by the reductions in the F_V/F_0 values, were more pronounced in plants of *A. blanchetiana* grown without Si. This resulted in an inhibition of electron transport, in addition to reducing the potential photosynthetic activity of PSII (Kalaji et al. 2018; Wang et al. 2018). F_V/F_0 describes the efficiency of the water-splitting complex on the donor side of the PSII, the most sensitive component in the photosynthetic process of the electron transport chain (Kalisz et al. 2016). K_P reductions can also demonstrate a physiological response to stress by Cd, indicating that there was partial inhibition of electron transport (Wang et al. 2016). In contrast, plants grown with Si showed a stress-alleviating effect from Cd stress by increasing the values of F_V/F_0 and K_P, which indicates an increase in photosynthetic activity.

The presence of Cd also caused an increase in V_J values, which was interpreted as a deceleration of electron transport from Q_A to quinone B (Q_B). This caused an accumulation of Q_A^- and a higher rate of fluorescence emission (Paunov et al. 2018), and this is an indicator of the closure of RCs of the PSII or the redox state of Q_A^- (Yin et al. 2019). A decrease in the rate of electron transport from Q_A to the second electron acceptor Q_B can cause damage by photoinhibition (Umar et al. 2019). In addition, the increase in F_0 values observed mainly in plants exposed to Cd is related to a smaller number of active RCs as confirmed by the lower RC/CS_M values. The values of V_J and F_0 verified in plants cultivated with Cd illustrated a decrease in primary photochemical activity. The reduction in V_J and the increase in F_V/F_0 in plants cultivated with Si suggests that the electron transfer between Q_A and Q_B has been improved, presenting less accumulation of Q_A^-. The F_0 reduction shows the highest density of

active RCs of PSII. This indicates that Si, by mitigating Cd stress, was able to ensure the best electron transport on the PSII acceptor side and protect the OEC function on the PSII donor side (Zhou et al. 2016).

The parameters related to the quantum yield in explants cultivated with Cd confirm the damage by photoinhibition. The decrease in φP_0 and φE_0, along with high values of φD_0, are associated with the occurrence of damage by photoinhibition in plants (Li et al. 2020a). According to Meng et al. (2016), the reduction of φE_0 values may indicate a lower proportion of open RCs of the PSII and less electrons used for carbon fixation, which generates more energy dissipated as heat (φD_0) than transported. These results were confirmed by the lower values of RC/CS_M in plants grown with Cd. Therefore, values of φP_0, φE_0, and φD_0 in plants grown with Cd led to a decrease in performance indexes ($PI_{(ABS)}$ and $PI_{(TOTAL)}$). The presence of Si contributed to partially mitigate the effects of Cd by maintaining the electron transport chain, evidenced by the higher values in φP_0, φE_0, and $PI_{(ABS)}$, which indicate an increase in the photosynthetic and photochemical activity of PSII (Lotfi et al. 2018). This may be due to an improved balance in the content of photosynthetic pigments.

Increase in ΦNO values obtained in plants grown in the highest concentrations of Cd and in the absence of Si suggest that the protection regulation mechanisms have become ineffective, besides indicating that the excess energy could not be effectively dissipated in the form of heat (Dias et al. 2018; Shu et al. 2019). ΦNO reflects the fraction of energy that is passively dissipated in the form of heat and fluorescence, mainly due to the closed RCs of the PSII. On the other hand, ΦNO was reduced in plants grown with Si. Decrease in the values of qN, ΦNPQ, and NPQ were obtained in plants exposed to high concentrations of Cd. The ΦNPQ parameter refers to the controlled heat dissipation that occurs in the RC of the PSII by inducing the pigments in the xanthophyll cycle and by proton gradient in the membranes of the thylakoid (Dias et al. 2018). Reduction in non-photochemical quenching parameters indicate that the mechanisms were inefficient in safely dissipating excess light energy and minimize the generation of ROS (Acosta -Motos et al. 2017; Wang et al. 2018). Conversely, their increase in *A. blanchetiana* plants grown with Si indicates that the plants had greater photoprotective capacity.

Regarding the ΦPSII, ETR, and qP parameters, the lower values obtained in plants grown in intermediate Cd concentrations suggest that there was a partial inhibition of electron transport and of the photochemical activity of PSII (Xin et al. 2019). This reduction points to a lower density of photon flux absorbed in the PSII (Wang et al. 2018). The small increase in ΦPSII and ETR values obtained at the highest Cd concentration can be interpreted, according to Baczer-Kwinta et al. (2019), as an intensification of the electron flow between the PSII and PSI. This is also possibly due to other processes involving electrons, such as photorespiration, Mehler reaction, and nitrate reduction (Baczer-Kwinta et al. 2019).

The anatomical, biochemical, and physiological responses induced by Cd allowed for *A. blanchetiana* plants to adjust, making it possible to withstand the exposed stress condition; however, it had a strong effect on their growth during in vitro cultivation. Plants grown in the highest Cd concentration exhibited a reduction in total fresh weight. In the absence of Si, the responses in the reduction of pigment content and disturbances in photosynthetic activity caused changes that indicated mechanisms mitigate stress. In addition, reduction of biomass and photosynthesis may be due to the Cd-induced reduction in nutrient absorption and adjustments to the plant ultrastructure and antioxidant system (Rizwan et al. 2016a, 2016b; Younis et al. 2016).

Conclusion

Anatomical, physiological, and biochemical modulations of *Aechmea blanchetiana* exposed to Cd in vitro allowed for the plants to fundamentally adjust to tolerate the excess Cd conditions, even with symptoms of toxicity. Protection mechanisms such as increased dissipation of excess excitation energy as heat allowed for plants to maintain the stability and function of the photosynthetic apparatus. However, most physiological symptoms of Cd toxicity were less pronounced with Si co-exposure. Supplementation with Si partially mitigated the effects of Cd by improving the efficiency of the energy flow of the electron transport chain, a large photoprotective capacity through the dissipation of excess excitation energy, and increased photosynthetic and photochemical activity of the PSII in *A. blanchetiana* plants. The results of the present study demonstrate that Si supplementation contributed to mitigating damage and increasing resistance to Cd in plants of *A. blanchetiana*, due to the lower level of deleterious effects on the photosynthetic pigments content and the performance of the photosynthetic apparatus.

Supplementary Information The online version contains supplementary material available at https:// doi. org/ 10. 1007/ s11240- 021- 02122-2.

Acknowledgements The authors would like to acknowledge the scholarship awarded by the CNPq (Brazilian National Council for Scientific and Technological Development), the CAPES (Coordination for the Improvement of Higher Education Personnel), and the FAPES (Espírito Santo State Research Foundation). The authors are also grateful to Luiz Carlos de Almeida Rodrigues for his technical assistance.

Author contributions RC and, LTC conducted experiments. RC and JPRM wrote the manuscript and, carried out the statistical analysis. ARF and ABPLG provided the structure and conditions to develop the experiments and contributed to the discussion of results. All the authors read and approved the final version of the paper.

Conflict of interest: The authors declare no conflict of interest.

References

Acosta-Motos JR, Ortuño MF, Bernal-Vicente A, Diaz-Vivancos P, Sanchez-Blanco MJ, Hernandez, J.A (2017) Plant Responses to Salt Stress: Adaptive Mechanisms. Agronomy 7(1):18. https://doi.org/10.3390/agronomy7010018

Adrees M, Ali S, Rizwan M, Rehman MZ, IbrahimM, Abbas F, Farid M, Qayyum MK, Irshad MK (2015) Mechanisms of silicon-mediated alleviation of heavy metal toxicity in plants: a review. Ecotoxicol Environ Saf 119:186–197. https://doi.org/10.1016/j.ecoenv.2015.05.011

Alzahrani Y, Kusvuran A, Alharby HF, Kusvuran S, Rady MM (2018) The defensive role of silicon in wheat against stress conditions induced by drought, salinity or cadmium. Ecotoxicol Environ Saf 154:187–196. https://doi.org/10.1016/j.ecoenv.2018.02.057

Amri CNABC, Mokhtar NABM, Shahari R (2019) Leaf anatomy and micromorphology of selected plant species in coastal area of Kuantan, Pahang, Malaysia. Sci Herit J 3(2):22-25. https://doi.org/10.26480/gws.02.2019.22.25

Andrade Júnior WV, Oliveira Neto CF, Santos Filho BG, Amarante CB, Cruz ED, Okumura RS, Barbosa AVC, Sousa DJP, Teixeira JSS, Botelho AS (2019) Effect of cadmium on young plants of *Virola surinamensis*. AoB Plants 11(3):plz022. https://doi.org/10.1093/aobpla/plz022

Anju M, Sanskriti G, Suresh BS, Nidhi S (2015) In vitro accumulation of cadmium chloride in papaya seedling and its impact on plant protein. Int J Ayurveda Pharma Res 2:54–62.

Arnon DI (1949) Copper enzymes in isolated chloroplasts. Polyphenoloxidase in *Beta vulgaris*. Plant Physiol 24 (1):1-15. https://doi.org/10.1104/pp.24.1.1

Asmar AS, Soares JDR, Silva RAL, Pasqual M, Pio LAS, Castro EM (2015) Anatomical and structural changes in response to application of silicon (Si) in vitro during the acclimatization of banana cv. 'Grand Naine'. Aust J Crop Sci 9:1236–1241

Aydoğan S, Erdağ B, Aktaş L (2017) Bioaccumulation and oxidative stress impact of Pb, Ni, Cu, and Cr heavy metals in two bryophyte species, *Pleurochaete squarrosa* and *Timmiella barbuloides*. Turk J Bot 41:464-475. https://doi.org/10.3906/bot-1608-33

Bączek-Kwinta R, Juzoń K, Borek M, Antonkiewicz J (2019) Photosynthetic response of cabbage in cadmium-spiked soil. Photosynthetica 57(3):731-739. https://doi.org/10.32615/ps.2019.070

Bauerle TL, Centinari M, Bauerle WL (2011) Shifts in xylem vessel diameter and embolisms in grafted apple trees of differing rootstock growth potential in response to drought. Planta 234(5):1045-1054. https://doi.org/ 10.1007/s00425-011-1460-6

Bertolino LT, Caine RS, Gray JE (2019) Impact of stomatal density and morphology on water-use eefficiency in a changing world. Frontiers in Plant Science 10:225. https://doi.org/10.3389/fpls.2019.00225

Bhat JA, Shivaraj SM, Singh P, Navadagi DB, Tripathi DK, Dash PK, Solanke AU, Sonah H, Deshmukh R (2019) Role of Silicon in Mitigation of Heavy Metal Stresses in Crop Plants. Plants 8(3):71. https://doi.org/10.3390/plants8030071

Bukatsch F (1972) Bemerkungen zur Doppelfarbung austrablau-safranin Mikrokosmos 61:255.

Costa WS, Yamamura RHR, Morcelli CPR, Sígolo JB (2020) Adição de resíduo de marmoraria em pastas cimentícias, avaliação de suas propriedades mecânicas e caracterização química. Journal of Engineering, Architecture and Technology Innovation 8:1-18.

Dias CS, Araujo L, Alves Chaves JA, DaMatta FM, Rodrigues FA (2018) Water relation, leaf gas exchange and chlorophyll a fluorescence imaging of soybean leaves infected with *Colletotrichum truncatum*. Plant Physiol Bioch 127:119–128. https://doi.org/10.1016/j.plaphy.2018.03.016

Etesami H, Jeong BR (2018) Silicon (Si): Review and future prospects on the action mechanisms in alleviating biotic and abiotic stresses in plants. Ecotoxicol Environ Saf 147:881–896. https://doi.org/10.1016/j.ecoenv.2017.09.063

Farooq MA, Ali S, Hameed A, Ishaque W, Mahmood K, Iqbal Z (2013) Alleviation of cadmium toxicity by silicon is related to elevated photosynthesis, antioxidant enzymes; suppressed cadmium uptake and oxidative stress in cotton. Ecotoxicol Environ Saf 96:242–249. https://doi.org/10.1016/j.ecoenv.2013.07.006

Feng J, Lin Y, Yang Y, Shen Q, Huang J, Wang S, Zhu X, Li Z (2018a) Tolerance and bioaccumulation of combined copper, zinc, and cadmium in *Sesuvium portulacastrum.* Mar Pollut Bull 131:416–421. https://doi.org/10.1016/j.marpolbul.2018.04.049

Feng J, Lin Y, Yang Y, Shen Q, Huang J, Wang S, Zhu X, Li Z (2018b) Tolerance and bioaccumulation of Cd and Cu in *Sesuvium portulacastrum.* Ecotoxicol Environ Saf 147:306–312. https://doi.org/10.1016/j.ecoenv.2017.08.056

Ferreira DF (2011) Sisvar: a computer statistical analysis system. Ciên Agrotec 35(6):1039-1042. https://doi.org/10.1590/S1413-70542011000600001

Franić M, Galić V, Mazur M, Šimić D (2017) Effects of excess cadmium in soil on JIP-test parameters, hydrogen peroxide content and antioxidant activity in two maize inbreds and their hybrid. Photosynthetica 55:1–10. https://doi.org/10.1007/s11099-017-0710-7

Ghassemi-Golezani K, Lotfi R (2015) The Impact of salicylic acid and silicon on chlorophyll *a* fluorescence in mung bean under salt stress. Russ J Plant Physiol 62:611–616. https://doi.org/10.1134/S1021443715040081

Giampaoli P, Tresmondi F, Lima GPP, Kanashiro S, Alves ES, Domingos E, Tavares AR (2012) Analysis of tolerance to copper and zinc in *Aechmea blanchetiana* grown in vitro. Biol Plant 56:83–88. https://doi.org/ 10.1007/s10535-012-0020-7

Giampaoli P, Wannaz ED, Tavares AR, Domingos, M (2016) Suitability of *Tillandsia usneoides* and *Aechmea fasciata* for biomonitoring toxic elements under tropical seasonal climate. Chemosphere 149:14-23. https://doi.org/10.1016/j.chemosphere.2016.01.080

Gupta R (2020) Manganese repairs the oxygen-evolving complex (OEC) in maize (*Zea mays* L.) damage during seawater vulnerability. J Soil Sci Plant Nutr 20:1387–1396. https://doi.org/10.1007 / s42729-020-00220-2

Kalaji HM., Jajoo A, Oukarroum A, Brestic M, Zivcak M, Samborska IA, Cetner MD, Łukasik I, Goltsev V, Ladle RJ (2016) Chlorophyll *a* fluorescence as a tool to monitor physiological status of plants under abiotic stress conditions. Acta Physiol Plant 4:1–11. https://doi.org/10.1007/S11738-016-2113-y

Kalaji MH, Goltsev VN, Zuk-Gołaszewska K, Zivcak M, Brestic M (2017a) Chlorophyll Fluorescence: Understanding Crop Performance—Basics and Applications; CRC Press, T&F Group: Abingdon, UK; p. 222.

Kalaji MH, Schansker G, Brestic M, Bussotti F, Calatayud A, Ferroni L, Goltsev V, Guidi L, Jajoo A, Li P et al (2017b) Frequently asked questions about chlorophyll fluorescence, the sequel. Photosynth Res 132:13–66. https://doi.org/ 10.1007/s11120-016-0318-y

Kalaji HM, Rastogi A, Živčák M et al (2018) Prompt chlorophyll fluorescence as a tool for crop phenotyping: an example of barley landraces exposed to various abiotic stress factors. Photosynthetica 56: 953-961. https://doi.org/10.1007/s11099-018-0766-z

Kalisz A, Jezdinský A, Pokluda R, Sękara A, Grabowska A, Gil J (2016) Impacts of chilling on photosynthesis and chlorophyll pigment content in juvenile basil cultivars. Hort Environ Biotech 57(4):330-339. https://doi.org/10.1007/s13580-016-0095-8

Kanashiro S, Ribeiro RCS, Gonçalves AN, Demétrio VA, Jocys T, Tavares A R (2009) Effect of calcium on the in vitro growth of *Aechmea blanchetiana* (Baker) L. B. Smith plantlets. J Plant Nutr 32(5):867-877. https://doi.org/10.1080/01904160902790341

Kaya C, Ashraf M, Alyemen MN, Ahmad P (2020) Responses of nitric oxide and hydrogen sulfide in regulating oxidative defence system in wheat plants grown under cadmium stress. Physiol Plant 168:345-360. https://doi.org/ 10.1007/s13580-016-0095-8

Khan A, Bilal S, Khan AL, Imran M, Al-Harrasi A, Al-Rawahi A, Lee I-J (2020) Silicon-mediated alleviation of combined salinity and cadmium stress in date palm (*Phoenix dactylifera* L.) by regulating physio-hormonal alteration. Ecotoxicol Environ Saf 188:109885. https://doi.org/10.1016/j.ecoenv.2019.109885

Kübarsepp L, Laanisto L, Niinemets Ü, Talts E, Tosens T (2019) Are stomata in ferns and allies sluggish? Stomatal responses to CO_2, humidity and light and their scaling with size and density. New Phytol 225:1-13. https://doi.org/10.1111/nph.16159

Li L, Pan XL, Mu GJ (2020a) Toxic effects of potassium permanganate on photosystem II activity of cyanobacteria *Microcystis aeruginosa*. Photosynthetica 58(1):54-60. https://doi.org/10.32615/ps.2019.155

Li W, Wang K, Chern M, Liu Y, Zhu Z, Liu J, Zhu X, Yin J, Ran L, He K, Xu L, He, Wang J, Liu J, Bi Yu, Qing H, Li M, Hu K, Song L, Wang L, Qi T, Hou Q, Chen W, Li Y, Wang W, Chen X (2020b) Sclerenchyma cell thickening through enhanced lignification induced by *OsMYB30* prevents fungal penetration of rice leaves. New Phytol 226:1850-1863. https://doi.org/10.1111/nph.16505

Lotfi R, Kalaji HM, Valizadeh GR, Khalilvand Behrozyar E, Hemati A, Gharavi-Kochebagh P, Ghassemi A (2018) Effects of humic acid on photosynthetic efficiency of rapeseed plants growing under different watering conditions. Photosynthetica 56:962-970. https://doi.org/10.1007/s11099-017-0745-9

Ma J, Cai H, He C, Zhang W, Wang L (2015) A hemicellulose-bound form of silicon inhibits cadmium ion uptake in rice (*Oryza sativa*) cells. New Phytol 206:1063–1074. https://doi.org/10.1111 / nph.13276

Malčovská SM, Dučaiová Z, Maslaňáková I, Bačkor M (2014) Effect of silicon on growth, photosynthesis, oxidative status and phenolic compounds of maize (*Zea mays* L.) grown in cadmium excess. Water Air Soil Pollut 225:2056. https://doi.org/10.1007/s11270-014-2056-0

Manquián-Cerda K, Escudey M, Zúñiga G, Arancibia-Miranda N, Molina M, Cruces E (2016) Effect of cadmium on phenolic compounds, antioxidant enzyme activity and oxidative stress in blueberry (*Vaccinium corymbosum* L.) plantlets grown in vitro. Ecotoxicol Environ Saf 133:316–326. https://doi.org/10.1016/j.ecoenv.2016.07.029

Martins JPR, Martins AD, Pires MF, Junior RAB, Reis RO, Dias GDMG, Pasqual M (2016) Anatomical and physiological responses of *Billbergia zebrina* (Bromeliaceae) to copper excess in a controlled microenvironment. Plant Cell Tissue Organ Cult 126(1):43-57. https://doi.org/ 10.1007/s11240-016-0975-8

Martins JPR, Rodrigues LCA, Santos ER, Batista BG, Gontijo A, Falqueto AR (2018) Anatomy and photosystem II activity of in vitro grown *Aechmea blanchetiana* as affected by 1-naphthaleneacetic acid. Biol Plant 62(2):211–221. https://doi.org/10.1007/s10535-018-0781-8

Martins JPR, Rodrigues LCA, Silva TS, Santos ER, Falqueto AR, Gontijo ABPL (2019). Sources and concentrations of silicon modulate the physiological and anatomical responses of *Aechmea blanchetiana* (Bromeliaceae) during in vitro culture. Plant Cell Tissue Organ Cult 137:397-410. https://doi.org/10.1007/s11240-019-01579-6

Martins JPR, Rodrigues LCA, Silva TS, Rossini FP, Gontijo ABPL, Falqueto AR (2020a) Morphophysiological responses of *Aechmea blanchetiana* (Bromeliaceae) to excess copper during *in vitro* culture. Plant Biosyst. https://doi.org/10.1080/11263504.2020.1756976

Martins JPR, Rodrigues LCA, Silva TS, Gontijo ABPL, Falqueto AR (2020b) Modulation of the anatomical and physiological responses of in vitro grown *Alcantarea imperialis* induced by NAA and residual effects of BAP. Ornam Hort 26(2):283-297. https://doi.org/10.1590/2447-536x.v26i2.2138

Meng LL, Song JF, Wen J, Zhang J, Wei JH (2016) Effects of drought stress on fluorescence characteristics of photosystem II in leaves of *Plectranthus scutellarioides*. Photosynthetica 54:414–421. https://doi.org/10.1007/s11099-016-0191-0

Murashige T, Skoog F (1962) A revised medium for rapid growth and bio assays with tobacco tissue cultures. Physiol Plant 15(3):473-497. https://doi.org/10.1111/j.1399-3054.1962.tb08052.x

Nahar K, Rahman M, Hasanuzzaman M, Alam MM, Rahman A, Suzuki T, Fujita M (2016) Physiological and biochemical mechanisms of spermine-induced cadmium stress tolerance in mung bean (*Vigna radiata* L.) seedlings. Environ Sci Pollut Res 23(21):21206–21218. https://doi.org/10.1007 / s11356-016-7295-8

Ögren E, Baker NR (1985) Evaluation of a technique for the measurement of chlorophyll fluorescence from leaves exposed to continuous white light. Plant Cell Environ 8:539-547. https://doi.org/10.1111/j.1365-3040.1985.tb01691.x

Oliveira JPV, Pereira MP, Duarte VP, Corrêa FF, Castro EM, Pereira FJ (2017) Cadmium tolerance of *Typha domingensis* Pers. (Typhaceae) as related to growth and leaf morphophysiology. Braz J Biol 78(3):509–516. https://doi.org/10.1590/1519-6984.171961

Parmoon G, Ebadi A, Jahanbakhsh S, Hashemi M, Moosavi SA (2019) Assessing photosynthetic performance of fennel (*Foeniculum vulgare* Mill) influenced by plant growth regulators and drought stress imposed at vegetative and reproductive stages. Ital J Agron 14:1319. https://doi.org/10.4081/ija.2019.1319

Paunov M, Koleva L, Vassilev A, Vangronsveld J, Goltsev V (2018) Effects of different metals on photosynthesis: cadmium and zinc affect chlorophyll fluorescence in durum wheat. Int J Mol Sci 19:787. https://doi.org/10.3390/ijms19030787

Piazzetta KD, Ramsdorf WA, Maranho LT (2018) Use of airplant *Tillandsia recurvata* L., Bromeliaceae, as biomonitor of urban air pollution. Aerobiologia 35(1):125-137. https://doi.org/10.1007/s10453-018-9545-3

Rizwan M, Meunier JD, Davidian JC, Pokrovsky OS, Bovet N, Keller C (2016a) Silicon alleviates Cd stress of wheat seedlings (*Triticum turgidum* L. cv. Claudio) grown in hydroponics. Environ Sci Pollut Res 23:1414–1427. https://doi.org/10.1007/s11356-015-5351-4

Rizwan M, Ali S, Qayyum MF, Ibrahim M, Rehman MZ, Abbas T, Ok YS (2016b) Mechanisms of biochar-mediated alleviation of toxicity of trace elements in plants: a critical review. Environ Sci Pollut Res 23:2230–2248. https://doi.org/10.1007/s11356-015-5697-7

Rizwan M,Ali S, QayyumMF, Ok YS, RehmanMZ, Abbas Z, Hannan F (2016c) Use of maize (Zea mays L.) for phytomanagement of Cd contaminated soils: a critical review. Environ Geochem Health 39(2):259-277. https://doi.org/10.1007/s10653-016-9826-0

Rodrigues LCA, Martins JPR, Júnior OA, Guilherme LRG, Pasqual M, Castro EM (2017) Tolerance and potential for bioaccumulation of *Alternanthera tenella* Colla to cadmium under in vitro conditions. Plant Cell Tissue Organ Cult 130:507–519. https://doi.org/10.1007/s11240-017-1241-4

Rosa WS, Martins JPR, Rodrigues ES, De Almeida Rodrigues LC, Gontijo ABPL, Falqueto AR (2018) Photosynthetic apparatus performance in function of the cytokinins used during the in vitro multiplication of *Aechmea blanchetiana* (Bromeliaceae). Plant Cell Tissue Organ Cult 133(3):339-350. https://doi.org/10.1007/s11240-018-1385

Schreck E, Sarret G, Oliva P, Calas A, Sobanska S, Guédron S, Barraza F, Point D, Huayta C, Couture RM, Prunier J, Henrique M, Tisserand D, Goix S, Chincheros J, Uzu G (2016) Is *Tillandsia capillaris* an efficient bioindicator of atmospheric metal and metalloid deposition? Insights from five months of monitoring in an urban mining area. Ecol Indic 67:227-237. https://doi.org/10.1016/j.ecolind.2016.02.027.

Schreiber U (1986) Detection of rapid induction kinetics with a new type of high-frequency modulated chlorophyll fluorometer. Photosynth Res 9: 261–272. https://doi.org/10.1007/BF00029749

Shu S, Yuan R, Shen J, Chen J, Wang L, Wu J, Sun J, Wang Y, Shirong G (2019) The positive regulation of putrescine on light-harvesting complex ii and excitation energy dissipation in salt-stressed cucumber seedlings. Environ Exp Bot 162:283–294. https://doi.org/10.1016/j.envexpbot.2019.02.027

Silva IV, Scatena VL (2011) Anatomia de raízes de nove espécies de Bromeliaceae (Poales) da região amazônica do estado de Mato Grosso, Brasil. Acta Bot Bras 25(3):618–627. https://doi.org/10.1590/S0102-33062011000300015

Son JA, Narayanankutty DP, Roh KS (2014) Influence of exogenous application of glutathione on rubisco and rubisco activase in heavy metal-stressed tobacco plant grown in vitro. Saudi J Biol Sci 21:89–97. https://doi.org/10.1016/j.sjbs.2013.06.002

Stirbet A, Lazár D, Kromdijk J (2018) Chlorophyll *a* fluorescence induction: Can just a one-second measurement be used to quantify abiotic stress responses? Photosynthetica 56(1):86-104. https://doi.org/10.1007/s11099-018-0770-3

Strasser RJ, Tsimilli-Michael M, Srivastava A (2004) Analysis of the Chlorophyll *a* Fluorescence Transient. *In*: Papageorgiou GC, Govindjee (eds) Chlorophyll *a* Fluorescence. Advances in Photosynthesis and Respiration. Springer, Dordrecht 19:321-362. https://doi.org/10.1007/978-1-4020-3218-9_12

Terletskaya N, Duisenbayeva U, Rysbekova A, Kurmanbayeva M, Blavachinskaya I (2019) Architectural traits in response to salinity of wheat primary roots. Acta Physiologiae Plantarum 41:157. https://doi.org/10.1007/s11738-019-2948-0

Umar M, Uddin Z, Siddiqui ZS (2019) Responses of photosynthetic apparatus in sunflower cultivars to combined drought and salt stress. Photosynthetica 57(2):627-639. https://doi.org/10.32615/ps.2019.043

Xin J, Zhao XH, Tan QL, Sun XC, Zhao YY, Hu CX (2019) Effects of cadmium exposure on the growth, photosynthesis, and antioxidante defense system in two radish (*Raphanus sativus* L.) cultivars. Photosynthetica 57:967–973. https://doi.org/10.32615/ps.2019.076

Yin Z, Lu J, Meng S, Liu Y, Mostafa I, Qi M, Li T (2019) Exogenous melatonin improves salt tolerance in tomato by regulating photosynthetic electron flux and the ascorbate–glutathione cycle. J Plant Interact 14:453-463. https://doi.org/10.1080/17429145.2019.1645895

Younis U, Malik SA, Rizwan M, Qayyum MF, Ok YS, Shah MHR, Rehman, RA, Ahmad N (2016) Biochar enhances the cadmium tolerance in spinach (Spinacia oleracea) through modification of Cd uptake and physiological and biochemical attributes. Environ Sci Pollut Res 23(21):21385–21394. https://doi.org/10.1007/s11356-016-7344-3

Wang YW, Xu C, Lv CF, Wu M, Cai XJ, Liu ZT, Song MX, Chen CX, Lv CG (2016) Chlorophyll *a* fluorescence analysis of high-yield rice (*Oryza sativa* L.) LYPJ during leaf senescence. Photosynthetica 54:422-429. https://doi.org/10.1007/s11099-016-0185-y

Wang Z, Li G, Sun H, Ma L, Guo Y, Zhao Z, Gao H, Mei L (2018) Effects of drought stress on photosynthesis and photosynthetic electron transport chain in young apple tree leaves. Biol Open 7(11):bio035279. https://doi.org/10.1242/bio.035279

Wellburn AR (1994) The Spectral Determination of Chlorophylls a and b, as well as Total Carotenoids, Using Various Solvents with Spectrophotometers of Different Resolution. J Plant Physiol 144(3):307-313. https://doi.org/10.1016/S0176-1617(11)81192-2

Zhou X, Zhao H, Cao K, Hu L, Du T, Baluška F, Zou Z (2016) Beneficial roles of melatonin on redox regulation of photosynthetic electron transport and synthesis of d1 protein in tomato seedlings under salt stress. Front Plant Sci 7:1823. https://doi.org/10.3389/fpls.2016.01823

Zrig A, Ben Mohamed H, Tounekti T, Khemira H, Serrano M, Valero D, Vadel AM (2016) Effect of rootstock on salinity tolerance of sweet almond (cv. Mazzetto). S Afr J Bot 102:50-59. https://doi.org/10.1016/j.sajb.2015.09.001

Zurek G, Rybka K, Pogrzeba M, Krzy zak J, Prokopiuk K (2014) Chlorophyll *a* Fluorescence in Evaluation of the Effect of Heavy Metal Soil Contamination on Perennial Grasses. PLoS ONE 9(3):e91475. https://doi.org/10.1371/journal.pone.0091475

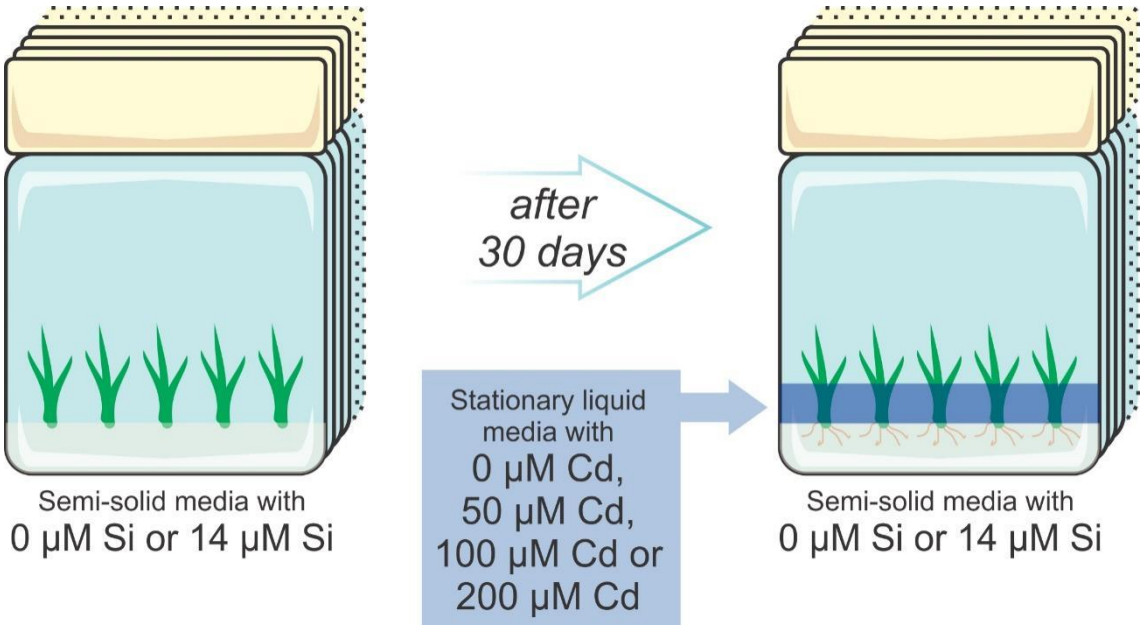

Fig. 1 Schematic representation of the experimental design from the first day of cultivation in agar-solidified culture media supplemented with 0 or 14 µM Si. After 30 days of growth, stationary liquid media with 0, 50, 100, or 200 µM Cd covered just the basal part of the leaves.

Table 1 Abbreviations of the parameters, formulas and description of the data derived from the transient fluorescence of chlorophyll *a*

Fluorescence parameters	Description
Extracted fluorescence parameters	
F_0	Initial fluorescence yield of dark-adapted sample with all PSII centers open
F_L	Fluorescence intensity at 0.15 µs
F_K	Fluorescence intensity at 0.3 µs
F_J	Fluorescence intensity at 0.3 µs
F_M	Maximum fluorescence yield of dark-adapted sample with all PSII centers closed
F_t	Fluorescence at time t after start of actinic Illumination
F_v/F_0	Ratio of photochemical to nonphotochemical quantum efficiencies (PSII potential activity)
K_P	The photochemical de-excitation rate constant in the excited antennae of energy fluxes for photochemistry
K_N	The nonphotochemical de-excitation rate constant in the excited antennae for non-photochemistry
Calculated parameters	
$V_J=(F_J-F_0)/(F_M-F_0)$	Relative variable fluorescence at the phase J of the fluorescence induction curve
$V_K=(F_K-F_0)/(F_M-F_0)$	Relative variable fluorescence at the phase K of the fluorescence induction curve
$W_K=(F_K-F_0)/(F_J-F_0)$	Represent the damage to oxygen evolving complex (OEC)
$W_L=(F_L-F_0)/(F_K-F_0)$	Represent the changes in the fluidity of the thylakoid membrane and damages to its function and structural integrity
$RC/CS_M=CSM/ABS=\varphi P_0\times(V_J/M_0)\times ABS/CSM$	Density of active reaction center per cross-section
Quantum yields and probabilities	
$\varphi P_0=TR_0/ABS=[1-(F_0/F_M]=F_v/F_M$	Maximum quantum yield of primary photochemistry at ($t=0$)
$\varphi E_0=ET_0/ABS=[1-(F_0/F_M)]\times\psi E_0=\varphi P_0\times\psi E_0$	Quantum yield of electron transport (at $t=0$)
$\varphi D_0=1-\varphi P_0=(F_0/F_M)$	Quantum yield of energy dissipation (at $t=0$)
Performance index	
$PI_{(ABS)}=RC/ABS\times[\varphi P_0/(1-\varphi P_0)]\times[\psi E_0/(1-\psi E_0)]$	The performance index on absorption basis
$PI_{(TOTAL)}=PI_{(ABS)}\times[\delta R_0/(1—\delta R_0)]$	Overall performance index, which measures the performance up until the final electron acceptors of PSI

For review see Strasser et al. (2004) and Wang et al. (2016)

Table 2 Abbreviations, formulas and description of the parameters of modulated chlorophyll fluorescence

Fluorescence parameters	Description
F_S	The steady-state fluorescence
F_0'	Minimal fluorescence yield of illuminated sample with all PS II centers open
F_M'	Maximal fluorescence yield of illuminated sample with all PSII centers closed
$\Phi PSII=Y(II)=(F_M'-F_S)/F_M'$	Effective photochemical quantum yield of PSII
$ETR=\Phi PSII\times 0.50\times PPFDa$	Rate of linear electron flow (PPFDa designates the rate of light absorption by a sample expressed in µmol m^2 s^{-1})
NPQ	Non-photochemical fluorescence dissipation (non-photochemical quenching)
$qP=(F_M'-F_S)/(F_M'-F_0')$	Photochemical quenching
$qN=(F_M-F_0')/(F_M-F_0)$	Non-photochemical quenching
ΦNPQ	Quantum yield induced light (ΔpH and zeaxanthin-dependent) from non-photochemical fluorescence dissipation
$\Phi NO=Y(NO)=F_S/F_M$	Quantum yield of non-regulated energy dissipation

For review see Wang et al. (2018)

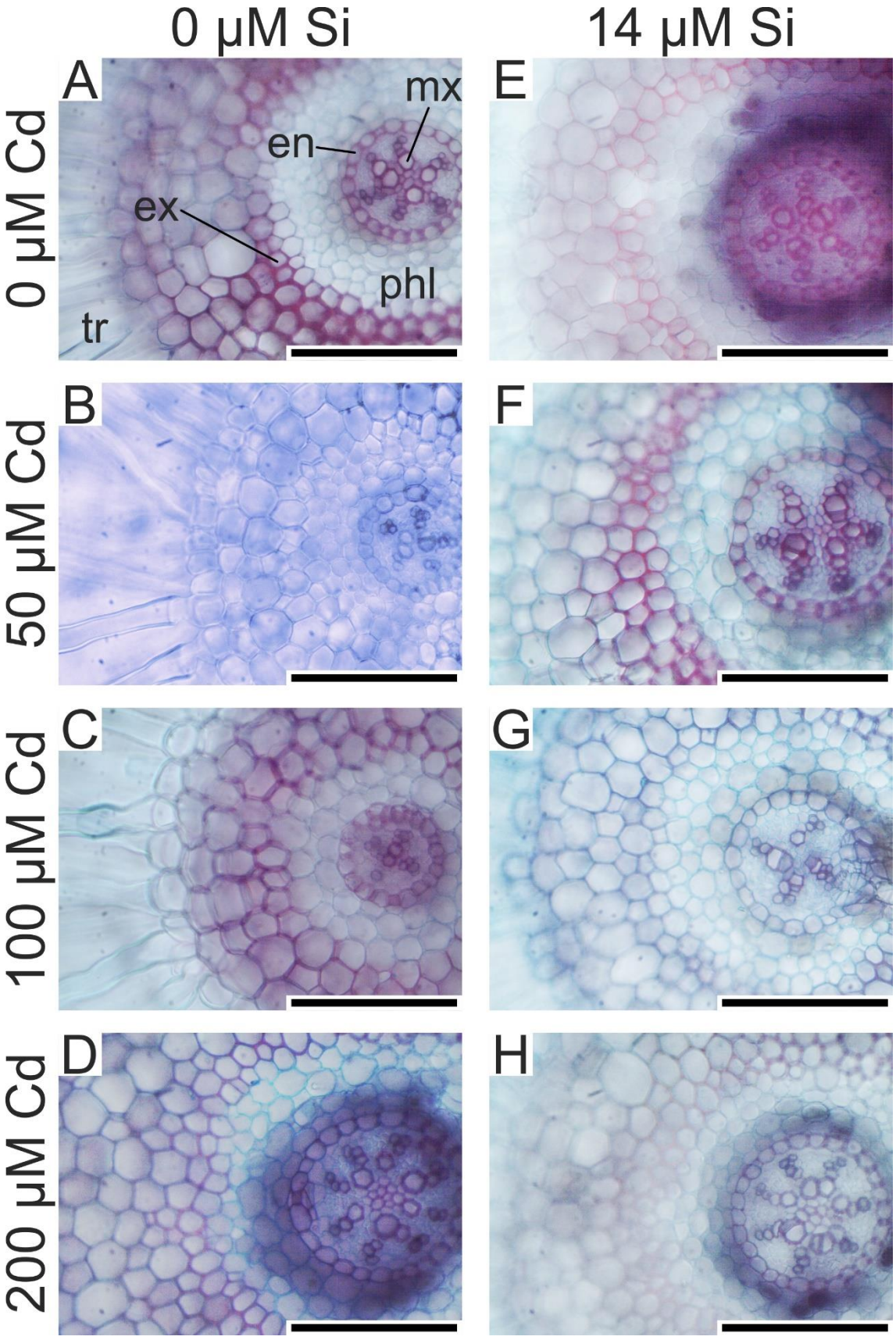

Fig. 2 Root cross-sections of *Aechmea blanchetiana* plants in the function of concentrations (0, 50, 100 and, 200 µM) of Cd and Si (0 and 14 µM) during *in vitro* culture. en-endodermis, ex-exodermis, tr- trichome (root hair), mx- metaxylem vessels and, phl-phloem. Bars = 100 µm

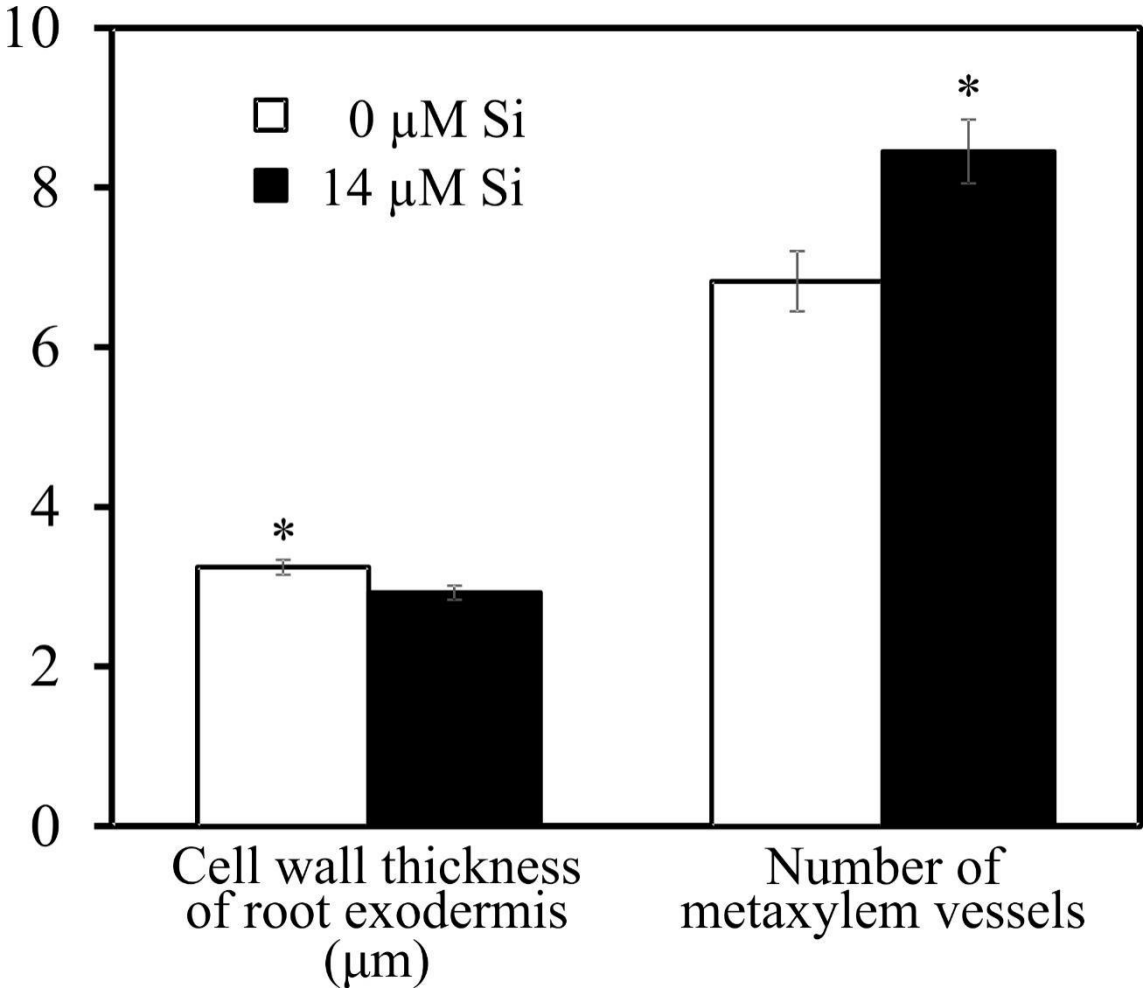

Fig. 3 Anatomical traits of the root of *Aechmea blanchetiana* with 0 or 14 µM of Si. Means (±SE), *n* = 5, followed by an asterisk (*) in each anatomical feature are significantly different according to the Tukey test with a 5% probability.

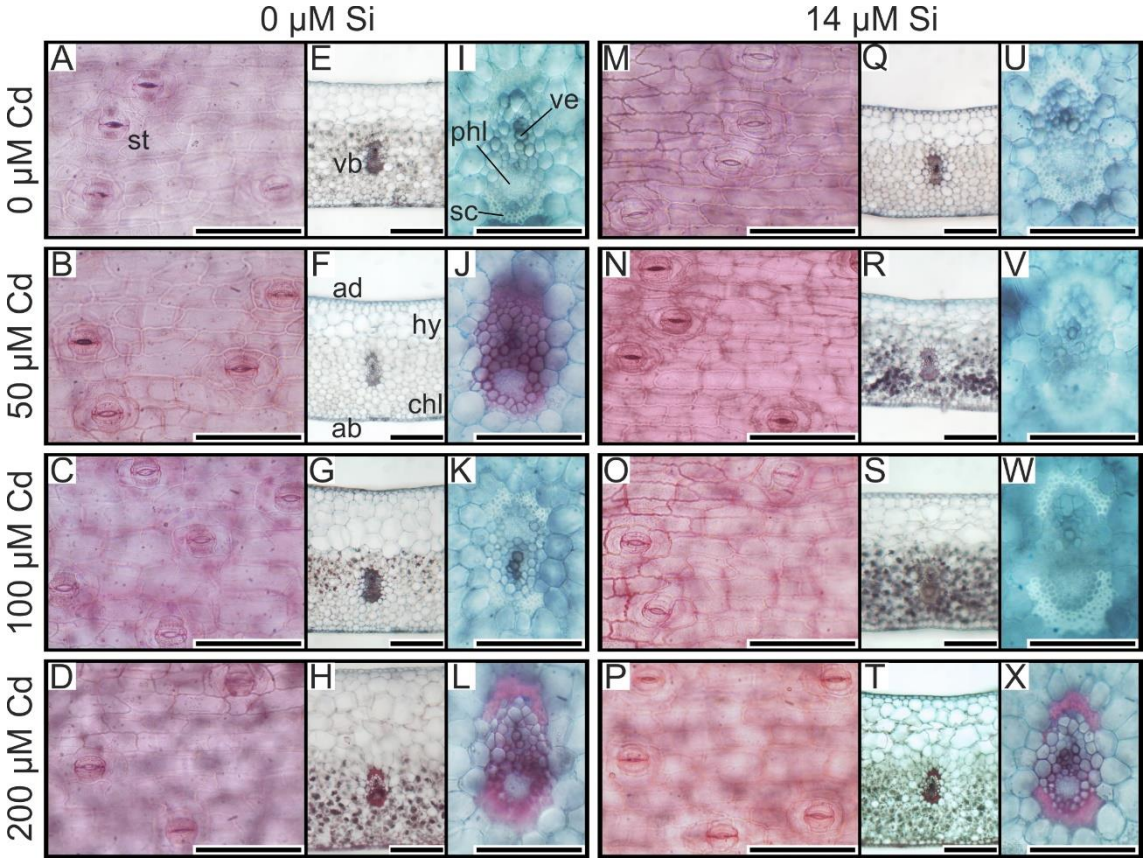

Fig. 4 Paradermal sections (a–d and m–p) and cross-sections (e–l and q–x) of leaves of *Aechmea blanchetiana* plants as a function of concentrations (0, 50, 100 and, 200 µM) of Cd and Si (0 and 14 µM) during *in vitro* culture. ad-adaxial epidermis, ab-abaxial epidermis, chl-chlorenchyma, hy-hydrenchyma, ph-phloem, sc-sclerenchyma, st-stomata, vb-vascular bundles, and ve-vessel elements (xylem vessels). Bars = 100 µm

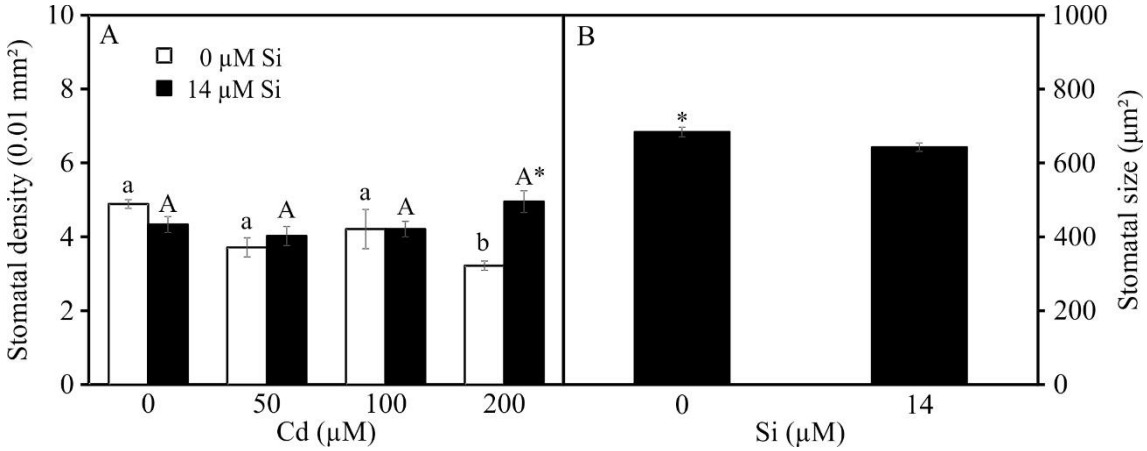

Fig. 5 (A) Stomatal density and (B) size of the stomata of leaves of *Aechmea blanchetiana* as a function of Si (0 or 14 µM) and Cd concentrations (0, 50, 100, 200 µM). (a) Means (±SE), *n* = 5, followed by the different letters in each Si concentration (lower case for 0 µM Si and upper case for 14 µM Si, comparing the Cd concentrations) and asterisk (*) in each Cd concentration (comparing the Si concentrations) are significantly different according to the Tukey test at 5% probability. (b) For each Si concentration analyzed (0 and 14 µM Si), the means (±SE) followed by an asterisk are significantly different according to the Tukey test at 5% significance.

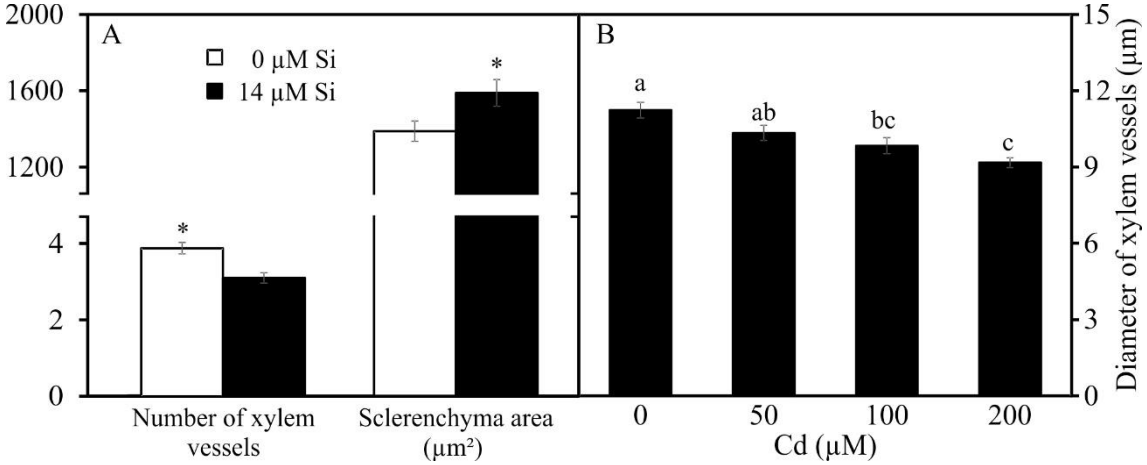

Fig. 6 Anatomical characteristics of *Aechmea blanchetiana* leaves as a function Si (0 and 14 µM) and Cd concentrations (0, 50, 100, 200 µM). For each anatomical trait, means (±SE), *n* = 5, followed by an asterisk (*) (comparing the Si treatments) and different letters (comparing the Cd treatments) are significantly different according to the Tukey test at 5% significance.

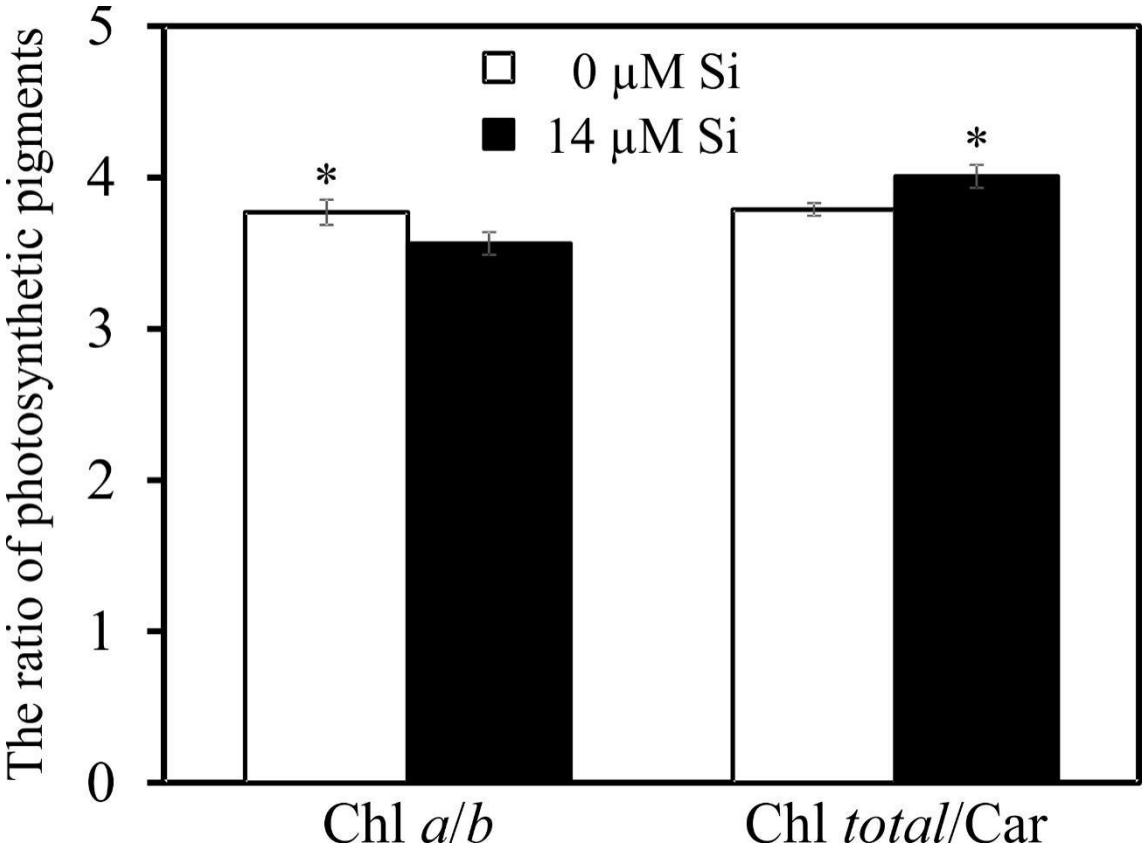

Fig. 7 Photosynthetic pigment content: chlorophyll *a/b* ratio (Chl *a*/b), total chlorophyll ratio for carotenoids (*total* Chl / Car) in *Aechmea blanchetiana* plants with 0 or 14 µM Si. Means (±SE), *n* = 8, followed by an asterisk (*) in each photosynthetic pigment ratio are significantly different according to the Tukey test with a 5% probability.

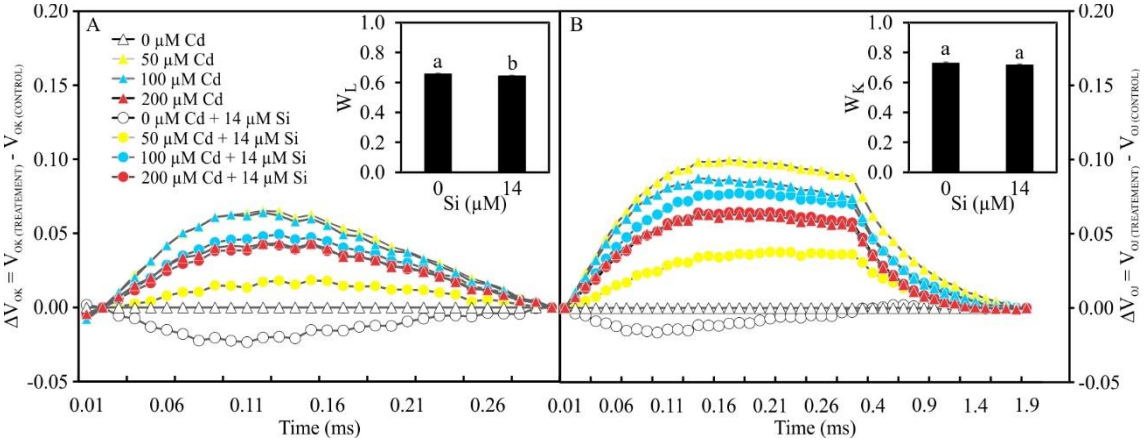

Fig. 8 Kinetic differences of *Aechmea blanchetiana* plants grown in medium with different concentrations of Cd [µM] and Si [µM]. (A) kinetic differences between steps O and K [$V_{OK} = (F_t - F_0)/(F_K - F_0)$], showing the L-band; W_L - represents changes in the fluidity of the thylakoid membrane and damage to its function and structural integrity. (B) kinetic differences between steps O and J [$V_{OJ} = (F_t - F_0)/(F_J - F_0)$], showing the K-band; W_K - represents the damage to the oxygen evolving complex (OEC); For each parameter, means (±SE), n = 15, followed by the same letter do not differ significantly according to the Tukey test, with a 5% probability.

Table 3 JIP test parameters in *Aechmea blanchetiana* plants as a function of the absence or presence of Si (0 or 14 µM Si)

JIP test parameters	0 µM Si	14 µM Si
F_V/F_0	1.77 ± 0.055^b	2.07 ± 0.060^a
F_0	661.06 ± 15.580^a	577.16 ± 14.888^b
V_J	0.66 ± 0.004^a	0.65 ± 0.004^b
V_K	0.51 ± 0.008^a	0.49 ± 0.007^a
φP_0	0.63 ± 0.007^b	0.66 ± 0.006^a
φE_0	0.21 ± 0.005^b	0.23 ± 0.005^a
φD_0	0.36 ± 0.007^a	0.33 ± 0.006^b
K_P	0.78 ± 0.024^b	0.92 ± 0.029^a
K_N	0.44 ± 0.005^a	0.44 ± 0.005^a
RC/CS_M	534.93 ± 15.264^a	569.93 ± 13.667^a
$PI_{(ABS)}$	2.30 ± 0.162^b	3.05 ± 0.201^a
$PI_{(TOTAL)}$	1.25 ± 0.076^a	1.34 ± 0.068^a

Means (±SE), $n = 15$, followed by the same letter in each JIP test parameter do not differ according to the Tukey test at 5% significance

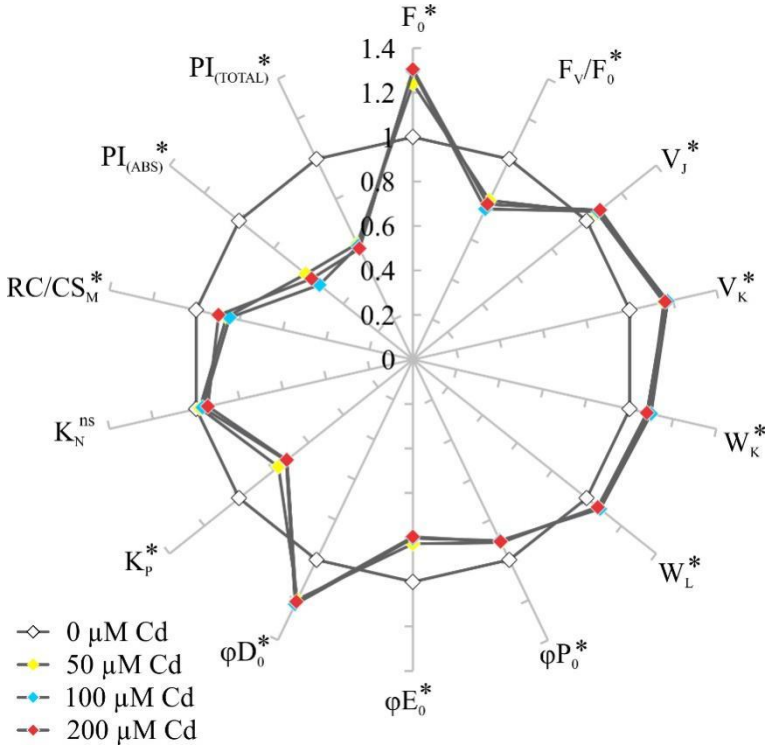

Fig. 9 Parameters of the JIP test in *Aechmea blanchetiana* plants as a function of Cd concentrations (0, 50, 100, 200 µM). Means (±SE), *n* = 15, followed by an asterisk (*) are significantly different according to the Tukey test with a 5% probability. All parameters of the JIP test were normalized in relation to the control data (0 µM Cd = 1). ^{ns} = not significant.

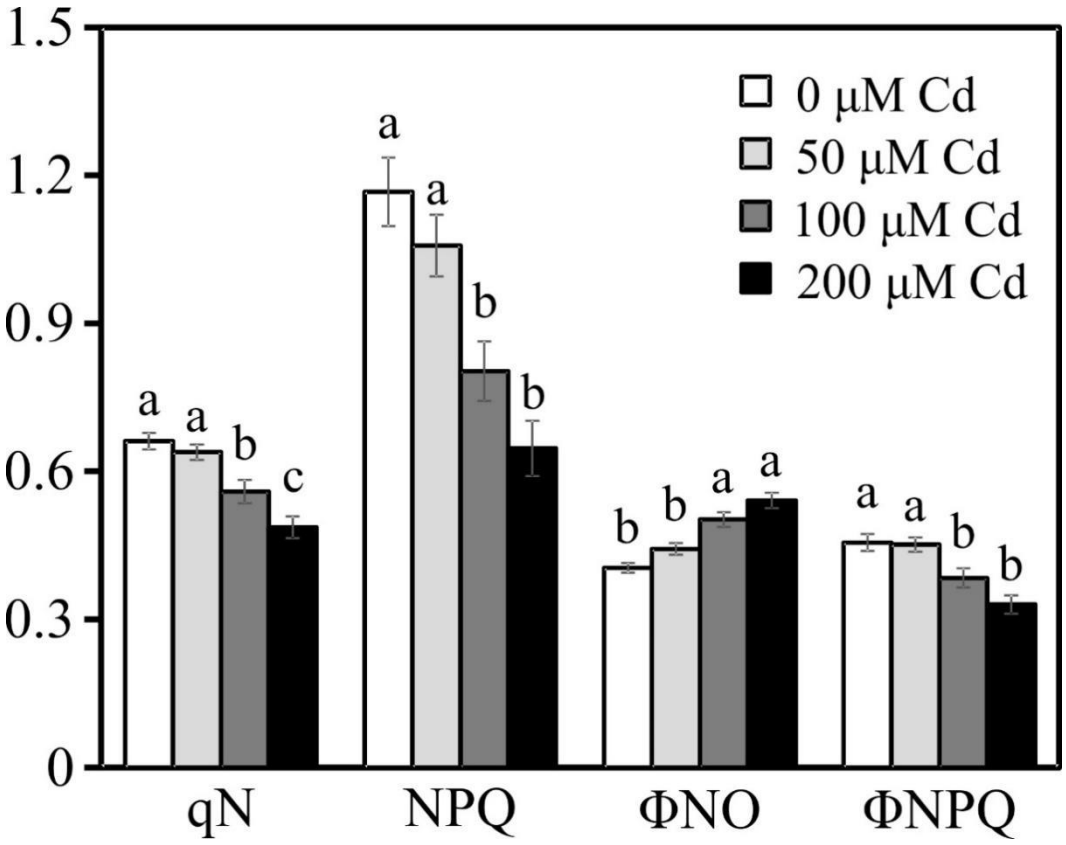

Fig. 10 Parameters of modulated chlorophyll *a* fluorescence related to energy dissipation in *Aechmea blanchetiana* plants as a function of Cd concentrations (0, 50, 100, 200 µM). Means (±SE), *n* = 12, followed by the same letter do not differ according to the Tukey test at 5% significance.

Table 4 Modulated fluorescence parameters related to energy dissipation in *Aechmea blanchetiana* plants as a function of the absence or presence of Si (0 or 14 µM Si)

Modulated fluorescence parameters	0 µM Si	14 µM Si
qN	0.56 ± 0.018^{b}	0.61 ± 0.015^{a}
NPQ	0.84 ± 0.050^{b}	0.99 ± 0.052^{a}
ΦNO	0.48 ± 0.012^{a}	0.45 ± 0.011^{b}
ΦNPQ	0.38 ± 0.015^{b}	0.42 ± 0.012^{a}

Means (±SE), $n = 12$, followed by the same letter in each modulated fluorescence parameter do not differ according to the Tukey test at 5% significance

Table 5 Effective photochemical quantum yield of PSII (ΦPSII), photochemical quenching (qP), and electron transport rate (ETR) as a function of Cd concentrations (0, 50, 100, 200 µM) in *Aechmea blanchetiana* plants

Cd (µM)	ΦPSII	qP	ETR
0	0.13 ± 0.006^{a}	0.26 ± 0.011^{a}	11.16 ± 0.54^{a}
50	0.10 ± 0.006^{b}	0.20 ± 0.011^{b}	8.42 ± 0.54^{b}
100	0.11 ± 0.006^{b}	0.21 ± 0.011^{b}	9.05 ± 0.54^{b}
200	0.12 ± 0.006^{ab}	$0.22 \pm 0{,}011^{b}$	10.25 ± 0.54^{ab}

Means (±SE), $n = 12$, followed by the same letter in the column do not differ according to the Tukey test at 5% significance

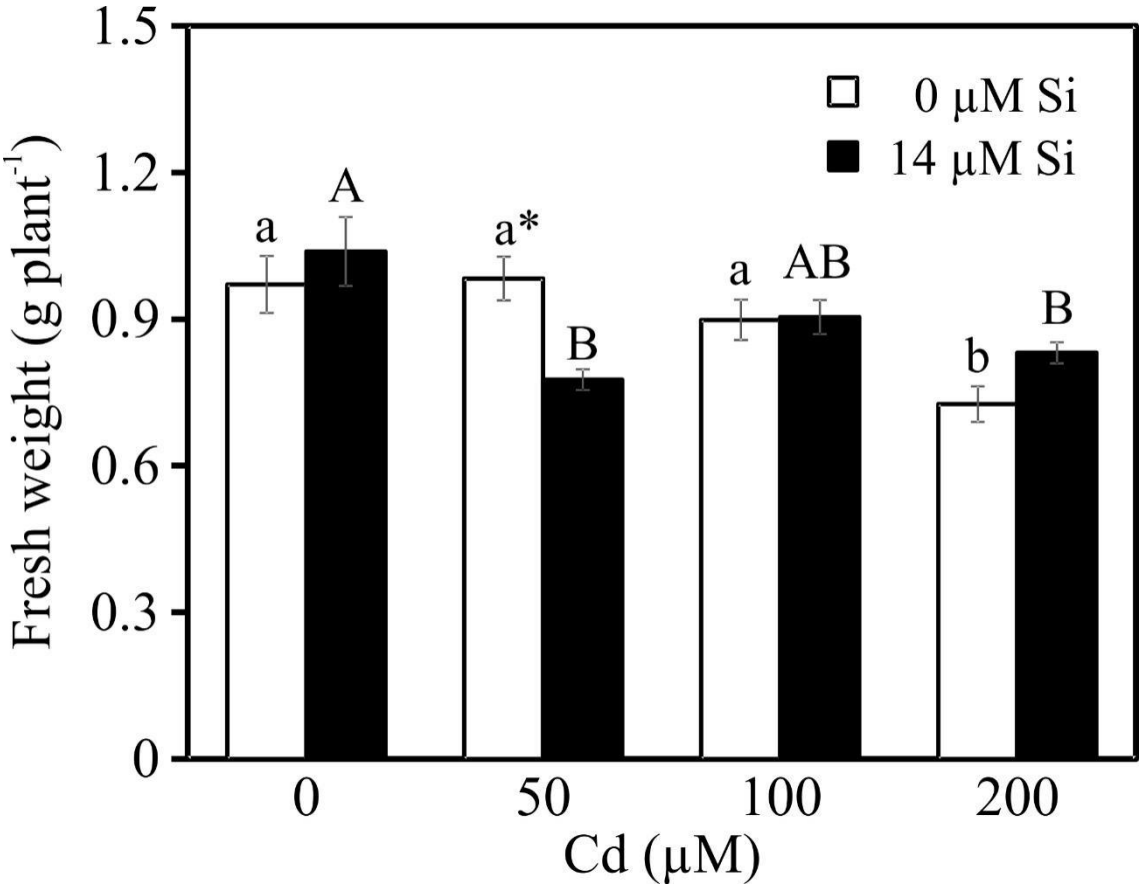

Fig. 11 Total fresh mass (shoot + roots) (g plant^{-1}) in *Aechmea blanchetiana* plants as a function of Cd concentrations (0, 50, 100, 200 µM) combined with 0 or 14 µM Si. Means (±SE), n = 5, followed by the different letters in each Si concentration (lower case for 0 µM Si and upper case for 14 µM Si, comparing the Cd concentrations) and asterisk (*) in each Cd concentration (comparing the Si concentrations) are significantly different according to the Tukey test at 5% probability.

CONCLUSÕES GERAIS

O presente estudo comprovou que as respostas induzidas pelo Si contribuem para a anatomia, fisiologia e maior crescimento de plantas de *A. blanchetiana* cultivadas *in vitro*. Em relação as fontes de Si, respostas em conjunto promovidas pelo $CaSiO_3$, como o aumento de ΦPSII, ETR e qP, contribuíram para aumentar o crescimento das plantas. Plantas crescidas com MgO_3Si promoveram respostas como o aumento no diâmetro dos vasos do xilema e da área de esclerênquima que permitiram o aumento da massa fresca total das plantas *in vitro*. No entanto, plantas cultivadas com K_2O_3Si apresentaram modulações anatômicas e fisiológicas que reduziram a atividade fotoquímica efetiva do FSII e o crescimento de plantas de *A. blanchetiana*. As concentrações 8 e 16 µM foram as que possuíram maior contribuição com a atividade fotoquímica efetiva do FSII. Dentre as fontes de Si testadas, o $CaSiO_3$ foi o que apresentou maior contribuição para o aumento do funcionamento efetivo do FSII e do crescimento das plantas.

Em condições de estresse *in vitro*, o NaCl e o Cd, são prejudiciais para o crescimento de plantas de *A. blanchetiana*, já que afetam a anatomia, a absorção de nutrientes e a fisiologia das plantas. Plantas de *A. blanchetiana* apresentam respostas de tolerância, implementando diferentes mecanismos para lidar com o estresse salino, como a espessura das paredes da exoderme mais finas, redução da densidade estomática e aumento da dissipação não-fotoquímica de fluorescência. O uso do Si reduz os danos gerados pelo estresse por meio de modulações na anatomia da raiz que permitem maior absorção de nutrientes essenciais para a atividade do sistema antioxidante. A maior atividade enzimática reduz o estresse oxidativo e possibilita alterações no funcionamento do aparato fotossintético. Essas modulações contribuíram para reduzir os danos nas plantas causados pelo estresse, como comprovado pela fluorescência da clorofila *a*.

Modulações em plantas de *A. blanchetiana* expostas ao Cd *in vitro* permitiram as plantas criarem ajustes fundamentais para suportarem a condição de excesso de Cd, mesmo em condições que induziram sintomas de toxicidade. Mecanismos de proteção como aumento da dissipação do excesso de energia de excitação como calor permitiram as plantas manterem a estabilidade e funcionamento do aparato fotossintético. Contudo, a maioria dos sintomas de toxicidade ao Cd foram melhorados

com a co-exposição de Si. A suplementação com o Si amenizou os efeitos do Cd por meio da melhoria na eficiência do fluxo de energia da cadeia de transporte de elétrons, uma grande capacidade fotoprotetora por meio da dissipação do excesso de energia de excitação, aumento da atividade fotossintética e fotoquímica do FSII das plantas de *A. blanchetiana*. Os resultados do presente estudo demonstram que a suplementação com o Si contribuiu para amenizar os danos e aumentar a resistência ao Cd em plantas de *A. blanchetiana* devido ao menor nível dos efeitos deletérios no conteúdo de pigmentos fotossintéticos e no desempenho do aparato fotossintético.